OPEN-FILE REPORT 06-9

Geologic Map of the Fairplay East Quadrangle, Park County, Colorado

By

Robert M. Kirkham[1], John W. Keller[2], Karen J. Houck[3], and Neil R. Lindsay[4]

[1] Consulting Geologist, Alamosa, CO
[2] Colorado Geological Survey, Denver, CO
[3] Dinosaur Tracks Museum, University of Colorado at Denver and Health Sciences Center, Denver, CO
[4] Colorado Geological Survey, Alamosa, CO

Bill Ritter Jr., Governor, State of Colorado
Harris D. Sherman, Director, Department of Natural Resources
Vince Matthews, State Geologist and Division Director, Colorado Geological Survey
Denver, Colorado
2006

FOREWORD

The Colorado Department of Natural Resources is pleased to present the Colorado Geological Survey's Open-File Report 06-9, *Geologic Map of the Fairplay East Quadrangle, Park County, Colorado***.** Its purpose is to describe the geologic setting of this 7.5-minute quadrangle. Field work for the project was conducted during the summer and fall of 2005.

This mapping project was funded jointly by the U.S. Geological Survey through Agreement No. 05HQAG0064 of the STATEMAP component of the National Cooperative Geologic Mapping Program, which is authorized by the National Geologic Mapping Act of 1997, and also by the Colorado Geological Survey using the Colorado Department of Natural Resources Severance Tax Operational Funds. The CGS matching funds come from the severance tax paid on the production of natural gas, oil, coal, and metals. Geologic maps produced by the CGS through the STATEMAP program are intended as multi-purpose maps useful for land-use planning, geotechnical engineering, geologic-hazards assessment, mineral-resource development, and ground-water exploration.

Vince Matthews
State Geologist and Division Director

TABLE OF CONTENTS

LIST OF FIGURES

LIST OF TABLES

INTRODUCTION

GEOGRAPHIC SETTING

The Fairplay East 7.5-minute quadrangle lies in the western part of South Park, a high-altitude intermontane valley in central Colorado. The map area covers approximately 57 square miles in Park County and includes the eastern part of the town of Fairplay and portions of the floor of South Park east and south of Fairplay (fig. 1). U.S. Highway 285, Colorado Highway 9, and numerous county-maintained and unimproved public and private roads provide good access to most of the quadrangle.

Topographically the quadrangle consists of gently southeastward-draining valleys separated by linear or slightly arcuate ridges that trend north or northwest (fig. 1). Reinecker Ridge lies along the eastern margin of the quadrangle, and Red Hill is in the central part of the quadrangle. Four named streams are shown on the base map: the Middle Fork of the South Platte River, Fourmile Creek, Trout Creek, and Crooked Creek, all of which are within the watershed of the South Platte River. Elevations range from a high of 10,558 feet above mean sea level on Reinecker Ridge to a low of about 9,170 feet where Trout Creek crosses the southern edge of the quadrangle.

Most land in the quadrangle is privately owned; the remainder is either state land or federal land. The Colorado Division of Wildlife manages several sections of land in the east-central part of the quadrangle along the crest of Reinecker Ridge and east of it. The Colorado Board of Land Commissioners manages a few tracts scattered across other parts of the quadrangle. The largest tract of contiguous Federal lands borders the state lands on Reinecker Ridge; other smaller tracts of federal lands are along the southern, western, and northern margins of the quadrangle. All federal lands within the quadrangle are administered by the Bureau of Land Management.

SCOPE OF WORK

Geologic mapping of the Fairplay East quadrangle was undertaken by the Colorado Geological Survey (CGS) as part of the STATEMAP component of the National Cooperative Geologic Mapping Program. This geologic map is the sixth map in this region prepared by the CGS as part of the STATEMAP program (fig. 2). The five other maps include Fairplay West quadrangle (Widmann and others, 2006), Alma quadrangle (Widmann and others, 2004a), Como quadrangle (Widmann and others, 2005), Breckenridge quadrangle (Wallace and others, (2003), and Copper Mountain quadrangle (Widmann and others, 2004b).

Mr. Kirkham was responsible for mapping the Paleozoic, middle Tertiary, most Mesozoic bedrock, and the Quaternary deposits. Mr. Keller mapped the late Cretaceous-Paleocene South Park Formation. Ms. Houck conducted detailed stratigraphic studies of the Minturn and Maroon Formations from Jacque Peak north of Leadville to the project area to establish the contact between the formations and correlate limestones within the formations. Mr. Lindsay served as the mapping field assistant, led efforts to trace individual limestone beds in the Minturn and Maroon Formations within the quadrangle, and assisted with the regional study of the Minturn and Maroon Formations.

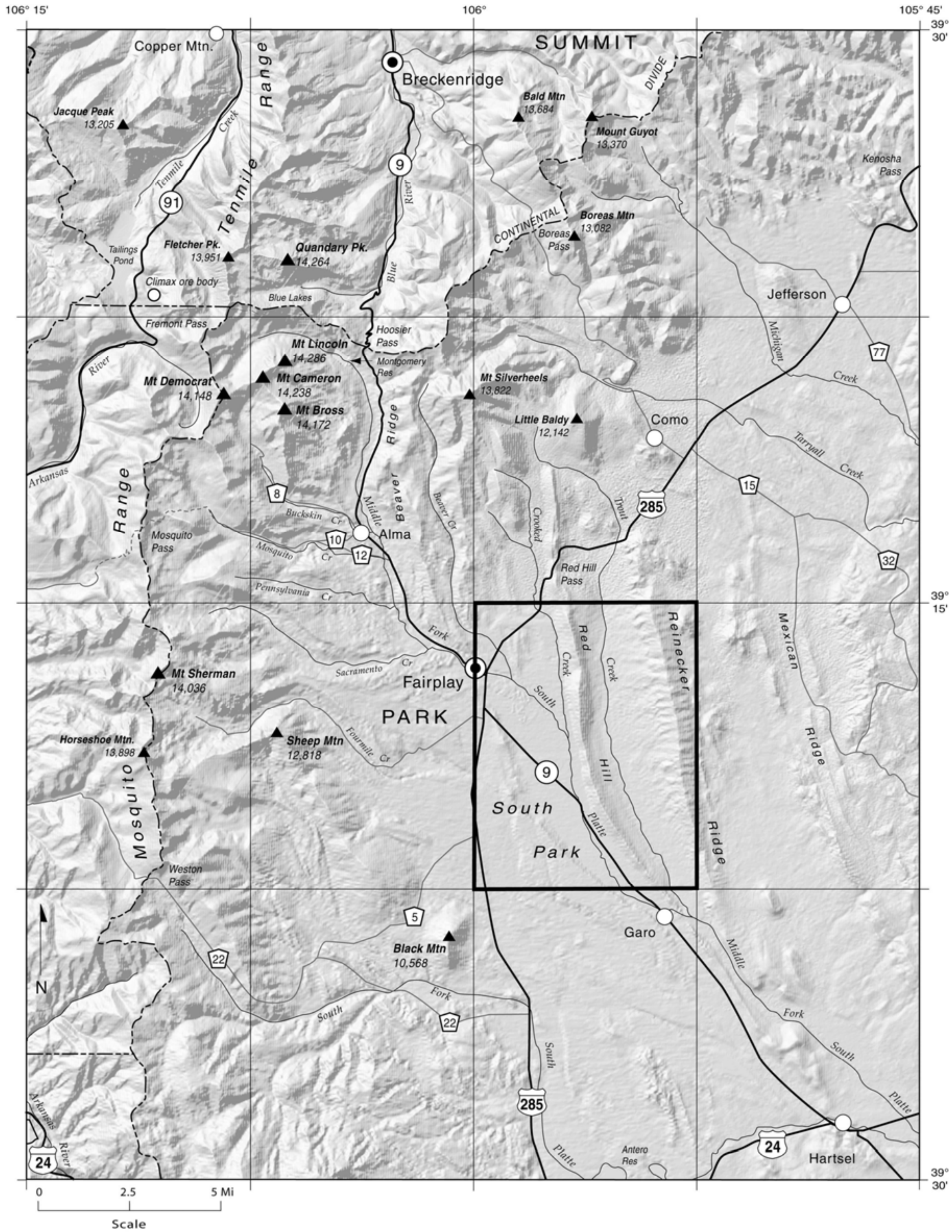

Figure 1. Shaded relief map of the project area and adjoining areas. The thick black line marks the Fairplay East quadrangle.

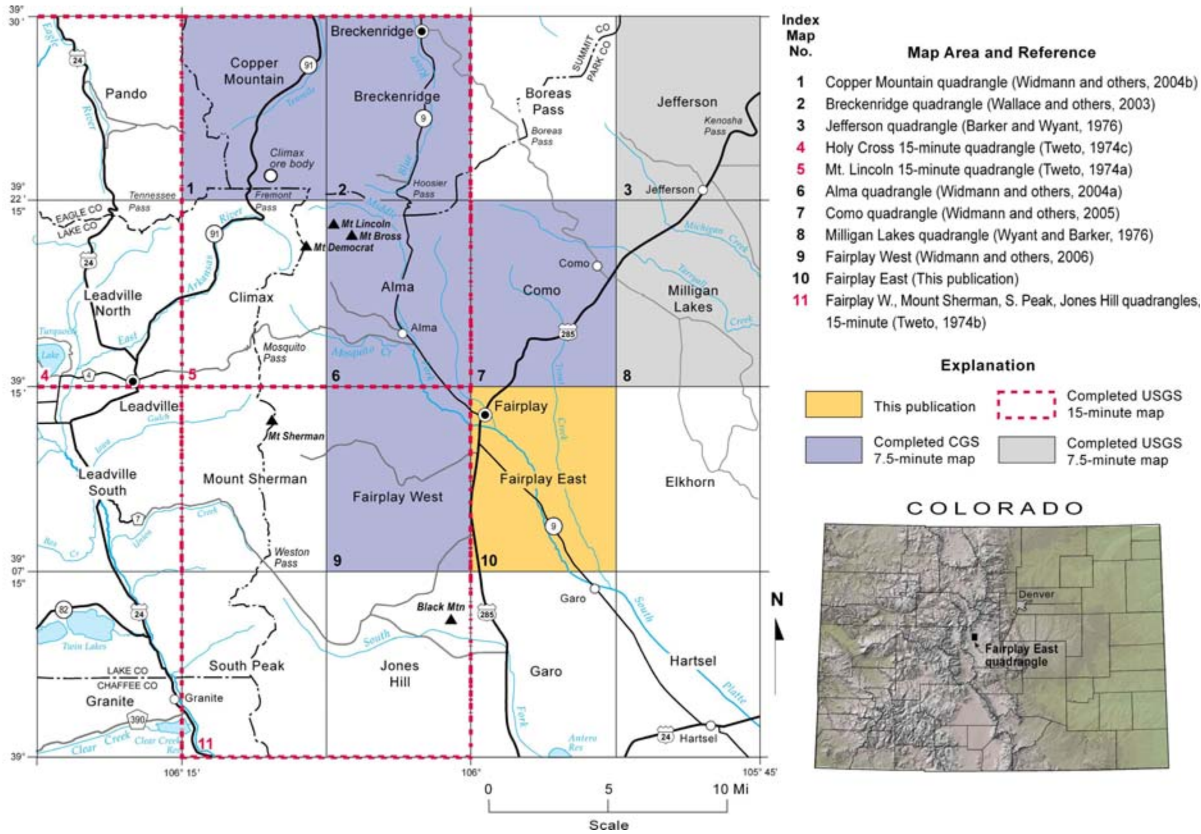

Figure 2. Location map of the Fairplay East quadrangle, and status of geologic mapping in adjacent areas.

Field work was conducted during the summer and fall of 2005. Geologic information and ground control collected in the field was plotted on 1:24,000-scale color aerial photographs flown for the Bureau of Land Management in 1982. Geographic coordinates for the ground control and geologic data points were determined using hand-held GPS receivers. The annotated aerial photographs were scanned, georeferenced, and imported into ERDAS Imagine OrthoBase, where they were photogrammetrically corrected and rendered in 3D. Line work was traced directly from ERDAS Imagine Stereo Analyst and exported as ESRI shapefiles into ArcGIS 9.1.

PREVIOUS STUDIES

Numerous prior published geologic maps and reports address all or parts of the Fairplay East quadrangle. These include the regional 1:500,000-scale geologic maps of Colorado by Burbank and others (1935) and Tweto (1979), the 1:250,000-scale geologic map of the Denver 1^o x 2^o quadrangle by Bryant and others (1981b), and the 1:125,00-scale geologic map of Stark and others (1949). The 1:48,000-scale map of Shoffner (1974) covers the eastern part of the quadrangle. Several geologic maps of areas adjacent to or near the Fairplay East quadrangle were published by the Colorado Geologic Survey and U.S. Geological Survey at scales of 1:24,000 and 1:62,500 (fig. 2).

The geology and origin of South Park was described by Stark and others (1949), De Voto (1961; 1971; 1972), and Sawatsky (1967). The Pennsylvanian and Permian stratigraphy and structure of the region was the subject of many prior studies (e.g. Brill, 1952; De Voto, 1965a, 1965b, 1980). Clement and Dolton (1970) provided a summary of the oil and gas exploration in South Park during the 1960s and 1970s. Hembre and TerBest (1997) and Steyaert and Wandrey (1997) discussed the petroleum potential of the area. Shoffner (1974) and Raynolds (2003) focused on the South Park Formation. Fatti (1974), Beggs (1977), Durani (1980), and Treviño and Keller (2004) reported on geophysical studies of the South Park basin. Singewald (1950) and Parker (1961, 1992) described the gold placers along the Middle Fork of the South Platte River.

TERMINOLOGY, NOMENCLATURE, AND METHODOLOGY

The nomenclature and ages in the geologic time scale of the Colorado Geological Survey (fig. 3) are used in this study. Grain-size terminology for sedimentary deposits (both bedrock and surficial deposits) follows the modified Wentworth grain-size scale (Ingram, 1989). This classification system defines pebbles, cobbles, and boulders as differing sizes of gravel. These terms are commonly used by many geologists for rounded clasts deposited in fluvial and beach environments (e.g. Jackson, 1997). We herein use these terms only to describe the size of the clasts, not the genetic origin. The term clast as used here refers to rock and mineral fragments larger than 2 mm in diameter, whereas matrix refers to surrounding material that is 2 mm or less in diameter (sand, silt, and clay). In clast-supported deposits, the majority of the material consists of clasts that are in point-to-point contact. Matrix-supported deposits are composed predominantly of material smaller than 2 mm, and most clasts are separated by or embedded in matrix. Terms used for sediment sorting are those of Folk and Ward (1957). Sedimentary rocks are named according to the classification system of Folk (1980). English units are used throughout the report except for microscropic observations, which are described in metric units. The 1927 North American datum is used for all UTM coordinates.

Selected samples were chemically analyzed for major elements. The analyses are listed in Appendix A, and the locations of the samples are shown on the geologic map. The total alkali-silica plot (TAS) of Le Bas and others (1986) was used to classify chemically analyzed volcanic rocks. Four samples from the quadrangle were dated using $^{40}Ar/^{39}Ar$ methods (see Appendices B and C).

Surficial geologic deposits in the quadrangle are divided into map units on the basis of either genesis or landform and also relative age. Most of the surficial deposits in the map area are not well exposed. The best exposures are in features such as mine pits, road cuts,excavations at homesites, and eroded stream banks. Due to limited exposures, the physical attributes of the surficial units, such as thickness, texture, stratification, and composition, are based on observations made at only a few locations, and their origin is often deduced only on the basis of geomorphic characteristics.

Surficial deposits with a minimum thickness of about 3 to 5 feet thick are shown on the map. Surficial deposits associated with distinct landforms locally may be thinner than 3 feet. Contacts for many surficial units were located using geomorphic characteristics, and some contacts are gradational. Areas mapped as surficial deposits may include small areas of bedrock that are not depicted on the map. Deposits of residuum are not mapped.

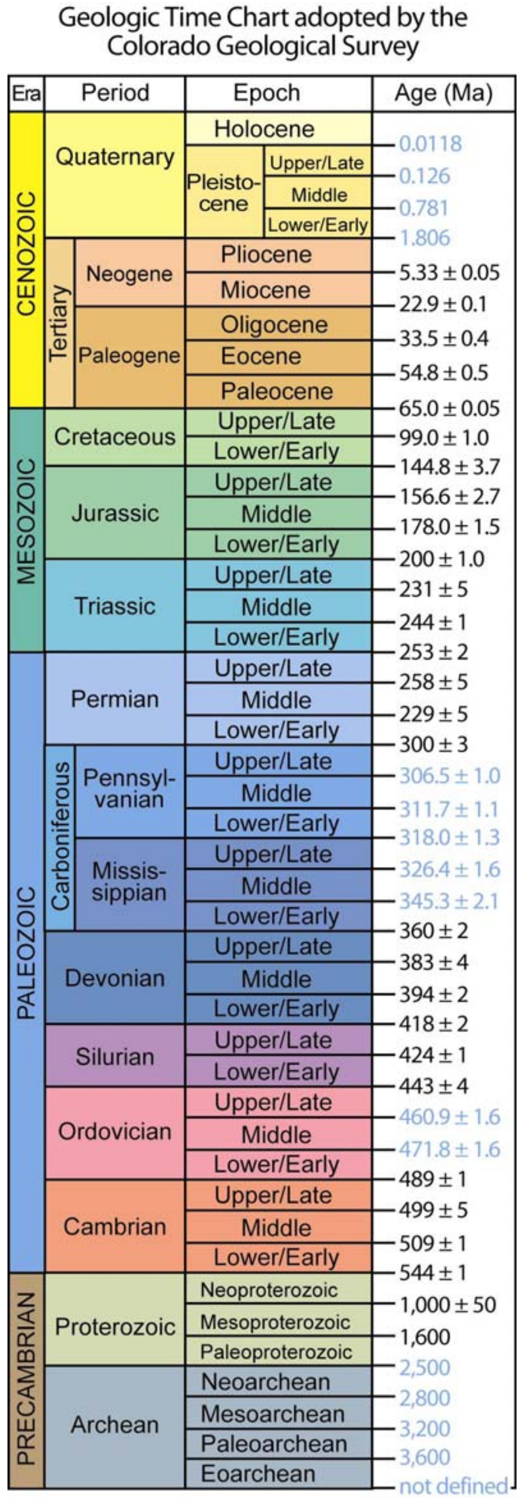

Figure 3. Geologic time scale used by the Colorado Geological Survey. Numerical ages shown in black are from the Geological Survey of Canada (Okulitch, 2002); ages shown in blue are from the International Commission on Stratigraphy (2005).

Absolute ages are not available for any of the surficial deposits in the map area. Characteristics such as stratigraphic relations, position in the landscape, degree of weathering, and, where exposed, pedogenic soil development were used to estimate the relative ages of the surficial deposits.

Glacial till and outwash deposited by glacial meltwater are correlated with oxygen isotope stages wherever possible in this report. Oxygen occurs in two common stable isotopes, ^{16}O and ^{18}O. The ratio of these two isotopes in water is temperature dependent. During cold glacial periods the $^{18}O/^{16}O$ ratio is high, and during warmer interglacial periods the ratio is low. By studying oxygen isotope ratios in thick ice caps and in fossils buried beneath the sea floor, changes in temperature over time can be evaluated (e.g. Martinson and others, 1987). An oxygen isotope stage consists of a lengthy time interval during which the temperature was generally either cold or warm. The modern warm interglacial period is assigned to oxygen isotope stage one, the last major glacial period (Pinedale glaciation) is oxygen isotope stage 2, and preceding interglacial and glacial periods are consecutively numbered. The Bull Lake glaciation is usually correlated with isotope stage 6.

Soil-horizon names used here are those of the Soil Survey Staff (1975) and Guthrie and Witty (1982), and the stages of secondary carbonate morphology are from Gile and others (1966), with the modifications of Machette (1985). Concurrent soil mapping by the U.S. Department of Agriculture's Natural Resource Conservation Service aided our attempt to use pedogenic soil development as a tool to determine relative ages of the surficial map units.

Bedrock outcrops and surficial deposits with a map width less than about 50 feet generally are not depicted on the map. Thin but important bedrock units, such as limestone beds, are represented on the map as single lines because they add to the stratigraphic and structural understanding of the geology in the area.

The U.S. Geological Survey’s Fairplay East 7.5-minute topographic map, which was published in 1956, serves as the base map for the geologic map. The topographic map was prepared using aerial photography flown in 1952. Therefore, cultural features that post-date the mid-1950s are not shown on the base map.

ACKNOWLEDGMENTS

This geologic mapping project was funded jointly by the Colorado Geological Survey and U.S. Geological Survey through the STATEMAP component of the National Cooperative Geologic Mapping Program, Award number 05HQAG0064. The State of Colorado provided funding through the Department of Natural Resources Severance Tax Operational Fund, which is derived from the production of gas, oil, and minerals.

The map and report benefited from the review comments of Richard De Voto and Beth Widmann. We thank Jim Cappa for his petrographic work on the tuff and his review of the section of the report that describes the tuff. Jim Shannon also examined thin sections of the tuff. Dave Stanford provided information on the water wells for the Red Hill Forest Ranches subdivision. Jane Ciener was the technical editor of the map and report. David Clark and Tom Neer, with Digital Data Services, prepared the digital geologic map for publication. Cartographic work for figures 1 and 2 was performed by Larry Scott. We thank the Colorado Historical Society for granting permission to reproduce the photograph of the South Park placer dredge and also Rachael Farnsworth, who helped secure that permission.

We appreciate the cooperation of numerous landowners and/or property managers who gave us permission to conduct field work on their land. Steve Rzepka, Bruce Plankinton, Bill Berger, Danny Middleton, Steve and Julie Petee, John Cooney, Rod Miley, Stan Kopunec, Charlie Gordon, Mark Balderston, and Mike Pfister were especially helpful. We also thank Art Girton and Sage Greising for their assistance in contacting several landowners. Special thanks to Rick and Michelle Carroll, whose house outside of Fairplay was our home during the field season, and who helped with landownership questions.

DESCRIPTION OF MAP UNITS

SURFICIAL DEPOSITS

Surficial deposits are organized into five groups on the basis of their genesis. The genetic groups are: human-made deposits; alluvial deposits; mass-wasting deposits; alluvial and mass-wasting deposits, undivided; and glacial deposits.

HUMAN-MADE DEPOSITS — Earth materials placed by humans

mw **Mine waste (Historic) —** Includes materials that resulted from mining operations. Most mine waste in the quadrangle is associated with gold placer operations that worked alluvial units Qa1 and Qa2 along the Middle Fork of the South Platte River or Beaver Creek. This material consists of light-brown piles of cobbles, pebbles, and boulders with minor sand and silt that was deposited by hydraulic or dredge mining. Mine waste from hydraulic mining typically forms hummocky or irregularly shaped piles, whereas the refuse from dredge mining forms sinuous or looping piles with a corrugated surface that is transverse to the long dimension of the pile (fig. 4). Area residents often refer to the sinuous piles southeast of Fairplay as the “intestines”. Recent mining operations for sand, gravel, landscaping rocks, and riprap are locally reworking the mine waste. The spoil from these recent operations also is included in the unit. Non-earthen materials such as scrap metal and timbers locally may be present in mine waste. Mine waste may exceed a thickness of 50 feet in places.

af **Artificial fill (Historic) —** Earth materials used as fill in road and dam construction. Artificial fill consists chiefly of sand, silt, rock debris, and clay that are at most about 40 feet thick.

ALLUVIAL DEPOSITS — Sediments deposited by flowing water in channels and on flood plains and by glacial meltwater in outwash fans and outwash plains. Alluvial deposits locally include significant amounts of organic material.

Qa1 **Alluvial unit one (Holocene) —** Mainly poorly sorted, clast-supported, unconsolidated, sandy gravel of all sizes, gravelly sand, silty sand, and sandy silt in modern channels, flood plains, and adjacent low-lying terraces that are as much as about 5 feet above modern channels. Deposits in alluvial unit one usually are stratified and may have cut-and-fill channels. Organic material is locally common. The unit may include interbedded or overlying, very poorly sorted, matrix-supported gravelly silt and sand that probably were deposited by debris flows from tributary drainages. Most clasts are fresh and sound, with little or no or decomposition. Clasts typically are subround to subangular, although a few are round or angular. Weakly developed pedogenic soil horizons have formed on deposits of alluvial unit one. The unit probably was deposited in oxygen isotope stage 1 during episodes of Holocene neoglaciation or flooding. Thickness of the unit is estimated to range from about 3 to 15 feet thick, but could be thicker in places.

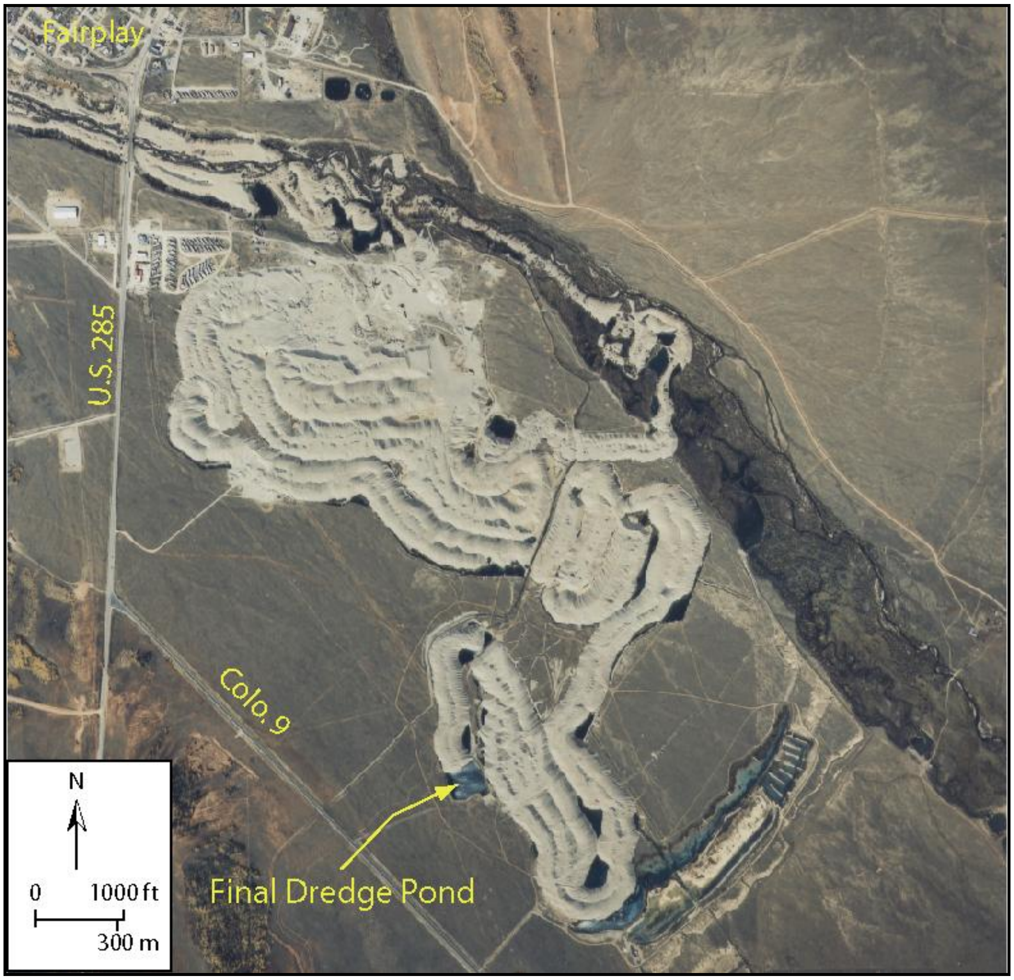

Figure 4. Aerial photograph of mine waste piles southeast of the town of Fairplay. Local residents refer to the sinuous and looping piles as the "intestines". The final dredge pond marks the last pond in which the dredge boat worked. (USDA photograph 612120 2495-124; flown September 29, 1997)

Qa2 **Alluvial unit two (upper Pleistocene) –** Alluvial unit two contains stratified, poorly sorted, clast-supported, sandy cobble and pebble gravel, gravelly sand, silty sand, and sandy silt that was deposited by glacial meltwater. Most clasts are subround to subangular and are unweathered or very slightly weathered. Extensive deposits of alluvial unit two are preserved in the valleys of the Middle Fork of the South Platte, Beaver Creek, and Fourmile Creek. To the west, in the Fairplay West and Alma quadrangles, these deposits grade to the Pinedale terminal moraine (Widmann and others, 2005; 2006). On the south side of the Middle Fork of the South Platte River, deposits of alluvial unit two underlie a broad outwash plain with terrace risers. The outwash plain extends beyond the south edge of the quadrangle. On the north side of the Middle Fork, in the vicinity of the “Coil” and “Buyer” ranches shown on the base map, deposits of alluvial unit two underlie a subtle fan-like landform with well-preserved channel geomorphology. The alluvial unit two deposits along Fourmile Creek are part of a broad outwash fan that extends westward into the Fairplay West quadrangle.

Streams are incised as much as 20 to 40 feet into alluvial unit two along the western margin of the quadrangle, but the depth of incision gradually decreases downstream. In places the depositional surfaces on alluvial unit two converge with the modern valley floor, which suggests alluvial unit two may underlie alluvial unit one at least locally. Pedogenic soils formed in alluvial unit two have weakly to moderately well developed Bw horizons, no or very weak and thin argillic Bt horizons, and very thin calcareous Cca horizons with stage I to weak stage II carbonate morphology. Stratigraphic relationships between alluvial unit two and the late Pleistocene tills west of the quadrangle, along with soil development and clast weathering, suggest deposition during the Pinedale glaciation (oxygen isotope stage 2), which extended from about 13 to 35 ka.

Singewald (1950) and Parker (1974) reported total gravel thicknesses in excess of 100 feet in and near the Fairplay placer in sections 2, 3, and 11, T. 10 S., R. 77 W. Parker’s data indicate gravel thicknesses vary significantly over relatively short distances. The presence of buried clay layers or “clayey gravel” in the logs of test holes led Parker (1974) to conclude that the clayey gravel was probably buried Bull Lake outwash (our unit Qa3), in which case the thickness of the alluvial unit two gravels would be substantially less than 100 feet. Driller’s logs of water wells spudded in alluvial unit two suggests gravel thicknesses in the valley of the Middle Fork below the Fairplay placer range from about 20 to 80 feet, and in the valley of Fourmile Creek the gravel attains thicknesses of at least 140 feet (Colorado Division of Water Resources well records). The gravel thicknesses reported in the driller’s logs may include stacked sequences of outwash of more than one age.

Qa **Alluvial units one and two, undivided (Holocene and upper Pleistocene) —** Includes deposits of alluvial unit one and alluvial unit two in the valley of South Crooked Creek that are not mapped separately because they are indistinguishable or cannot be mapped separately at a scale of 1:24,000.

Qa3 **Alluvial unit three (upper middle Pleistocene) —** Sediment in unit Qa3 is similar to that contained in unit Qa2, but it is older and usually higher in the landscape than unit Qa2. Deposits of alluvial unit three are mapped in two areas within the quadrangle. In the northwest part of the quadrangle the sediment was probably deposited by meltwater from Beaver Creek valley. These sediments are 30 to 40 feet above South Crooked Creek upstream of Highway 285, but they rapidly converge with the valley floor downstream of the highway and appear to disappear beneath alluvial unit one in the center of the E ½ of section 35, T. 9 S., R. 77 W.

The second area with deposits of alluvial unit three is along the western margin of the quadrangle. These sediments, which likely were deposited by meltwater from glaciers in the valleys of the Middle Fork of the South Platte River and Fourmile Creek, are found in (1) a narrow and elongated remnant that rims the western side of the bedrock ridge between the valleys of the Middle Fork and Fourmile Creek; (2) isolated islands surrounded by younger alluvial sediments, and (3) a remnant that overlies Tertiary sediments (unit Ts) along the east side of Fourmile Creek. Typically, the original depositional surfaces associated with alluvial unit three are about 20 feet or less above adjacent streams, and the islands of unit Qa3 appear to grade beneath adjacent younger alluvial deposits at the downstream ends of the islands. Parker (1974) described buried clayey gravels in the subsurface beneath areas mapped as alluvial unit two downstream of Fairplay. He concluded the buried clayey gravels were Bull Lake outwash (our unit Qa3) and the overlying sandy gravels were Pinedale outwash (our unit Qa2).

Gravel clasts contained within unit Qa3 typically are slightly or moderately weathered. Pedogenic soils formed on deposits of unit Qa3 commonly have moderately well-developed argillic Bt horizons with blocky or sometimes very weak prismatic structure and stage I carbonate morphology and Bk horizons that have stage II to very weak stage III carbonate morphology. In Fairplay West quadrangle alluvial unit three locally grades to terminal moraines correlated with the late middle Pleistocene Bull Lake glaciation (Widmann and others, 2006), which occurred during oxygen isotope stage 6. However, some deposits of alluvial unit three in the Fairplay East quadrangle may have been deposited during oxygen isotope stage 4. Alluvial unit three is a maximum of about 20 to 25 feet thick where exposed, but its thickness may vary significantly. Water wells drilled into alluvial unit three in the west-central part of the quadrangle pentetrated as much as 57 feet of gravel; a water well located in the center of section 27 near the northwest corner of the quadrangle encountered 17 feet of "overburden", all of which probably is gravel in alluvial unit three (Colorado Division of Water Resources water well records). Parker (1974) reported thicknesses as great as 51 feet for the buried clayey gravels that may correlate with our unit Qa3.

Qa4 **Alluvial unit four (middle Pleistocene) –** Sediment in alluvial unit four is similar to that contained in alluvial unit two; however, many of the Laramide intrusive and Precambrian clasts within the deposit are moderately to strongly weathered. The unit is also rich in multi-colored chalcedony clasts (fig. 5). The bright red and yellow colors on some of the clasts are a result of weathering, as the coloration does not extend into the interior of these clasts. The chalcedony clasts probably were eroded from the Maroon Formation. A large remnant of unit Qa4 underlies the high-level surface on the drainage divide between Fourmile Creek and the Middle Fork of the South Platte River in the southwest part of the quadrangle (fig. 6). The geomorphology of this large remnant suggests it was part of a larger outwash fan fed by meltwater from the Middle Fork.

The height of alluvial unit four above the adjacent modern streams decreases in a downstream direction. At the northern end of the large remnant, the deposits are about 140 feet above Fourmile Creek, whereas at the southern margin of the quadrangle the deposits are only about 40 feet above the creek. These deposits are about 240 feet above the Middle Fork at their upstream end and about 160 feet higher than the river at the south edge of the map area. The relatively rapid convergence of these deposits with modern streams demonstrates the futility of efforts to correlate the deposits using height above modern streams, as was done by Stark and others (1949). Pedogenic soils formed on unit Qa4 are somewhat similar to those on unit Qa3, except the Bk horizon usually has weak to moderate stage III morphology.

Exposed thicknesses of alluvial unit four typically are 5 to 20 feet, but it locally may be much thicker. A small valley up to about 40 feet deep is eroded into alluvial unit four in and south of the S ½ of section 26. No definitive evidence of the underlying bedrock was noted in the walls and bottom of this valley, which suggests the gravel thickness may exceed 40 feet in that area. A 92-feet-deep water well in the SW ¼ SE ¼ of section 35 apparently was drilled into alluvial unit four but did not reach bedrock (Colorado Division of Water Resources water well records).

Figure 5. Chalcedony clasts in alluvial unit four (unit Qa4).

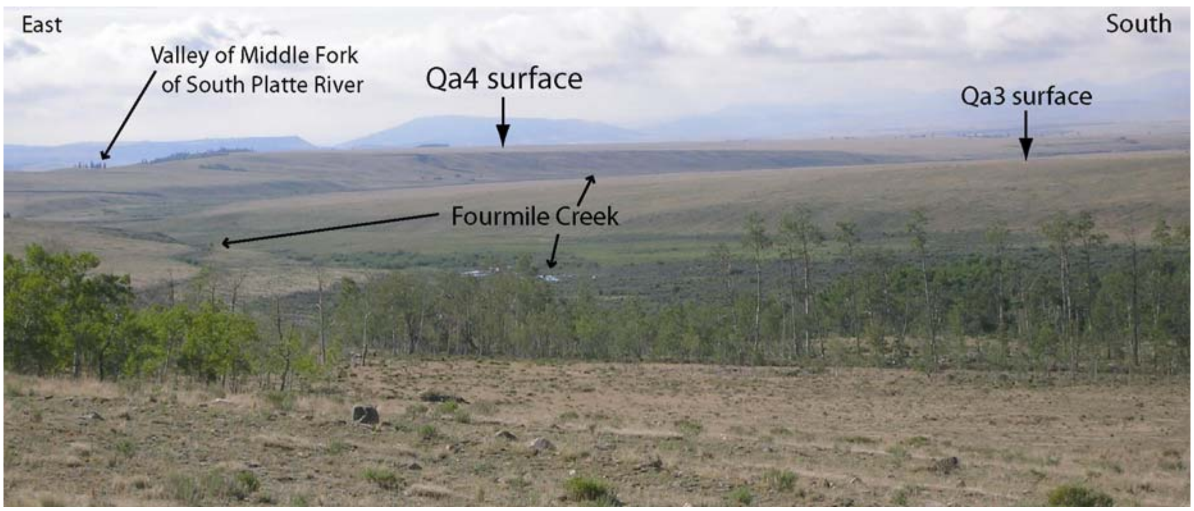

Figure 6. The gently south-southwest sloping, prominent surface on the drainage divide between Fourmile Creek and the Middle Fork of the South Platte River is underlain by alluvial unit four. The surface is a remnant of an outwash fan deposited by meltwater from the Middle Fork. Fourmile Creek flows east in the foreground of the image and makes a nearly right-angle turn to the south as it approaches the ridge capped by alluvial unit four. A remnant of alluvial unit three is preserved on the south side of the east-flowing section of the creek. Photograph taken in the Fairplay West quadrangle looking southeast across the valley of Fourmile Creek.

MASS-WASTING DEPOSITS – Mass-wasting deposits accumulate on hillslopes and adjacent valley floors. They are transported downslope primarily by gravity and not transported within, on, or under another medium such as flowing water or wind (Jackson, 1997). Water can be an important element in mass wasting, and it commonly triggers the movement. However, water is merely a part of the moving mass, not the transporting agent. Colluvium, landslide deposits, and talus are the principal types of mass-wasting deposits in the quadrangle. The classification system of Cruden and Varnes (1996) is used to describe the type of slope movement.

Qc **Colluvium (Holocene and upper Pleistocene) —** Includes deposits of poorly sorted, sandy or silty, fine to coarse gravel and gravelly sand or silt that are on hillslopes or at the foot of them. Colluvium can be rich in boulders below cliffs and rocky outcrops. As used here, colluvium generally follows the definition of Hilgard (1892) in that it (1) is derived locally and transported only short distances, (2) is not distributed by channelized water flow, (3) contains clasts of varying size, (4) has little or no sedimentary structures or stratification, features which are typically caused by channelized flow of water, and (5) may include minor amounts of sheetwash and debris-flow deposits. Unit Qc also locally includes landslide deposits and talus that either are too small to differentiate at the map scale or which are difficult to clearly discern on aerial photographs. Clasts in colluvium typically are angular to subangular, except in areas where the bedrock or surficial deposits in source areas for the colluvium contain well-rounded clasts. Maximum thickness of colluvium is estimated at about 25 feet.

Qls **Landslide deposits (Quaternary) —** Landslide deposits consist of heterogeneous, mostly unsorted and unstratified debris that commonly is characterized by hummocky topography and lobate form. Most landslide deposits in the quadrangle are located on the east side of Red Hill, which is an east-dipping hogback held up by the Dakota Sandstone. These landslide deposits are rich in angular clasts of sandstone derived from the Dakota, but also locally contain clasts of shale and clayey matrix from the Benton Group. The slope failures probably involve sandstone-rich colluvium that slides on the underlying shales of the Benton Group. A prominent slump-like landform exists on the east side of the crest of Red Hill at the north edge of the quadrangle and is denoted on Plate 1 by the pattern superimposed on the unit color used for landslide deposits. Unfortunately, there are no outcrops or exposures of the material under the landform. Some previous workers (e.g. Stark and others, 1949; Navas, 1966) interpreted the landform as a fault-bounded block of bedrock. Bryant and others (1981b) mapped a single fault here and depicted the slope below the slump-like landform as a landslide. We generally concur with the mapping of Bryant and others (1981b) but prefer to interpret the slump-like landform as a nearly intact but dislocated block of rock that is part of the landslide.

Several other small landslides occur in the quadrangle. They are on the steep slopes on the east side of Red Hill, on the west side of Reinecker Ridge, and on the west wall of the Middle Fork valley. Some of these deposits appear to be a result of rapid thin-skinned slope failures involving colluvium or residuum on steep slopes. Landslide deposits typically are a maximum of about 30 feet thick, but the large landslide at the north edge of the quadrangle may be much thicker.

ALLUVIAL AND MASS-WASTING DEPOSITS — These deposits include alluvial and colluvial material that are mapped as a single unit because they are juxtaposed and are too small to show individually, or they have contacts that are not clearly defined. Fan deposits and piedmont deposits are included in this category because, in addition to alluvium, they also include significant volumes of debris-flow sediment, which is generally considered to be a form of mass wasting (e.g. Cruden and Varnes, 1996; Hungr and others, 2001).

Qf **Fan deposits (Holocene and upper Pleistocene) —** Includes sediment in small, geomorphically distinct fans at the mouths of tributary valleys. Fan deposits are chiefly poorly sorted, clast-supported sandy gravel and gravelly sand deposited as alluvium during storm events, but locally they include debris-flow deposits that are composed of matrix-supported, poorly sorted, silty or sandy gravel. Clasts contained in younger fan deposits are mainly subangular to angular. Maximum thickness of the younger fan deposits is estimated at 20 feet.

Qac **Alluvium and colluvium (Holocene and upper Pleistocene) —** Unit Qac consists of alluvial sediments in (1) channels, flood plains, and low terraces in tributary drainages, and (2) colluvium and sheetwash along valley margins and hillslopes. The alluvial component of the unit is very poorly sorted to well sorted and ranges from sandy pebble, cobble, and boulder gravel to stratified fine sand and silt. Clasts in the alluvial component are subangular to subround. The colluvial part consists of very poorly sorted, unstratified or poorly stratified, gravelly to silty sand, sandy to silty gravel and gravelly sandy silt. Clasts in the colluvial part chiefly angular to subangular. The unit locally includes debris-flow deposits, which typically are matrix-supported gravelly silt, and also small landslides or soil slips. Thickness of unit Qac is estimated to range from 3 to 25 feet thick.

Qp **Piedmont deposits (Pleistocene) —** Fine- to coarse-grained alluvium and debris-flow deposits compose the piedmont deposits that mantle drainage divides on both sides of Reinecker Ridge. The sediments were eroded from the South Park Formation, carried down the ephemeral valleys by storm runoff or snow melt, and deposited on the piedmont at the base of the ridge. The deposits lie about 3 to 30 feet above the modern drainages. They probably were deposited at various times during the Pleistocene. The deposits are typically 3 to 10 feet thick. In many places along the western side of the ridge the piedmont deposits form a very thin mantle that conceals the underlying Pierre Shale. These areas are depicted on the geologic map by the multiple-unit symbol Qp/Kp.

GLACIAL DEPOSITS — Includes sediment deposited by or adjacent to glacial ice. These deposits are mapped as till, which is nonsorted and nonstratified sediment deposited directly by ice without reworking by glacial meltwater, but the unit locally includes stratified alluvial sediment, debris-flow deposits, and mass-wasting deposits.

Qti **Till (middle Pleistocene) —** Deposits of till exist in two locations in the northwest corner of the quadrangle. Both are in the valley of the Middle Fork of the South Platte River and are contiguous with and correlative to deposits of till unit Qti_2 in the Fairplay West quadrangle (Widmann and others, 2006). The deposits are eroded remnants of lateral and terminal moraines and consist chiefly of nonsorted and nonstratified subangular to subround boulders, cobbles, and pebbles in a sandy or silty matrix. Sand-sized and smaller particles commonly comprise more than 50 percent of the deposit, although gravel-sized material locally is more abundant. Stratified, thinly bedded sand and fine gravel, debris-flow deposits, and mass-wasting deposits may locally be included in the map unit.

The geomorphic features on the moraine on the south side of the river are less distinct than those on late Pleistocene moraines in Fairplay West quadrangle (Widmann and others, 2006). Most geomorphic features of the moraine on the north side of the river have been altered by human activity; they appear to be similar to landforms on late middle Pleistocene or older moraines. The clasts in till within the quadrangle are more decomposed than those found in late Pleistocene till in the Fairplay West quadrangle. Weathering rinds on clasts in till in the quadrangle also are thicker than those developed on clasts in nearby late Pleistocene tills. Pedogenic soils formed on till in the quadrangle are thicker, more oxidized, and contain more illuvial clay than the soils on the late Pleistocene tills to the west. These relative weathering characteristics lead us to conclude that most till deposits in the quadrangle probably were deposited during the late middle Pleistocene Bull Lake glaciation (oxygen isotope stage 6), which ended about 130 ka, or during older glaciations in the middle Pleistocene. Maximum thickness of unit Qti is estimated at about 60 feet.

UNDIFFERENTIATED SURFICIAL DEPOSITS

Q **Surficial deposits, undivided (Quaternary) –** Shown only on cross sections

BEDROCK

TERTIARY SEDIMENTARY AND VOLCANIC ROCKS

Ts **Sedimentary rocks (Oligocene) –** Weakly to moderately indurated sedimentary rocks of probable Oligocene age crop out in two areas. One of these areas is along the drainage divide between the Middle Fork of the South Platte River and Fourmile Creek in sections 22, 23, and 27, T. 10 S., R. 77 W. The second area consists of a single exposure in a borrow pit on the west side of the Trout Creek valley in the SE ¼ of section 19, T. 10 S., R. 76 W. The Oligocene sedimentary rocks along the drainage divide crop out in an area about 2,000 feet wide and 6,500 feet long. These deposits, along with an underlying thick tuff (fig. 7), were deposited in a paleovalley herein named the Fairplay paleovalley.

The basal strata in the Oligocene sedimentary rocks are well exposed in gullies above the tuff. They consist chiefly of red-brown mudstones with lenses of matrix-supported and clast-supported pebble conglomerate and thin beds of light- to medium-gray sandstone and rare thin tuffaceous beds. The mudstone beds are typically 1 to 15 feet thick, conglomerate beds attain a maximum thickness of about 5 feet, sandstone beds are generally at most 1 to 2 feet thick, and tuffaceous beds are less than 1 foot thick. Conglomerate clasts in the basal part of the unit are chiefly red-brown mudstone, fine-grained red-brown sandstone, and light- to medium-gray, fine- to medium-grained sandstone eroded from Upper Paleozoic formations. Clast rounding is distinctive, in that both subround and angular clasts co-exist in the same lens (fig. 8). Clasts composed of limestone, tuff, Tertiary intrusive rocks, and Precambrian metamorphic and intrusive lithologies are present but relatively sparse in the basal part of the unit.

The Oligocene sedimentary rocks also are exposed in tributary gullies and eroded banks along Fourmile Creek on the west side of the drainage divide. Because all the rocks in the paleovalley dip southwest and no faults with post-middle Tertiary movement were identified between the two areas, we assume the strata on the west side of the drainage divide are stratigraphically higher in the unit than the strata that are exposed above the tuff on the east side of the drainage divide. The strata in what we believe is the upper part of the unit consist mostly of greenish-gray or red-brown mudstone, tan sandstone, clast-supported conglomeratic sandstone and conglomerate, and a higher percentage of Tertiary intrusive rocks and Precambrian metamorphic and intrusive rocks that often are strongly decomposed. Most clasts in the upper part of unit Ts are subrounded; the distinct bimodal clast rounding noted in the conglomerate beds in the basal part of the unit immediately above the tuff were not observed in the upper part of the unit. Cross section B-B' suggests a minimum thickness of 900 feet for the Oligocene sedimentary rocks in the Fairplay paleovalley, but this estimate assumes that no unrecognized significant faults cut them.

Brown (1940) reported fossil mollusks (*Polygyra*[?] *leidyi* and *Gonyodiscus hendersoni*) and vertebrate fossils (leptictid sp., *Palaeolagus* sp., and *Leptomeryx* sp.) in the sedimentary rocks in the Fairplay paleovalley. These fossils, along with the stratigraphic position of the sediments above a thick tuff unit, led Brown to correlate the sedimentary rocks in the Fairplay paleovalley with his Oligocene upper Antero Formation, which is exposed in the axis of the Antero syncline southeast of Antero Reservoir. However, De Voto (1964) concluded that the lithologies of the middle Tertiary sedimentary strata in the quadrangle were not sufficiently distinct to allow precise correlation of the rocks to either the upper or lower members of the Antero Formation.

A very small area on the west side of Trout Creek valley is underlain by a deposit of sedimentary rocks that are included in unit Ts (fig. 9). The lateral extent of this deposit is uncertain, as the deposits were observed only in a borrow pit and could not be traced from the pit. The light-red-brown, tan, and light-gray sediments consist of weakly indurated beds of fine-grained sandstone that may be silty, tuffaceous, or slightly pebbly (fig. 10). A veneer of colluvium that is rich in angular clasts of sandstone derived from the Dakota Sandstone blankets the strata exposed in the pit. Intriguing landforms that consist of low-relief, northeast-trending ridges and swales are associated with this deposit (fig. 11). Relief between adjacent ridges and swales ranges from about 1 to 10 feet, and the unusual landforms extend over a mile to the north-northwest and south-southeast from the pit. Small isolated areas with similar ridge-and-swale topography continue to the south edge of the quadrangle. On the basis of float associated with these landforms, shallow exposures (<1 foot deep) into the subtle ridges, and the exposure in the pit, we conclude that colluvium rich in angular clasts of sandstone underlies the ridge-and-swale landforms and that deposits of unit Ts may underlie the colluvium.

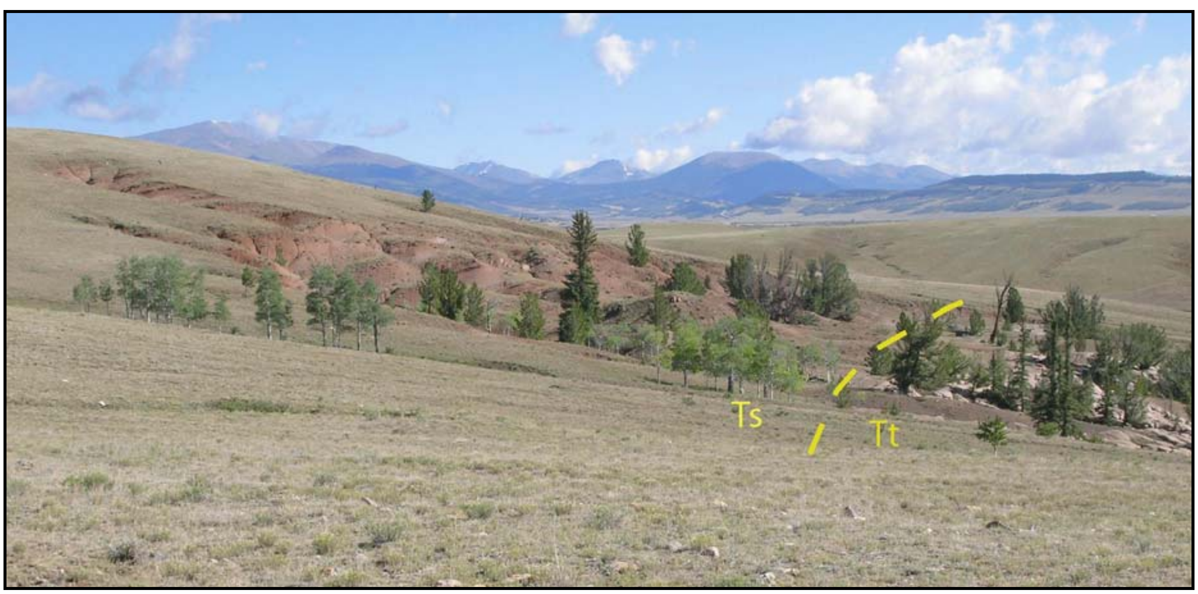

Figure 7. Overview of southwest-dipping Oligocene sedimentary rocks (Ts) and tuff (Tt) in the Fairplay paleovalley near the center of the E½ of section 22, T. 10 S., R. 77 W. The approximate contact between the overlying sedimentary rocks (on left) and underlying tuff (on right) is shown by the dashed yellow line. View is to north.

Figure 8. Closeup view of a lens of conglomerate in Oligocene sedimentary rocks (Ts). Note the angular to subangular light-colored clasts of sandstone and subround to round red-brown clasts of mudstone.

Figure 9. Oligocene sedimentary rocks exposed in a borrow pit on the west side of Trout Creek valley. View is to northwest. A veneer of colluvium, which is rich in angular clasts of sandstone, mantles the fine-grained Oligocene sediments.

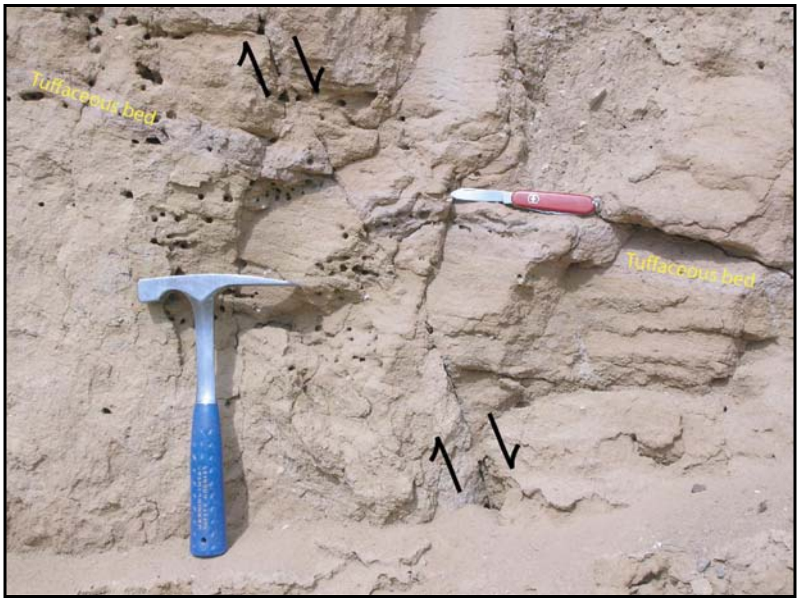

Figure 10. Close-up view of the Oligocene sedimentary rocks exposed in a borrow pit on the west side of Trout Creek valley that are shown in figure 9. View is to northwest. Note the thin bed of light-gray tuffaceous fine-grained sandstone beneath the red pocket knife, which is offset a few inches by a high-angle normal fault with down-to-north displacement.

Figure 11. Aerial photograph of Trout Creek valley. North is to the left. Note the narrow linear belt of short, northeast-trending, subparallel ridges and swales, which is outlined by the yellow arrows oriented parallel to the ridges and swales. The belt of ridge-and-swale topography trends north-northwest, parallels the strike of Mesozoic bedrock in the area, and is over 3 miles long. A yellow asterisk marks the pit in which Oligocene sedimentary rocks are exposed. (U.S. Bureau of Land Management photograph, project CO-81CC, frame 11-35B-10; flown October 6, 1982)

Tt Tuff (Oligocene) — A massive tuff fills the basal part of the Fairplay paleovalley on the drainage divide between Fourmile Creek and the Middle Fork of the South Platte River. The light-gray, crystal-lithic tuff is poorly welded and weathers to rounded knolls that are cut by shallow, steep-walled gullies (fig. 12). The tuff is clearly visible from Highway 9 near where the road crosses the Middle Fork, and it contrasts sharply with the overlying reddish-brown sediments (fig. 7). The tuff has a fine-grained matrix comprised mostly of glass shards. The angular glass shards in the matrix are poorly compacted, and some have classic bubble triple junctions. No, or very little, devitrification affects the glass shards. The matrix also includes sparse very small crystals of biotite and feldspar (possibly sanidine), very rare anorthoclase, and less than 2 percent unidentified opaque minerals.

The tuff is rich in crystals, lithic fragments, and pumice fragments. Approximately 85 to 90 percent of the crystals are broken, anhedral, single crystals of feldspar. They average about 0.5 mm in length, with a maximum length of 2 mm. Some feldspar crystals have resorption borders. Others have Carlsbad or albite twinning. A few euhedral feldspar crystals exist in the tuff matrix, but most of the euhedral feldspar crystals are within the porphyritic pumice fragments. Euhedral crystals of biotite comprise about 10 to 15 percent of the phenocryst assemblage. The biotite phenocrysts average about 0.5 mm in length, but some are as long as 1.8 mm.

Pumice fragments typically comprise 10 to 20 percent of the rock by volume, but locally they can constitute as much as about 40 percent of the rock. The pumice fragments are not collapsed, and gas-bubble cavities are intact, evidence that indicates the tuff is poorly welded. The pumice fragments are eutaxitic and glassy and have occasional euhedral crystals of biotite, sanidine, and plagioclase. Most pumice fragments observed in thin section were 1 to 2 mm in diameter, but one was 10 mm long. Pumice fragments as much as 8 inches in length were observed in outcrop (fig. 13). Under crossed polars the pumice fragments go mostly to complete extinction, an indication of very little devitrification.

Figure 12. The Oligocene tuff weathers to rounded knolls that are cut by shallow, steep-walled gullies.

Figure 13. Pumice fragments typically compose 10 to 20 percent of the tuff in unit Tt and can be as much as about 40 percent of the rock.

Angular to subangular fragments of mostly sandstone, mudstone, and equigranular and hypabyssal igneous rocks generally compose less than 1 percent of the rock, but locally they are more abundant. Evidence of significant thermal alteration was not noted in hand specimens of the xenoliths.

Chemical analyses were obtained on a pumice clast (sample E309P; Appendix A) and a whole-rock sample of the tuff (sample E266). Obvious lithic material was removed from the whole-rock sample prior to analysis. The pumice clast was 66.3 percent $Si0_2$, and the whole-rock sample was 67.4 percent $Si0_2$. Both samples plot in the dacite field of the TAS chart of Le Bas and others (1986). Faint evidence of bedding or flow foliation was noted in a few outcrops of the tuff, but for the most part it is massive with little or no internal stratification.

A sample collected from a pumice clast within unit Tt (sample E309P) was submitted to the University of Alaska Fairbanks Geochronology Laboratory for $^{40}Ar/^{39}Ar$ dating. They reported a weighted average age of 33.47 ± 0.15 Ma (see Appendices B and C).

Table 1. $^{40}Ar/^{39}Ar$ ages of igneous rocks and igneous clasts in sedimentary deposits in the Fairplay East quadrangle.

Unit	Samples dated during this study (see Appendices B & C)		Previously published ages (from Widmann and others, 2005)	
	Age	**Material dated**	**Age**	**Material dated**
Tt	33.47 ± 0.15 Ma (weighted average age of 10 phenocrysts from sample # E309P)	plagioclase from pumice clast		
Tsc	66.6 ± 0.5 Ma (sample JK099)	biotite from clast	64.08 ± 0.11 Ma	biotite from clast
	66.4 ± Ma (sample JK083)	biotite from clast		
TKsr	68.8 ± 0.8 Ma (sample JK119)	hornblende from flow	66.94 ± 0.25 Ma (minimum age)	hornblende from flow

Prior workers correlated unit Tt with either the Antero Formation (De Voto, 1964; Bryant and others, 1981b) or the lower member of the Antero Formation (Brown, 1940), which suggests unit Tt may be the Antero tuff. However, unit Tt also is potentially correlative with the Badger Creek Tuff or Grizzly Peak Tuff (Shannon, 1988; Fridrich and others, 1991; McIntosh and Chapin, 2004). The size of the pumice clasts suggests the source was proximal to the tuff deposit. The age dates on feldspar phenocrysts from a pumice clast in unit Tt are inadequate to allow us to confidently correlate unit Tt with any of the known and named ash-flow tuffs.

Unit Tt attains a maximum thickness of about 350 feet in the thalweg of the paleovalley. It pinches out to the south and north as the floor of the paleovalley rises in elevation, and is cut off to the west by the previously unrecognized Fairplay fault.

PALEOCENE AND UPPER CRETACEOUS SOUTH PARK FORMATION

Only the lower part of the Paleocene and Upper Cretaceous South Park Formation crops out in the quadrangle. It is exposed on and east of Reinecker Ridge. Strata in the lower part of the formation are subdivided in the map area into four members, three of which are informal members and one is a formal member. In descending order, the members are the (1) fine-grained sedimentary member; (2) coarse-grained conglomeratic member; (3) Reinecker Ridge Volcanic Member; and (4) lower volcaniclastic sedimentary member. Refer to the Stratigraphy chapter for a summary description of prior published work on the South Park Formation.

Tsf **Fine-grained sedimentary member (Paleocene) –** This unit underlies the low-relief strike valley on the east side of Reinecker Ridge. The fine-grained sedimentary member either forms a lens within the coarse-grained conglomeratic member (Tsc) or intertongues with it. The fine-grained sedimentary member is poorly lithified, easily eroded, and very poorly exposed. Two small exposures of the unit were observed along the southeast side of the quadrangle; bedding attitudes were measured at both locations. Only the upper part of the member is exposed at the two outcrops. In these limited exposures, the member consists of light- to medium-reddish-brown, pinkish-brown, and gray, arkosic, slightly micaceous, gritty, silty sandstone, sandy siltstone, and sparse conglomeratic sandstone. The matrix is highly calcareous and argillaceous. Sandstone beds are fine to coarse grained and poorly sorted. The fine-grained sedimentary unit is massive to faintly bedded. Bedding attitudes are difficult to confidently decipher. Sand-sized grains are predominantly angular to subangular quartz, with lesser biotite, feldspar, and lithic fragments.

Conglomeratic sandstone beds locally include rounded white clasts up to 4 inches in diameter (mostly smaller than 1 inch). The white clasts consist of white, fine-grained volcanic rock, probably devitrified tuff, and contain small feldspar crystals that appear to be partly resorbed. The matrix in the clasts is very fine grained. No glass shards were observed, but this may be due to devitrification.

Low topographic saddles within the strike valley of unit Tsf are mantled with residuum or surficial deposits composed of medium- to dark-reddish-brown, silty and sandy sediment with rare pebbles. Only sparse boulders and cobbles are present on the saddles; they probably were eroded from nearby topographically higher beds in the coarse-grained conglomeratic member.

Thickness of the fine-grained member is estimated at about 250 to 300 feet in the NE 1/4 of section 4, T. 10 S., R. 76 W. Here, the low-relief strike valley of the fine-grained member is flanked on the west by the hogback of the main Reinecker Ridge and on the east by a subsidiary hogback, both of which are underlain by the erosion-resistant conglomeratic member. To the south, the fine-grained member gradually thins, and it eventually pinches out against the coarse-grained conglomeratic member in the southwestern part of the adjacent Elkhorn quadrangle. The main hogback of Reinecker Ridge and the subsidiary hogback merge at that location.

North of section 4 the subsidiary hogback is cut off by a fault, and the eastern piedmont of Reinecker Ridge slopes gradually eastward without the topographic disruption of the subsidiary hogback. In this area, bedrock is concealed by surficial deposits, most of which are thick enough to be shown on the geologic map. We suspect that the fine-grained sedimentary member underlies the piedmont slope north of section 4 as far east as the South Park fault. If this interpretation is correct, then the fine-grained member thickens in the E ½ of section 33. Further north, in the southeast part of section 28, the piedmont slope terminates against one of the strands of the South Park fault. The fine-grained member has not been recognized north of this fault strand.

Tsc **Coarse-grained conglomeratic member (Paleocene)** — This unit underlies the crest and eastern slope of Reinecker Ridge, as well as the subsidiary ridge east of Reinecker Ridge. The unit, which is very poorly exposed, consists of clast-supported, polymictic, pebble, cobble, and boulder conglomerate locally interbedded with thin zones of sandstone and siltstone that may be partially volcaniclastic or tuffaceous. One bed of gray, biotite-bearing crystal-lithic tuff was noted in unit Tsc in a ditch on the Como quadrangle (Widmann and others, 2005), but none were observed on the Fairplay East quadrangle. The coarse-grained conglomeratic member is weakly lithified.

Because the boulders and cobbles that comprise the unit are mostly composed of hard, indurated lithologies, the unit is resistant to erosion. Reinecker Ridge is the highest hogback in the northern part of South Park, even higher than the hogback of Red Hill, which is underlain by Dakota Sandstone. Where underlain by unit Tsc, the ground surface is strewn with subangular to well-rounded pebbles, cobbles, and, boulders (fig. 14). Boulders two to five feet in diameter are common in the unit. Boulders as large as eight feet in diameter were observed on Reinecker Ridge, which indicates the member was deposited in a very high-energy environment. Subtle benches and topographic breaks are apparent on the western and eastern slopes of Reinecker Ridge. Cobbles and boulders are rare on these landforms, which suggests they are underlain by thin, lenticular beds of finer-grained clastic and/or tuffaceous strata that are interbedded with the conglomeratic beds.

Some clasts in the conglomeratic member are strongly decomposed and have thick weathering rinds, but others are little affected by weathering and are still very sound. Clast lithologies include various intermediate and felsic intrusive rocks, andesite from the Reinecker Ridge Volcanic Member (unit TKsr), red Pennsylvanian and Permian sandstones, dense andesite or basalt that is not from unit TKsr, rare hornfels and skarn derived from contact-metamorphosed Pennsylvanian and Permian rocks, rare Dakota Sandstone (Kd), and black, cherty pebbles from an undetermined formation. Intrusive rock types are the most abundant clasts, and they also tend to be the largest clasts. These clast lithologies suggest the provenance was to the west or northwest, possibly the Mosquito Range near Leadville and Alma (Wyant and Barker, 1976; De Voto, 1988). De Voto (1988) observed that the conglomerate clasts reflect the erosional unroofing of the Sawatch anticline to the west. Silicified wood is locally present but not abundant. Fragments of Proterozoic crystalline rock were not observed. Andesite clasts from the Reinecker Ridge Volcanic Member are abundant only near the base of the formation and become increasingly scarce in younger beds. The estimated maximum thickness of the coarse-grained conglomeratic member of the South Park Formation in the Fairplay East quadrangle is around 1,300 feet.

New $^{40}Ar/^{39}Ar$ dates obtained on two clasts from the coarse-grained conglomeratic member help constrain its age. Sample JK083 is a dense, very dark-gray basalt or andesite cobble from a conglomerate bed near the crest of Reinecker Ridge. Biotite from sample JK083 yielded an age of 66.4 ± 0.4 Ma (table 1 and Appendix B). The surface of the cobble was pitted, perhaps due to weathering of plagioclase phenocrysts. Sample JK099 was a boulder of medium-grained, hornblende-rich, equigranular quartz monzonite or quartz diorite that also was collected near the crest of Reinecker Ridge. Biotite in sample JK099 yielded an age of 66.6 ± 0.5 Ma (table 1 and Appendix B). An $^{40}Ar/^{39}Ar$ age of 64.08 ± 0.11 Ma was obtained from biotite in a clast of fine-grained granitic intrusive rock from unit Tsc on Reinecker Ridge in the Como quadrangle (Widmann and others, 2005). These dates indicate the conglomeratic member is younger than 64 Ma.

The provenance of the coarse-grained member of the South Park Formation is probably the Mosquito Range. The lithologies and ages of intrusive clasts in unit Tsc are similar to dated intrusions in the Mosquito Range. Bookstrom and others (1987) reported a K-Ar age of 63.6 ± 2.3 Ma (early Paleocene) on biotite from an "aplitic" rhyolite porphyry dike, one of a large swarm of such dikes that cut granodiorite porphyry in upper Buckskin Gulch upstream of the town of Alma. On the basis of the description given for the sample, it is petrologically similar to the clast of "rhyolite" or intrusive fine-grained granite from unit

Figure 14. In areas underlain by the conglomeratic member of the South Park Formation, boulders and cobbles litter the ground surface. View looking south along the crest of Reinecker Ridge.

Tsc in the Como quadrangle that yielded an $^{40}Ar/^{39}Ar$ age of 64.08 ± 0.11 Ma (Widmann and others, 2005). Granodiorites and monzonites in the Buckskin Gulch intrusive center near Alma yielded isotopic ages ranging from 71 to 41 Ma (Bookstrom, 1989). McDowell (1971) obtained a K-Ar date of 64.7 ± 1 Ma from biotite in "Laramide porphyry" in the Leadville North quadrangle.

TKsr Reinecker Ridge Volcanic Member (Paleocene and Upper Cretaceous) — The Reinecker Ridge Volcanic Member is exposed on the lower slopes on the west side of Reinecker Ridge and in the uplifted fault block east of Reinecker Ridge near the northeast corner of the quadrangle. It forms the steep western base of Reinecker Ridge in the north half of the quadrangle, where the ridge rises sharply from the flat valley floor of Trout Creek.

The member consists of a sequence of lava flows, flow breccias, volcaniclastic breccia, and agglomerate with rare, thin, intercalated, fine-grained sedimentary beds. The volcanic rocks are purplish gray, reddish brown, and greenish gray; some are mottled deep red and light gray. In TAS plots the flows and flow breccias are classified as trachyandesite, andesite, and dacite (Widmann and others, 2005). Flows and flow breccias (both the clasts and the matrix) are usually porphyritic, with small phenocrysts of plagioclase, hornblende, and locally augite in an aphanitic groundmass. Hornblende typically forms the most conspicuous phenocrysts, but some flows contain augite and little or no hornblende. A few thin, discontinuous lenses of medium-gray to green-gray and tan, locally fossiliferous,non-calcareous, fine- to very-fine-grained sandstone and siltstone are interbedded with the volcanic rocks, but these are rare and poorly exposed. A poorly preserved, unidentified conical mollusk shell impression was found in a sedimentary bed in the Como quadrangle (Widmann and others, 2005).

Beds of flow breccia are more prevalent than dense, massive unbrecciated volcanic flows in the member. The flow breccias are monolithologic, in that the matrix material is compositionally similar to the angular to subrounded breccia clasts (fig. 15). The flow breccias probably were created by auto-brecciation of andesitic flows as they cooled and differentially solidified while in motion. Some flow horizons contain an unusual texture characterized by leucocratic andesitic spheroids set in a dark-reddish-brown to dark-gray andesitic matrix. These spheroids weather to distinctive round to oval pellets averaging about 0.25 to 0.5 inch in diameter (Widmann and others, 2005). This ‘pelleted’ volcanic unit is not a breccia but is a textural variant of non-fragmental andesite flows (Widmann and others, 2005). This andesitic subunit was given the informal term ‘variolitic andesite member’ by Stark and others (1949), who recognized that the leucocratic spheroids were probably not true varioles.

Another distinctive subunit within the Reinecker Ridge Volcanic Member was called the red and white member by Stark and others (1949). This subunit is a volcanic breccia that we refer to as the red and white breccia. The subunit occurs as several relatively thin lenses within the overall package of volcanic rocks. It is more common in the higher parts of the sequence. The matrix of this fragmental rock is dark red to reddish brown and consists of tiny lithic fragments, broken crystal fragments, and abundant hematite. Clasts are whitish-gray, angular, equidimensional fragments of dacite that range from approximately 0.05 to 3.0 inches in diameter. Along with plagioclase, both biotite and hornblende phenocrysts are present in the dacitic clasts of the red and white breccias. Biotite was not observed in the trachyandesite or andesite flows or flow breccias, but it was observed in the red and white breccia. Biotite grains are commonly surrounded by a halo of fine-grained hematite. Outcrops of red and white breccia were too irregular and scattered to map separately at the scale of this project.

Figure 15. Clasts and matrix in the volcanic breccias within the Reinecker Ridge Volcanic Member of the South Park Formation have a similar andesitic composition. (outcrop is on west side of Reinecker Ridge)

The flows and flow breccias of the Reinecker Ridge Volcanic Member are usually porphyritic, with phenocrysts comprising 40 to 60 percent of the rock. They are similar to the flows and flow breccias in the Como quadrangle, which Widmann and others (2005) described as follows:

> The typically small (0.03 to 0.08 inch) phenocrysts consist of plagioclase (20 to 35 percent), hornblende (less than 1 to 35 percent), augite (0 to 25 percent), and opaque minerals (1 to 4 percent). No quartz phenocrysts were observed. The groundmass of hornblende-bearing trachyandesite flows contains potassium feldspar, but potassium feldspar is not present as phenocrysts. The groundmass is commonly hematite rich. Hematite, sometimes with chlorite, locally fills small, spheroidal vugs. Plagioclase phenocrysts are zoned and locally show evidence of very rapid crystal growth. Plagioclase is commonly partially altered to sericite. Hornblende phenocrysts are lath shaped and locally as long as 0.3 inches. In thin section, hornblende phenocrysts are usually patchy green and red-brown and are typically partly altered to chlorite and iron oxides. The rarer augite-bearing andesite flows are harder, denser, and less altered than the hornblende-bearing trachyandesites and contain little or no potassium feldspar in the groundmass.

Seven whole-rock samples collected from the Reinecker Ridge Volcanic Member in the Como quadrangle were chemically analyzed (Widmann and others, 2005). Six of the seven analyses plot in two diffuse clusters on a TAS diagram (see fig. 12 in Widmann and others, 2005). One cluster is in the trachyandesite field, and the other is along the boundary between the dacite and trachydacite fields. A sample of a dark-gray, dense, augite-bearing flow of limited areal extent plots near the center of the andesite field, outside the clusters of the more alkaline samples.

With the exception of scattered cliffy outcrops, most areas underlain by the member are mantled by angular cobble- and pebble-sized detritus. This debris everywhere obscures contacts with the adjacent or underlying volcaniclastic rocks of unit Ksvc and the Pierre Shale (unit Kp). Nowhere was the contact with these older formations observed. On the basis of the few outcrops where volcanic layering is clearly discernible and measurable, the volcanic rocks underlying Reinecker Ridge dip on average 28° to the east and northeast in the quadrangle. Local variations may reflect the influence of paleotopography during extrusion and deposition of the flows and breccias or differential tectonic tilting subsequent to emplacement. Volcanic flow layering in the isolated, fault-bounded hill east of Reinecker Ridge is steeper.

We obtained a new Ar $^{40}Ar/^{39}Ar$ age of 68.8 ± 0.8 Ma from fresh hornblende in sample JK119, a light-brownish-gray porphyritic andesitic flow with prominent hornblende phenocrysts (table 1 and Appendix B). The sample was collected from a flow exposed in a small prospect adit in the SW ¼ of section 5, T. 10 S., R. 76 W. on the lower west side of Reinecker Ridge. A minimum $^{40}Ar/^{39}Ar$ age of 66.94 ± 0.25 Ma was obtained from hornblende in the lowest exposed flow of trachyandesite porphyry in the southern part of the Como quadrangle (Widmann and others, 2005). These dates indicate flows in the basal part of the member are Upper Cretaceous. Rocks in the upper part of the member probably are Paleocene.

In the Fairplay East quadrangle, the Reinecker Ridge Volcanic Member ranges in thickness from 0 to about 900 feet. To the north in the Como quadrangle, Widmann and others (2005) reported a maximum estimated thickness in excess of 1,000 feet. Within the Fairplay East quadrangle, the member gradually thins southward and pinches out in the SE ¼ of section 8, T. 10 S., R. 76 W. South of this location the unit crops out intermittently as discontinuous lens-shaped masses that probably were deposited in paleovalleys. Since the member thickens northward, the source of the volcanic rocks probably is in that direction. The Reinecker Ridge Volcanic Member conformably overlies and perhaps is interbedded with the lower volcaniclastic sedimentary member of the South Park Formation (unit Ksvs). Where unit Ksvs is absent, the Reinecker Ridge Volcanic Member unconformably overlies the Pierre Shale.

Ksvs **Lower volcaniclastic sedimentary member (Upper Cretaceous) —** This unit includes two lenses of volcaniclastic sedimentary rocks that underlie andesitic rocks of the Reinecker Ridge Volcanic Member on the lower western slopes of Reinecker Ridge. The lower volcaniclastic sedimentary member is the oldest and stratigraphically lowest member in the South Park Formation in the quadrangle. The unit consists chiefly of poorly sorted, reddish-brown to greenish-brown, medium- to coarse-grained, argillaceous, volcaniclastic sandstone that is well bedded. It is moderately well lithified and forms small outcrops. Although the top of the member is poorly exposed, it appears to intertongue with overlying thin volcanic flows or flow breccia that are included in the Reinecker Ridge Volcanic Member.

Petrographically, unit Ksvs consists of medium- to coarse-grained, angular, and broken crystal fragments and andesitic(?) lithic fragments set in a fine-grained, argillaceous, iron-oxide-rich, non-calcareous matrix. Crystal fragments consist of plagioclase, hornblende, augite, and minor quartz. No biotite was observed. This mineral assemblage, along with the absence of biotite, is similar to the phenocryst content in andesitic flows and flow breccias in the overlying Reinecker ridge Volcanic Member. The maximum thickness of the lower volcaniclastic member is 460 feet. An unconformity separates unit Ksvs from the underlying Pierre Shale. Because the lower volcaniclastic member underlies the Reinecker Ridge Volcanic member and the basal flows of that member are Upper Cretaceous, we conclude the lower volcaniclastic member also is Upper Cretaceous.

MESOZOIC SEDIMENTARY DEPOSITS

Kp **Pierre Shale (Upper Cretaceous) —** The Pierre Shale consists chiefly of medium- to dark-gray, calcareous, marine shale with relatively thin zones of brownish-gray to olive-drab sandstone. The formation underlies the broad valley floor of Trout Creek and the piedmont on the east side of Reinecker Ridge, but it is very poorly exposed and usually concealed by surficial deposits or residuum. Small windows of shale crop out in a few of the gullies and ditches in the quadrangle. The shaly beds can be bentonitic. Ledges of sandstone, perhaps equivalent to the Hygiene or Apache Creek Member, are exposed in a few areas along the east side of Trout Creek near the north edge of the mapped area. The sandstone beds are fine- to very fine-grained subarkose and are moderately well cemented. Sand grains are mostly subround quartz; minor amounts of feldspar and mafic and opaque minerals also are present. A prominent lens of microcrystalline calcite crops out in a gully on the east side of Reinecker Ridge in the SW ¼ of section 27, T. 9 S., R. 76 W. The lens is a maximum of 3 inches thick, and the calcite crystals are roughly aligned in columns oriented perpendicular to bedding. Small fragments of the calcitic material found lying on the ground surface near the lens and also in other parts of the quadrangle might be mistaken for fragments of mollusk fossils, but the in-place lens suggests formation in a discrete stratigraphic horizon that perhaps is an altered bed of bentonite (D.C. Noe, 2005, personal commun.). The Pierre Shale conformably overlies the Niobrara Formation.

About 4,300 feet of Pierre strata were penetrated by the Amoco Reinecker Ridge well (cross section A-A'). In our model, the well is nearly perpendicular to bedding, which means the preserved partial section of the Pierre is probably slightly less than 4,300 feet in the quadrangle. An unknown thickness of upper Pierre was removed when an angular unconformity was cut across it at the end of the Cretaceous prior to deposition of the South Park Formation.

In contrast, Stark and others (1949) estimated the total thickness of Pierre Shale in South Park to only range from 2,300 to 2,700 feet. In cross sections by Clement and Dolton (1970) the Pierre is depicted as being slightly over 4,000 feet thick. In nearby quadrangles Barker and Wyant (1976) and Wyant and Barker (1976) estimated the total thickness of the Pierre at about 6,000 feet. The estimates by Barker and Wyant may be close to the original thickness of the Pierre in the Fairplay East quadrangle.

Kn **Niobrara Formation (Upper Cretaceous) –** The Niobrara Formation underlies surficial deposits and residuum between the eastern base of Red Hill and Trout Creek. The formation is very poorly exposed in the quadrangle and is mapped as a distinct unit only near the northern edge of the quadrangle. To the south, in areas that lack exposure and float, the Niobrara is lumped into a unit of undivided Cretaceous rocks (unit Ku) that also includes parts of the Benton Group and Pierre Shale. In adjacent areas, two members comprise the Niobrara: the Fort Hays Limestone Member, a gray fossiliferous marine limestone about 40 to 100 feet thick; and the overlying Smoky Hill Shale Member, a medium- to dark-gray, yellow-weathering, calcareous, marine shale about 350 feet thick (Barker and Wyant, 1976; Wyant and Barker, 1976; Widmann and others, 2005). Two very small exposures of the Niobrara were found during the project. One exposure near a spring in the NE ¼ of section 36, T. 9 S., R. 77 W. contains a few thin beds of limestone that resemble the Fort Hays Limestone Member. A short distance east, yellow-brown weathered calcareous shale of the Smoky Hill Shale Member is exposed in a borrow ditch along a county road that is not shown on the base map. The Niobrara Formation disconformably overlies the Benton Group.

Kb **Benton Group (Upper Cretaceous) –** The Benton Group underlies surficial deposits and residuum on the steep eastern slope of Red Hill. The unit is very poorly exposed; it was observed only in three road cuts in section 1, T. 9 S., R. 77 W. In adjacent areas three formations constitute the group (Barker and Wyant, 1976; Wyant and Barker, 1976). In ascending order these formations are the Graneros Shale, Greenhorn Limestone, and Carlile Shale. The Graneros Shale is a dark-gray shale about 300 feet thick; the Greenhorn Limestone includes gray shaly limestone and brown fetid calcareous sandstone with globigerinid foraminifers; and the Carlile Shale is chiefly black shale that is capped by a brown, fossiliferous, fetid, calcareous sandstone called the Juana Lopez Member (Barker and Wyant, 1976; Wyant and Barker, 1976). Barker and Wyant (1976) and Wyant and Barker (1976) reported a total thickness of about 600 feet for the Benton Group, with the Graneros Shale being about 300 feet thick and a combined thickness of about 300 feet for the Greenhorn and Carlile. Widmann and others (2005) described a total thickness of only 250 feet for the entire group. The Benton Group conformably overlies the Dakota Sandstone.

Ku **Pierre Shale, Niobrara Formation, and Benton Group, undivided (Upper Cretaceous) –** Cretaceous strata beneath the valley floor on the west side of Trout Creek are mostly concealed by a thin mantle of surficial deposits. Identification of individual bedrock formations or the contacts between them is not feasible in this area, yet the mantle of surficial deposits is not thick enough to warrant mapping the area as a surficial unit. Therefore, this area is mapped as undivided Cretaceous rocks. Most areas mapped as unit Ku probably are underlain by the Niobrara Formation, but the upper part of the Benton Group and the basal part of the Pierre Shale also may be present.

Kd **Dakota Sandstone (Lower Cretaceous) —** Good exposures of the Dakota Sandstone appear sporadically along the crest of Red Hill, which is a hogback ridge of hard, well-indurated rocks in the formation. Road cuts through the ridge crest reveal excellent exposures of some Dakota strata (fig. 16). The formation consists mostly of tan or light-gray, coarse- to fine-grained quartzose sandstone, sedimentary quartzite, conglomeratic sandstone, and conglomerate, all of which typically weather yellow brown. Sandstone beds are moderately well sorted, and cross-bedding is common. Conglomeratic lenses are prevalent near the base of the unit. They contain subround to round pebbles and granules of chert or quartz; some lenses are arkosic, and angular ripup clasts from the underlying Morrison Formation are locally present. Thin beds of light- to dark-gray, greenish-gray, and light-brown shale occur in the unit, most commonly in the middle part. At the ground surface the estimated thickness of the Dakota ranges from about 200 to 250 feet; the Petroleum Information scout card for the Amoco Reinecker Ridge well reports a thickness of only 177 feet. The Dakota Sandstone disconformably overlies the Morrison Formation.

Figure 16. Road cut exposure of a sandstone bed in the Dakota Sandstone along the crest of Red Hill. Note the natural outcrop of the bed on the right (west) side of the road cut and the rapidly thickening mantle of colluvium rich in clasts of Dakota Sandstone on the left (east) side. Rock hammer at base of exposure provides scale.

Jm **Morrison Formation (Upper Jurassic) —** The Morrison Formation underlies the upper reaches of the hillslope on the west side of Red Hill, but it is very poorly exposed because it is less resistant to erosion than the overlying Dakota Sandstone and underlying Garo Sandstone. The only outcrops discovered during the project were thin, discontinuous ledges of gray limestone and sandstone, the largest of which was about 1 foot thick and 8 feet long. In nearby areas the formation is described as chiefly green, red, and gray, commonly bentonitic claystone and interlayered fine- to medium-grained sandstone, siltstone, and limestone that is a total of 200 to 350 feet thick (Stark and others, 1949; Barker and Wyant, 1976; Widmann and others, 2005). The Morrison Formation disconformably overlies the Garo Formation.

PALEOZOIC SEDIMENTARY ROCKS

Pg **Garo Sandstone (Permian)** — Good outcrops of the Garo Sandstone form cliffs adjacent to the Middle Fork of the South Platte River in section 13, T. 10 S., R. 77 W., an area where the river has cut into the base of the hill (fig. 17). Strata in these outcrops are chiefly light-pink to red or light-gray, fine- to medium-grained, quartz-rich, generally calcareous sandstone. Most beds are moderately well sorted; some have bimodal sizes of sand grains. Quartz grains are generally round or subround; coarser grains are sometimes frosted. Large-scale cross-bedding is locally prominent, as are small round nodules of uncertain origin. The Garo Sandstone is generally less micaceous and more calcareous than the Maroon Formation.

Age of the Garo Sandstone is uncertain. Some workers assigned it to the Permian, while others correlate it with the Jurassic Entrada Sandstone. Refer to the Stratigraphy chapter for a summary of these discussions. We utilize the age assignment and stratigraphic relationships of De Voto (1965a, 1965b), who prefers a Permian age for the Garo Sandstone and believes the Garo conformably overlies the Maroon Formation and was deposited synchronously with the uppermost shales of the Maroon in adjacent areas. A complete section of the Garo Sandstone was not exposed in the quadrangle, therefore the thickness is not precisely known. De Voto (1965a) reported a thickness of 62 feet in a measured a section about 4 miles south of the quadrangle, but the formation rapidly thickens to 217 feet about one-half mile further south. The thickness at Red Hill Pass about one mile north of the quadrangle is approximately 225 feet (Widmann and others, 2005).

Figure 17. Prominent cliffs of Garo Sandstone along the east bank of the Middle Fork of the South Platte River north of where Highway 9 crosses the river. Note large scale cross-bedding in part of the outcrop.

PIPm **Maroon Formation (Lower Permian to Upper and Middle Pennsylvanian)** —The Maroon Formation underlies much of the western one-third of the quadrangle, but it is concealed by surficial deposits in most of this area. The Maroon Formation is mapped as a separate unit only in the northwest corner of the quadrangle between Crooked Creek and the Middle Fork of the

South Platte River and on the west side of Red Hill where only the uppermost part of the formation crops out.

Red to orange-red laminated siltstone is the dominant lithology in the Maroon Formation. Several beds of conglomerate, sandstone, conglomeratic sandstone, limestone, and shale exist in the lower half of the formation. The limestone and sandstone beds become less prevalent higher in the formation. Minor amounts of sandstone but no limestone were observed in the rare outcrops that expose the uppermost Maroon strata on the west side of Red Hill.

Siltstone beds in the Maroon Formation crop out very poorly; they weather to valleys and gentle slopes that are covered by surficial deposits or red silty residuum. The conglomerate and sandstone are pink to light red, micaceous, and arkosic, and typically are in interbedded lenses about 5 to 40 feet thick. The conglomerate beds and some of the sandstone beds are more resistant to erosion than the siltstone and form small ridges and isolated hills. Most conglomerate clasts are composed of quartz, feldspar, and granitic intrusive lithologies. Most sandstones in the lower half of the formation are coarse- to very coarse-grained; conglomeratic sandstones contain pebbles up to 2 inches in diameter. Conglomerate beds contain clasts up to 5 inches in diameter. Trough and planar cross-bedding are the most common sedimentary structures. Red shale and beds of laminated fine sandstone are also present but not common.

Gray limestone beds that are about 6 inches to 5 feet thick occur sporadically throughout the lower half of the Maroon Formation and are denoted on the map by dark blue lines. They are typically separated by 100 to 350 feet of siliciclastic rocks. Most of these limestone beds are micritic, but fossil hash, intraclasts, stromatolites, and detrital sand were also observed in places. The limestone beds are somewhat resistant to erosion; in places they form small ridges. Limestone also occurs as nodules in siltstone or shale.

In addition to individual limestone beds, three limestone-rich zones up to 60 feet in thickness were identified in the lower half of the Maroon Formation. Two of the zones can be traced for several miles, though individual beds within the zones have limited lateral extent. We designate these two zones as informal members, the Fairplay and Silverheels limestone members. Another 50-feet-thick zone containing at least three limestone beds also is present about 2,400 feet above the base of the formation. Limestone beds within these zones tend to have a greater variety of constituents (fossil fragments, intraclasts, stromatolites, bioturbation, etc.) than the other Maroon limestone beds and are more likely to contain calcareous algae. The lateral extent of the limestone members to the south of the quadrangle is currently not known.

The Maroon Formation is about 5,300 to 5,600 feet thick in the northern part of the quadrangle. Thickness in the southern part is not known because the lower contact is poorly exposed and numerous faults disrupt the section. The Maroon Formation is thought to conformably overlie the Minturn Formation (Tweto, 1949; Tweto and Lovering, 1977).

FL **Fairplay limestone member** – The Fairplay limestone member is denoted on the geologic map and cross sections by brackets labeled “FL”. The member spans two limestone beds shown on the map, and it consists of interbedded gray micritic limestone, red siltstone, and minor pink coarse sandstone in a zone about 40 to 60 feet thick. Stromatolites, fossil hash, bioturbation, and calcareous algae were observed in the limestone beds, which are about 0.5 to 4 feet thick. The Fairplay limestone member lies about 1,900 feet above the base of the Maroon Formation.

SL **Silverheels limestone member** — A single limestone line labeled “SL” on the geologic map marks the position of the informal Silver Heels limestone member. This member consists of interbedded gray micritic limestone, red siltstone, and pink coarse sandstone in a zone about 10 to 30 feet thick. The limestone beds, which contain calcareous algae, fossil hash, intraclasts, bioturbation, and arkosic sand grains, are less than 1 foot to about 5 feet thick. The Silverheels limestone member lies about 1,500 feet above the base of the Maroon Formation and can be traced northward onto the slopes of Mount Silverheels.

PPgm **Garo Sandstone and Maroon Formation, undivided (Permian to Middle Pennsylvanian)** — This undivided unit is used in the south-central part of the quadrangle where poor exposures prevent identification of the contact between the Garo Sandstone and Maroon Formation.

Pm **Minturn Formation (Middle Pennsylvanian)** — The upper part of the Minturn Formation underlies the western part of the quadrangle. An estimated 600 feet of strata in the upper part of the formation are present in the northwestern part of the quadrangle in the area where the contact with the Maroon Formation is identified. To the south, the Maroon and Minturn Formations are combined into a single unit because the contact between them is poorly exposed. The Minturn strata consist of interbedded siltstone, sandstone, and minor limestone. The siltstone is poorly exposed. It tends to weather to valleys and gentle slopes covered by surficial deposits or red silty residuum. Coarse sandstone occurs in tabular to lens-shaped deposits about 10 feet thick. It is light-pink to red in color, arkosic, and micaceous. Quartz, feldspar, and granite clasts are common in the gravel-size fraction. Subround and round clasts up to an inch in diameter were observed. Bedding is massive, planar, planar cross-bedded, and/or trough cross-bedded. Beds of laminated fine sandstone are locally present.

Limestone occurs in beds up to 5 feet thick and as nodules in siltstone. Mappable Minturn limestone beds are shown on the geologic map by light-colored lines. Many limestones are gray and micritic, although some are recrystallized to a coarser texture and are pinkish or reddish. Calcareous algae and fossil hash were observed. Though individual beds of limestone have limited lateral extent, limestone-rich zones up to 150 feet thick can be traced north at least as far as the Continental Divide. The uppermost of these, the Jacque Mountain Limestone Member, marks the top of the Minturn Formation.

The exact thickness of the Minturn Formation cannot be determined in the Fairplay area. The base of the formation is not exposed in the quadrangle, and the London fault disrupts the lower part of the Minturn section where exposed in the Fairplay West quadrangle (Widmann and others, 2006). In areas to the north the formation is at least 6,000 feet thick (Widmann and others, 2005; Tweto, 1949). In the Fairplay West quadrangle the Minturn Formation is underlain by either the Belden Formation or Leadville Limestone. The Leadville/Minturn contact is disconformable; the Belden/Minturn contact is gradational and conformable (Brill, 1944; Widmann and others, 2006).

The Jacque Mountain Limestone Member consists of red, laminated siltstone with several 1- to 5-feet-thick beds of gray, micritic limestone at the top of the Minturn Formation. Although the limestones are commonly recrystallized, ghosts of calcareous algae and fossil hash were observed. Large cephalopods occur rarely in these limestones, and one was observed approximately one mile north of the quadrangle. Ooids were not observed in these beds in the Fairplay East quadrangle, but they are present to the north in the Como and Breckenridge quadrangles. In the northern part of the Fairplay East quadrangle the Jacque Mountain Member is about 150 feet thick. The uppermost limestone bed in the Jacque Mountain Member is labeled on plate 1, but the basal limestone bed is typically concealed and therefore not labeled on the map.

The Jacque Mountain Limestone Member is present in the SE ¼ of section 21, T. 9 S., R. 77 W. near the northwest corner of the quadrangle. Here, mapped limestone beds coincide with the top and bottom of the member; another mapped limestone bed is in the middle part of the member. In the next outcrop to the south, in the SE ¼ of section 28, the upper and middle limestone beds in the Jacque Mountain Limestone Member are recognized and mapped, but the basal limestone member was not found. Further south, in the SE ¼ of section 4, T. 10 S., R. 77 W., the basal limestone of the Jacque Mountain Limestone Member was identified and mapped, but the upper limestone bed was observed only near the county road and could not be traced from that exposure. In the NE ¼ of section 15 the basal limestone bed was again identified and mapped, but the limestone bed at the top of the member was not.

PIPmm Maroon and Minturn Formations, undivided (Lower Permian to Middle Pennsylvanian) – This undivided unit is used in the west-central and southwest parts of the quadrangle where poor exposures and numerous faults prevent identification of the contact between the Maroon and Minturn Formations. The approximate position of the contact is constrained by the white lines used for the Minturn limestone beds and the dark blue lines used for the Maroon limestone beds.

STRATIGRAPHY

The oldest rocks in the Fairplay East quadrangle are the Minturn and Maroon Formations, which are Pennsylvanian and Permian in age. They underlie much of the western part of the quadrangle but usually are concealed by surficial deposits. The age of the Middle Pennsylvanian Minturn Formation is fairly well constrained by fossils. The Maroon Formation is generally considered to be Early Permian to Middle Pennsylvanian, but definitive age control is lacking.

The Minturn and Maroon Formations are composed of a thick succession of varied sedimentary rock types such as conglomerate, sandstone, siltstone, shale, and limestone, and show abrupt changes laterally and vertically. They were originally deposited as sediments on alluvial plains and in shallow tropical seas of the Central Colorado Trough (Tillman, 1971; Walker, 1972; De Voto, 1980). This trough was surrounded by the actively rising Ancestral Rocky Mountains. As the ancient mountains rose, arkosic sediment was eroded from the uplifts and carried into the trough (Mallory, 1972). Paleocurrent and grain-size measurements made in sandstone and conglomerate between Hoosier Pass and Fairplay show that sediments in the Fairplay area came from the north and northeast, possibly from the area around Breckenridge. The Late Paleozoic Era was a time of frequent sea-level changes, which also contributed to the lithologic variation in rocks of this age in many parts of the world, including Colorado (Ross, 1985; Heckel, 1986). The lithologic variation causes difficulty in dividing the succession into easily recognizable formations. Several different schemes have been used in the past. Wallace and others (2003) and Widmann and others (2004a, 2005) summarize the schemes, which generally fall into two categories.

Early workers such as Emmons (1889), Singewald (1942), and Koschmann and Wells (1946) realized that marine horizons with thin limestone beds were traceable over distances of several miles, and they used these beds to divide the stratigraphic section into intervals or formations. Tweto (1949) picked the top of the Jacque Mountain Limestone Member as the boundary between the Minturn and Maroon Formations. Other workers (e.g. De Voto, 1965a, b; Taranik, 1974) used a color change from dominantly gray rocks to dominantly red ones as the contact between these formations. Although the color change has the advantage of being easy to see and map, it changes position in the section by hundreds or even thousands of feet on a regional scale (Schenk, 1989). The marine horizons are more difficult to find and trace in the field but have the advantage of maintaining the same stratigraphic position in the section.

To facilitate regional-scale mapping of the Upper Paleozoic rocks in central Colorado, a correlation project was undertaken in which an attempt was made to trace the Robinson, Elk Ridge, White Quail, and Jacque Mountain limestone members of the Minturn Formation from their type areas in the Copper Mountain quadrangle to the Fairplay area. In the Breckenridge, Alma, Como, and Fairplay East quadrangles, an approximately 150-feet-thick interval of interbedded limestone and siltstone was identified about 6,000 feet above the top of the Leadville Limestone, which is at the same stratigraphic position as the Jacque Mountain Limestone Member in the Copper Mountain quadrangle. At some localities the limestone beds exhibit the distinctive features of the Jacque Mountain Limestone, such as ooids and large cephalopods. At other localities the limestones change facies and show other features such as phylloid algae, algal laminations, and intraclasts. However, they are still identifiable by their position in the section and the occurrence of several limestone beds in an interval about 150 feet thick. We correlate this interval with the Jacque Mountain Limestone Member.

Though individual limestone beds do not continue for long distances, the entire Jacque Mountain Limestone Member was traced on the ground for a distance of at least 5 miles in the Fairplay East, Como, and Alma quadrangles. Igneous intrusions and erosional removal prevented continued tracing of the interval further north, but a zone of thin limestone beds occurs at the same stratigraphic horizon in the Breckenridge quadrangle; these contain ooids and large cephalopods and were identified as the Jacque Mountain Limestone Member by Singewald (1942), Brill (1952), Taranik (1974), and Tweto and Lovering (1977). For these reasons, we use the highest limestone bed in the Jacque Mountain Limestone Member as the contact between the Minturn and Maroon Formations in the quadrangle. Unfortunately, the Jacque Mountain Limestone is presently recognized only in the northwest part of the quadrangle. To the south, poor exposure and complex faulting preclude precise identification of the contact. The Minturn and Maroon Formations are mapped as a single undivided unit in that area.

Equivalents of the Robinson and White Quail Limestone Members were also found to extend into the Fairplay area. They crop out in the Fairplay West quadrangle (Widmann and others, 2006) and exist in the subsurface of the Fairplay East quadrangle (see cross section A-A’). In the Fairplay East and Como quadrangles additional laterally persistent intervals of multiple limestone beds occur in the Maroon Formation. Two of these are herein informally named the Fairplay and Silverheels limestone members and are identified on the geologic map. The Fairplay limestone member is about 1,900 feet above the base of the Maroon Formation, and the Silverheels limestone member is about 1,500 feet above the base. The positions of other minor limestone beds in the Minturn and Maroon Formations are also shown on the geologic map. In general the number of limestone beds increases toward the south, and they appear higher and higher in the section, although not in the uppermost Maroon strata that are exposed on the west side of Red Hill.

The siliciclastic rocks of the Minturn and Maroon Formations in the area from Hoosier Pass to Fairplay are generally similar to those in the Minturn and Pando areas, but the proportions of various rock types are quite different. At Minturn and Pando the Minturn and Maroon

Formations are dominated by conglomerate and sandstone (Tweto, 1949; Tweto and Lovering, 1977), whereas from Hoosier Pass to Fairplay these formations are predominantly siltstone. Conglomerate and sandstone are present but in lesser quantities that progressively decrease to the south. Because siltstone is less resistant to erosion than conglomerate or sandstone, areas underlain by the Minturn and Maroon Formations in the quadrangle tend to be topographically low. The Minturn Formation includes a thick evaporite sequence south of the quadrangle (e.g. Brill, 1952; De Voto, 1965, 1971). Although no evaporite was observed in outcrop within the quadrangle, the presence of sinkholes attributed to evaporite karst in the southern parts of the Fairplay East and Fairplay West quadrangles (Shawe and others, 1995) suggests evaporite may also be present within the Minturn Formation in the southern part of the mapped area.

The Garo Sandstone lies above the Minturn and Maroon formations in the quadrangle. It crops out on the western side of Red Hill. The age of the Garo Sandstone and its relationships to underlying formations has been debated in the literature for decades. Most workers initially considered the Garo to be Jurassic in age and probably correlative with the Entrada Sandstone (e.g. Miller, 1937; Stark and others, 1949; Ettinger, 1964). Stark and others (1949) reported unconformities both above and below the Garo Sandstone, which supported that age assignment. De Voto (1965a, b), however, described evidence that the lower part of the Garo Formation interfingered with the uppermost part of the Maroon Formation. He also noted that a sandy dolomitic limestone with a Permian alga previously described by Johnson (1935) lies about 80 feet stratigraphically below the base of the Garo and that the thickness changes in the Garo are mostly a result of facies changes. On the basis of this evidence, De Voto (1965a, b) concluded that the Garo Sandstone is Permian in age, is laterally equivalent to the Maroon, and is overlain by an unconformity but does not rest on an unconformity.

Lozano (1965) did not find the evidence described by De Voto (1965a, b) but continued to use a Permian age for the formation. Most recent studies have returned to the earlier interpretations. Bryant and others (1981b) mapped the unit as the Jurassic Entrada Sandstone. Hembre and TerBest (1997) also suggested the unit was probably correlative with the Entrada, as did Steyaert and Wandrey (1997), who said the Garo unconformably overlies the Maroon Formation, but neither described much evidence to support their positions. Until the authors have an opportunity to study the pertinent outcrops near Badger Springs southeast of the quadrangle, we will use the age assignment and stratigraphic relationships of De Voto (1965a, b), who to date appears to have done the most thorough studies of the formation.

No Triassic strata exist in the quadrangle. The closest Triassic rocks crop out near Boreas Pass several miles to the north (Poole and Stewart, 1964). Either the Triassic strata were never deposited in the mapped area, or they were removed by pre-Late Jurassic erosion. The Upper Jurassic Morrison Formation disconformably overlies the Garo Sandstone, and a thick sequence of Lower and Upper Cretaceous sedimentary rocks disconformably overlies the Morrison. The Dakota Sandstone constitutes the basal part of the Cretaceous section and signals the beginning of the transgression of the Western Interior Seaway into the region during the Early Cretaceous. A thick, conformable sequence of Upper Cretaceous marine rocks were deposited over the Dakota in the region. In ascending order, this sequence includes the Benton Group, Niobrara Formation, and Pierre Shale. Except for the Dakota Sandstone, the Mesozoic sedimentary rocks are very poorly exposed in the quadrangle. Because of the poor exposures, many areas underlain by the Benton, Niobrara, and Pierre are combined into a single unit.

East of the quadrangle, and east of the South Park fault, the Upper Cretaceous Fox Hills Sandstone and Laramie Formation conformably overlie the Pierre Shale. Within the quadrangle, however, the Paleocene and Upper Cretaceous South Park Formation unconformably rest on the Pierre. The Fox Hills and Laramie must have been removed by erosion west of the South Park fault before the basal part of the South Park Formation was deposited at the end of the Cretaceous.

Only the lower part of the South Park Formation crops out in the quadrangle. We subdivide these rocks into four members, three informal and one formal member. In ascending order, the members are (1) an Upper Cretaceous lower volcaniclastic sedimentary member; (2) the Reinecker Ridge Volcanic Member; (3) a coarse-grained conglomeratic member; and (4) a fine-grained sedimentary member. The South Park Formation rests unconformably on the middle part of the Pierre Shale (Sawatsky, 1967) in the Fairplay East quadrangle; elsewhere in South Park it unconformably overlies the Laramie Formation, the Fox Hills Sandstone, Permian rocks, and Proterozoic basement rocks (Stark, 1949, p. 59). The upper part of the South Park Formation, which Chapin and Cather (1983) suspect is Eocene, is not present in the quadrangle.

Washburne (1910) originally included all the Lower Tertiary rocks in South Park within the Shoshone Formation, but that nomenclature was later abandoned. Johnson (1935, 1937) studied these rocks and correlated them with the Denver Formation on the basis of fossil leaf impressions. Stark and others (1949), Ettinger (1964), De Voto (1965b), and others continued the use of that name. Paleontological age control is poor, however. No fossil pollen data and no vertebrate fossils have been described from the South Park Formation (Raynolds, 2003). Furthermore, the Denver Formation was deposited in the Denver basin during the Laramide orogeny, and that basin was physically separated from the South Park basin by the Laramide Front Range uplift.

Sawatsky (1967) designated all of the lower Tertiary rocks that previously were called the Denver Formation, including the andesitic volcanic rocks on Reinecker Ridge, as the South Park Formation, a nomenclature that has persisted to the present. Wyant and Barker (1976) applied the formal name Reinecker Ridge Volcanic Member to andesitic volcanic rocks and conglomeratic sediments in the lower part of the South Park Formation. They included coarse conglomeratic strata, which in the Fairplay East and Como quadrangles form the crest of Reinecker Ridge, in their Volcanic Member. Because the conglomeratic strata are lithologically and genetically distinct from the underlying andesitic flows and breccias, we follow the approach of Bryant and others (1981b) and map the units separately as the formal Reinecker Ridge Volcanic Member (unit TKrs) and the informal coarse-grained conglomeratic member (unit Tsc).

The newly recognized lower volcaniclastic sedimentary member of the South Park Formation (Kvsr) consists of sedimentary and pyroclastic detritus locally deposited in paleovalleys cut into the Pierre Shale. The volcanic debris was probably generated during the initial pulse of early Laramide volcanic activity. The angularity of crystal fragments and volcanic lithic fragments in the volcaniclastic sandstones are indicative of short transport distances, therefore the volcanic field was near modern Reinecker Ridge.

As volcanism continued, the area was covered by the thick sequence of flows and flow breccias that comprise the Reinecker Ridge Volcanic Member. A basal flow in the Reinecker Ridge Volcanic Member in the quadrangle yielded an $^{40}Ar/^{39}Ar$ age of 68.8 ± 0.8 Ma (table 1 and Appendix B). A minimum $^{40}Ar/^{39}Ar$ age of 66.94 ± 0.25 Ma was obtained on the lowest exposed volcanic flow in the Como quadrangle (Widmann and others, 2005). These dates indicate the lowest flows in the Reinecker Ridge Volcanic Member are Upper Cretaceous, not Paleocene as previously reported by Sawatsky (1967). No dates are available for flows at the top of the Reinecker Ridge Volcanic Member; they may be early Paleocene in age.

Stark and others (1949) originally assigned the name Basin Ridge Group to the rocks now referred to as the Reinecker Ridge Volcanic Member of the South Park Formation. They subdivided the Basin Ridge Group into three members, including a rhyolite unit that overlies the andesitic rocks on Reinecker Ridge. Our mapping in this quadrangle and in the Como quadrangle (Widmann and others, 2005) does not confirm the presence of this rhyolite unit, nor did mapping by Sawatsky (1967). Rhyolite flows are not exposed in outcrop on Reinecker Ridge in either of the quadrangles, but abundant clasts of equigranular fine-grained granitic rock with sparse phenocrysts of biotite, probably hypabyssal granite, exist within the coarse-grained conglomeratic member of the South Park Formation (unit Tsc), which overlies the Reinecker Ridge Volcanic Member. One of these clasts in the coarse-grained conglomerate member in the Como quadrangle yielded an $^{40}Ar/^{39}Ar$ age of 64.08 ± 0.11 Ma (Widmann and others, 2005). This early Paleocene age provides a maximum age for the coarse-grained conglomeratic member at that location; the bed from which the clast was collected, as well as overlying beds in the coarse-grained conglomeratic member, must be younger than 64 Ma.

Two new $^{40}Ar/^{39}Ar$ dates obtained on clasts in the coarse-grained conglomeratic member in the Fairplay East quadrangle provide additional age constraints on the member. A dense, very dark-gray basaltic or andesitic clast collected from the top of Reinecker Ridge yielded an age of 66.4 ± 0.4 Ma, and a date of 66.6 ± 0.5 Ma was obtained from a medium-grained granitic clast, also from the top of Reinecker Ridge (table 1 and Appendix B). These dates lead us to conclude that the coarse-grained conglomeratic member probably is Paleocene in age, but it could be younger.

The ages of the dated intrusive clasts in the coarse-grained conglomeratic member correspond fairly well with dates obtained from petrographically similar Laramide-age intrusions in the Alma and Leadville areas in the Mosquito Range (Bookstrom, 1987; Bookstrom and others, 1989; McDowell, 1971). We postulate that a major source area for clasts in the coarse-grained conglomeratic member of the lower South Park Formation in the Reinecker Ridge area is the Mosquito Range, west and northwest of the Fairplay East quadrangle. K-Ar ages of the Tertiary intrusive rocks in the South Park-Breckenridge region are generally younger, ranging from about 35 to 51 Ma

The fine-grained sedimentary member of the South Park Formation is interbedded with the coarse-grained conglomeratic member. Prior to this project, the fine-grained member had not been mapped separately. The member is less resistant to erosion than the coarse-grained conglomeratic member and underlies a north-south-trending, low-relief strike valley on the east side of Reinecker Ridge. The low-relief strike valley is flanked on the west by the topographically prominent hogback of Reinecker Ridge and on the east by a subsidiary hogback, both of which are underlain by the conglomeratic member. Some of the east-flowing ephemeral streams that drain the eastern side of the Reinecker Ridge hogback make right-angle bends as they enter the low strike valley underlain by the fine-grained sedimentary member. These ephemeral streams make another sharp bend as they turn into water gaps cut through the subsidiary hogback held up by erosion-resistant beds in the coarse-grained conglomeratic member that stratigraphically overlie the fine-grained member.

The fine-grained member thins southward across the quadrangle and pinches out against the coarse-grained member a short distance off the quadrangle in the adjacent Elkhorn quadrangle. In the northern part of the quadrangle poor exposures and faulting obfuscate stratigraphic relationships between the fine-grained member and conglomeratic member. The fine-grained member either is a lens within the Paleocene coarse-grained member or intertongues with it. Because of these factors, a Paleocene age is assigned to the fine-grained member.

Two deposits of middle Tertiary rocks are preserved in a paleovalley cut into Upper Paleozoic rocks. This paleovalley, which we call the Fairplay paleovalley, is exposed on the drainage divide between Fourmile Creek and the Middle Fork of the South Platte River. A thick, massive, poorly welded, crystal-lithic tuff fills the bottom of the paleovalley (figs. 7 and 12). The floor of the paleovalley can be traced in outcrop by following the contact between the tuff and underlying Paleozoic rocks (fig. 18). The thalweg or axis of the paleovalley crops out in a gully well below the prominent tuff outcrop. The floor of the paleovalley rapidly rises in elevation to the south of the thalweg but then remains fairly flat until the southern margin of the paleovalley is cut off by a middle Pleistocene unconformity at the base of alluvial unit four (Qa4). The northern side of the paleovalley also quickly climbs in elevation from the thalweg, but a short distance further north a modern tributary valley cuts out the tuff.

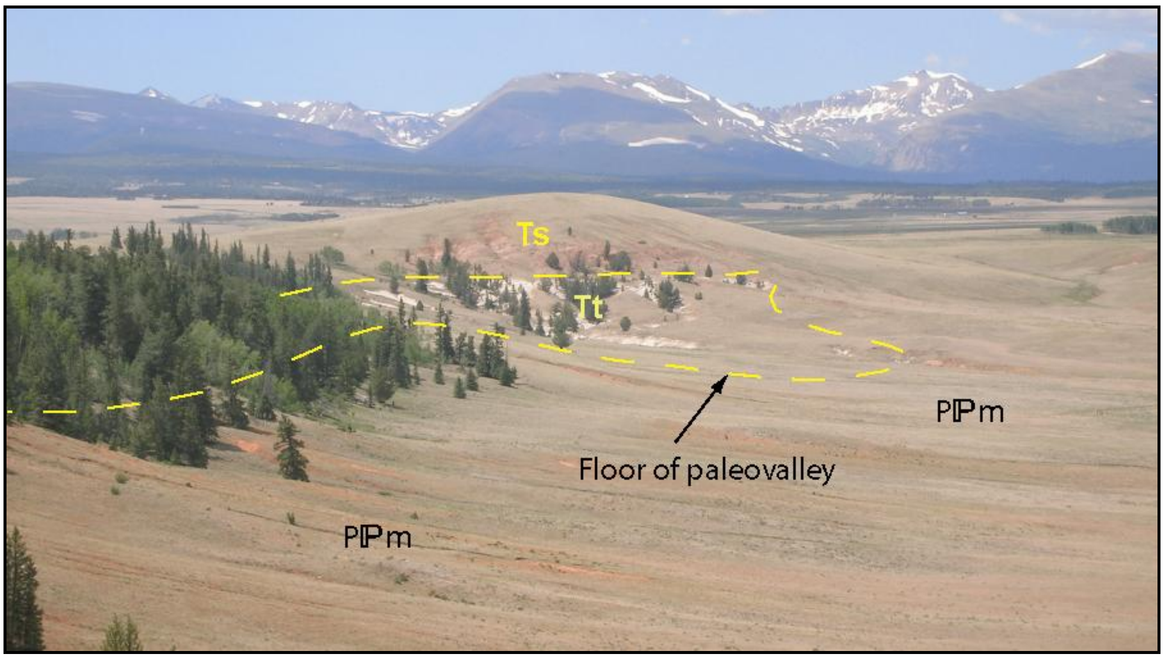

Figure 18. Photograph of the Fairplay paleovalley, looking northwest. The paleovalley was cut into east-dipping beds in the Maroon Formation (P₱m). Oligocene tuff (Tt) and sedimentary rocks (Ts) fill the paleovalley. Both the tuff and sedimentary rocks in the paleovalley dip west, opposite of the underlying east-dipping Paleozoic rocks. Paleocurrent measurements on imbricated clasts in the Oligocene sedimentary rocks indicate an eastward flow direction in the paleovalley. In this perspective the deep thalweg or axis of the paleovalley is clearly evident. To the south (left) of the thalweg, the floor of the paleovalley rapidly climbs in elevation, but then flattens and continues southward for nearly one-half mile. The tuff crops out in trees south of the thalweg. The floor of the paleovalley also rises quickly on the north side of the thalweg, and the tuff nearly pinches out completely a short distance north of the thalweg.

A thick sequence of middle Tertiary sedimentary rock (unit Ts) overlies the tuff in the paleovalley. In the basal part of unit Ts the clasts are angular to subround and consist mostly of reworked sedimentary clasts eroded from Upper Paleozoic formations. Tertiary intrusive lithologies and Precambrian metamorphic and intrusive lithologies comprise a higher percentage of the clasts in the stratigraphically higher parts of the unit. A poorly exposed remnant of middle Tertiary sedimentary rocks may mark the northern edge of the paleovalley.

Previous workers (e.g. Brown, 1940; Bryant and others, 1981b) included the tuff and overlying sedimentary rocks in the Oligocene Antero Formation. On the basis of fossils in the sedimentary rocks, Brown (1940) placed them in the upper Antero Formation; however, De Voto (1964) questioned this correlation. Since the underlying tuff yielded a weighted average $^{40}Ar/^{39}Ar$ date of 33.47 ± 0.15 Ma, the tuff and overlying sediments probably are Oligocene, but their correlation with other rocks in the region remains uncertain.

Glaciation and stream incision during the Quaternary modified the late Tertiary landscape and created the modern topography seen today. North-trending outcrops of erosionally resistant beds in the Dakota Sandstone and South Park Formation underlie the most prominent landforms in the quadrangle, Red Hill and Reinecker Ridge. During the Pleistocene, glaciers formed in the Mosquito Range to the west and flowed down the major valleys. Till deposited by the glaciers is widespread to the west in the Fairplay West quadrangle (Widmann and others, 2006). Only the distal end of the late middle Pleistocene moraines in the Middle Fork of the South Platte River extended into the Fairplay East quadrangle (unit Qti), but outwash from at least three of the glacial periods covers much of the western part of the quadrangle.

A remnant of an outwash fan from one of the middle Pleistocene glaciations (alluvial unit four) caps much of the drainage divide between Fourmile Creek and the Middle Fork of the South Platte River. The preserved geomorphology of the fan remnant suggests the outwash was carried by glacial meltwater that flowed down the Middle Fork of the South Platte River valley. The western margin of the middle Pleistocene fan deposited by the ancestral Middle Fork extended to, and probably beyond, the modern position of Fourmile Creek.

The middle Pleistocene outwash of alluvial unit four is anomalously rich in clasts of chalcedony. Exposed surfaces of clasts that lie on the ground surface have multi-colored bright patinas (fig. 5). A logical source for the chalcedony clasts is the Upper Paleozoic rocks that are subjacent to the Fairplay paleovalley. Thin lenses of chalcedony were observed in an outcrop of the Maroon Formation on the east side of the drainage divide south of the Fairplay paleovalley (fig. 19). Silica-rich solutions escaping from the tuff in the bottom of the paleovalley may have facilitated the formation of chalcedony lenses and veins. Younger outwash gravels near and downstream of the paleovalley do not contain enriched quantities of chalcedony clasts.

Sometime between the middle Pleistocene, when alluvial unit four was deposited, and the late middle Pleistocene, when alluvial unit three was deposited, streams incised through the alluvial unit four outwash fan and began to carve the modern valleys of Four Mile Creek and the Middle Fork. Some late middle Pleistocene (Bull Lake?) outwash from the Middle Fork spilled into the modern valley of Fourmile Creek, but none of the outwash of alluvial unit four carried by Fourmile Creek entered the modern valley of the Middle Fork. By the late Pleistocene the valleys were sufficiently incised, and the outwash from both streams was confined to their respective modern valleys.

Widespread remnants of thin Pleistocene piedmont deposits overlie the highly erodible Pierre Shale on both the east and west sides of Reinecker Ridge. These remnants lie at various heights above adjacent drainages, which leads us to conclude that the piedmont deposits are not all the same age.

Spectacular examples of stream piracy exist in South Park (De Voto, 1971; Widmann and others, 2005). Trout Creek, which now flows through the quadrangle, was one of the streams affected by piracy. Prior to the Holocene, upper Trout Creek, which drains an area between Mount Silverheels and Little Baldy Mountain north of the quadrangle (fig. 1), flowed into the South Branch of Park Creek and completely by-passed the Fairplay East quadrangle. However,

Figure 19. Lens of bluish-gray chalcedony in the Maroon Formation on the east side of the drainage divide between Fourmile Creek and the Middle Fork of the South Platte River, south of the Fairplay paleovalley (SW ¼ of section 25, T. 10 S. R. 77 W.).

headward incision in the highly erodible Pierre Shale strike valley between Red Hill and Reinecker Ridge eventually captured upper Trout Creek. At the point of capture in the Como quadrangle, the creek has subsequently cut about 40 to 50 feet deep through the late Pleistocene outwash that was deposited in the now-abandoned Trout Creek paleovalley. No late Pleistocene outwash is recognized in modern Trout Creek valley within the quadrangle. This evidence places the time of capture at, or shortly after, the end of the late Pleistocene Pinedale glaciation.

A thin veneer of light-brown to light-gray, calcareous silty clay locally overlies the late Pleistocene outwash of alluvial unit two in the Middle Fork valley (fig.20). Classic examples of “popcorn” textures are developed in the silty clay (fig. 20), which susggests the material is highly expansive and rich in smectitic clays. The area covered by the silty clay is delineated on the geologic map by the wavy pattern superimposed on the color/pattern used for unit Qa2. The deposit was found only on the west side of the Middle Fork valley and downstream of the Fairplay paleovalley. The veneer of calcareous silty clay may have accumulated chiefly as a precipitate formed by years of evaporation of calcium-rich ground water that was wicked up from an underlying shallow ground-water table. The bentonitic component may result from weathering and alteration of tuffaceous material that was rich in volcanic glass. The tuff potentially could have been an air-fall ash; however, it was probably deposited during the Holocene, as it overlies late Pleistocene gravel, and Holocene tephras are not known to exist anywhere in Colorado. A more likely source of the tuffaceous material is the middle Tertiary tuff in the Fairplay paleovalley. We theorize that during one or more storm events, tuffaceous material was eroded from the prominent gullies that are carved into outcrops of tuff (fig. 12), which are located upvalley from and on the same side of the valley as the silty clay. The eroded tuffaceous material was deposited on alluvial unit two as a relatively thin veneer during the

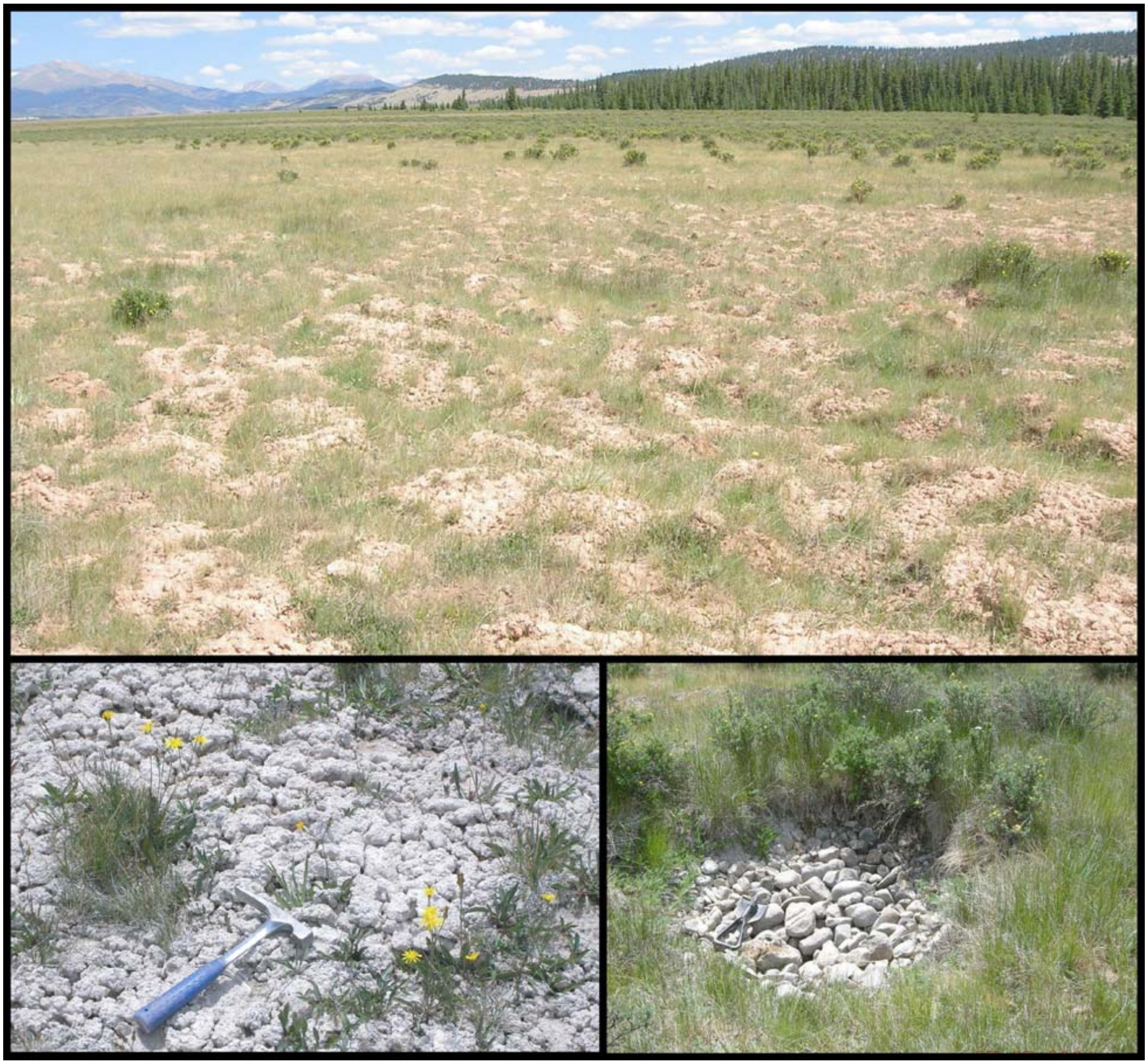

Figure 20. Light-brown, very bentonitic, calcareous silty clay overlies alluvial unit two in the Middle Fork valley downstream of the Fairplay paleovalley. Inset photograph in lower left illustrates the typical "popcorn" texture formed on the deposit, which has high shrink-swell properties. In the inset photograph in lower right, rounded cobble gravel clasts are exposed in depressions that extend through the layer of silty sediment.

Holocene and was modified as the glass weathered to smectitic clay and as calcium carbonate accumulated.

A sample of calcareous silty clay was chemically analyzed (sample E142; Appendix A). The major-element composition of the clay is dramatically different than the tuff. The tuff contains significantly more silica, aluminum, iron, sodium, potassium, titanium, and barium, and significantly less calcium and magnesium than the silty clay. Alteration of volcanic glasses in the tuff to smectitic clay may explain the differences in chemistry. Comparisons of rare-earth-element ratios and high-field-strength ratios, if available, might help to shed light on the origin of the bentonitic material.

Multiple, small diameter, shallow topographic depressions are scattered across areas capped by the silty clay (fig. 20); the depressions are especially abundant in the northwest part of this silty clay area. Matrix-free deposits of clast-supported cobble gravel are visible in the bottoms of most depressions. The cobbles are similar to those in the underlying outwash. We suspect the depressions are a result of periglacial activity. The cobbles were probably elevated by frost heave.

Landslide deposits are present but not widespread in the quadrangle. Most of the landslides were small, shallow rotational slumps or translational failures on steep slopes. Several small unmapped landslides may exist within areas mapped as colluvium on the east side of Red Hill. The largest landslide in the mapped area is on the east side of Red Hill in the north-central part of the quadrangle; it extends northward into the Como quadrangle. A large bench-like landform at the head of the landslide is interpreted as a bedrock slump block, although no exposures of the material were observed.

STRUCTURE

South Park basin is a Laramide-age structural depression that has been modified by post-middle Tertiary extensional tectonism. The western side of the South Park basin coincides in part with the eastern limb of the large Sawatch anticline (Tweto, 1979), and the west-vergent Elkhorn thrust forms the eastern margin of the basin. Precambrian rocks are thrust over lower Tertiary and older rocks by the Elkhorn thrust. The Michigan-San Isabel syncline formed in rocks beneath and adjacent to the thrust and is the structurally deepest part of South Park basin (Sawatsky, 1967; Bryant and others, 1981b). North-northwest-trending reverse and/or thrust faults with down-to-west displacement locally disrupt east-dipping bedrock on the west side of South Park basin. One of the larger of these faults, the South Park fault, forms the eastern margin of Reinecker Ridge within the quadrangle. Several other structures (e.g. Mexican Ridge anticline and syncline, Hartsel anticline, McDannald fault, Michigan-San Isabel syncline) are east of the quadrangle between the Elkhorn thrust and South Park fault.

Most lower Tertiary and older strata beneath the quadrangle dip east. They are within the eastern limb of the Laramide Sawatch anticline. Previous workers mapped few or no faults in the Upper Paleozoic rocks in the quadrangle. However, detailed mapping of these rocks on the drainage divide between Fourmile Creek and the Middle Fork of the South Platte River revealed the presence of a complex swarm of faults. Most of the faults are easily identified on aerial photography. Thin limestone and sandstone beds that are apparent on aerial photographs and that can be traced in outcrop abruptly terminate against these faults. However, the sense of movement and amount of displacement on most of these faults cannot be determined with available data.

Several small displacement faults cut the Dakota Sandstone and other formations on Red Hill. Most of these faults are depicted on the map as having dip-slip movement, but folded beds adjacent to a few of these faults are suggestive of deformation due to drag caused by oblique-slip or strike-slip motion. Arrows are used on the geologic map to depict the relative horizontal movement on these faults, which may be minor tear faults of Laramide age. At least one of these faults runs beneath the large landslide on the east side of Red Hill, suggesting fracturing along the fault may have contributed to slope instability.

A small amplitude, tight anticline formed in the Dakota Sandstone is exposed in a road cut about one thousand feet southwest of the northeast corner of section 12, T. 10 S., R. 77 W. This block of Dakota is stratigraphically out of place and, as seen on aerial photography, is within a landslide.

The horizontal distances between the contacts of Mesozoic formations that outcrop on the west side of Red Hill and the contact between the Pierre Shale and South Park Formation on the west side of Reinecker Ridge gradually decrease from north to south across the quadrangle. This relationship could be caused by one or more of the following phenomena. (1) A fault that offsets the coarse conglomeratic member of the South Park in a down-to-west vertical direction in the Hartsel quadrangle may extend northward into the southeast corner of the Fairplay East quadrangle. If this fault continues further north beneath the valley of Trout Creek, it could cut out enough stratigraphic section to cause the above described shortening of horizontal distance. (2) Strikes in the Dakota Sandstone gradually swing from a nearly north-south orientation to a northwest strike as Red Hill approaches the southern edge of the quadrangle. The dips in the Dakota also increase from 10^{o} to 25^{o} eastward where the strikes are nearly north-south, to 25^{o} to 35^{o} northeastward where the bedding strikes northwest. This increase in dip also could explain part or all of the reduction in horizontal distances. (3) The South Park Formation rests on an unconformity eroded into the Pierre Shale. The unconformity may cut deeper into Pierre strata near the southern end of the quadrangle. The third interpretation is preferred by the authors.

The South Park fault is a major Laramide reverse-slip structure with down-to-west motion. It juxtaposes Upper Cretaceous Pierre Shale on the east over Paleocene strata in the South Park Formation on the west. Within the quadrangle the fault zone typically consists of two strands, each with down-to-west displacement. Individual strands die out and/or merge several times within the quadrangle. Where two strands exist, most displacement is focused on the eastern strand where the Pierre Shale is faulted over the South Park Formation.

Ettinger (1964) shows the southern end of the South Park fault as a high-angle fault. Sawatsky (1967) describes it as a moderate- to high-angle fault. The fault plane is not exposed in outcrops in the Fairplay East quadrangle. We suspect the fault dips east at a low to moderate angle, chiefly on the basis of the sinuosity of the fault trace as it crosses low-relief ridges and valleys and on our cross section A-A, which uses information from the Amoco Reinecker Ridge no. 1 well. Our interpretations of the well rely only upon publicly available geophysical logs and formation tops reported on Petroleum Information scout tickets; no cuttings or well-site geology reports were discovered.

The Reinecker Ridge well was spudded in the Pierre Shale about 1,600 feet east of the mapped location of one of the strands of the South Park fault. Unfortunately, the precise surface location of the fault cannot be pinpointed along cross section A-A’ because no outcrops exist there, and thin veneers of surficial deposits complicate interpretations using residuum. The well was cased to a depth of 759 feet, and from the bottom of the casing to a depth of 1,750 feet there are many high resistivity beds that we suspect are within the South Park Formation. From 1,750 to 6,028 feet the geophysical logs have responses typical of the Pierre Shale. From 6,028 feet to the bottom of the well at 7,611 feet the scout ticket reports an apparently complete section of Mesozoic rocks from the Niobrara through the Morrison Formations. The well may have extended into the Garo Sandstone and perhaps Maroon Formation. These data support a conclusion that the well cuts the east-dipping fault strand somewhere in the cased part of the well, probably near the bottom of the cased interval. A plane projected from the approximate fault location shown on the geologic map to the bottom of the well casing has an east dip of about 25°. In light of the uncertainties associated with the surface location of the fault and the position of the fault in the well, we conclude the fault plane dips about 20 to 35° east.

Sawatsky (1967) reported a maximum of 5,500 to 6,500 feet of down-to-west throw on the South Park fault. The fault displacement cannot be accurately determined in the quadrangle with available data, but the data do indicate the fault has experienced thousands of feet of displacement since the late Cretaceous.

In the E ½ of section 33, T. 9 S., R. 76 W., two subtle topographic benches were noted in Pleistocene piedmont deposits along the approximately located trace of the South Park fault (see special fault symbol with tick marks on the geologic map for locations of the benches). The benches are anomalous in that the surface capped by the piedmont deposits slopes gently eastward except for the subtle benches. The origin of the benches is uncertain. They could be due to differential erosion along the fault or to minor fault movement since deposition of the Pleistocene piedmont deposits.

The regional Hayden lineament described by Maughan and Perry (1986) extends through the quadrangle. It may coincide with the South Park fault, or perhaps an unmapped fault beneath the valley floor of Trout Creek. An absence of upper Paleozoic rocks east of the South Park fault led Sawatsky (1967) and De Voto (1971) to surmise that the South Park fault may have served as the western boundary of the ancestral Front Range Highland during the late Paleozoic.

Sawatsky (1967) and De Voto (1971) reported that beds in the Upper Cretaceous rocks dip east about 5° more than do strata in the South Park Formation. This led them to conclude that the block west of the South Park fault was tilted about 5° eastward prior to deposition of the South Park Formation. Bedding attitudes measured during this investigation suggest there is significant variability in dips in each formation, and conclusions based on dip changes within the quadrangle would be speculative. However, the absence of the Upper Cretaceous Laramie Formation, Fox Hills Sandstone, and upper part of the Pierre Shale in the area west of the South Park fault, along with the unconformity between the Pierre Shale and South Park Formation, require significant eastward tilting and major erosion prior to deposition of the South Park Formation. Major post-South Park Formation thrusting also is required to account for the juxtapositioning of the Pierre Shale over the South Park Formation.

Cross sections by some workers (e.g. Bryant and others, 1981b) show an anticline in the hanging wall immediately adjacent to the South Park fault. We found supportive evidence for this concept in the SW ¼ of section 27 in the northeast corner of the quadrangle. Here, a series of attitudes were measured on beds of Pierre Shale in a gully. All beds dipped east except for the westernmost exposed bed, which dipped west. Unfortunately, the area between the beds with opposing dips was not exposed and the crest of the theorized anticline where the beds would roll over was concealed. Hanging wall folds are somewhat better exposed to the north in the Como quadrangle in the SW ¼ of section 16, where measured attitudes in the Pierre Shale suggest the presence of an anticline and syncline pair in the hanging wall (Widmann and others, 2005).

The middle Tertiary tuff and sedimentary rocks preserved in the Fairplay paleovalley dip west at 6 to 25°, which is the opposite direction of the dip in all older rocks in the quadrangle. The middle Tertiary rocks project westward towards east-dipping upper Paleozoic rocks in the Minturn Formation that are exposed in the Fairplay West quadrangle at elevations higher than the Tertiary rocks in the paleovalley (Widmann and others, 2006). These relationships require the presence of a concealed fault with considerable down-to east displacement between the middle Tertiary rocks in the paleovalley and the upper Paleozoic rocks to the west. We name this concealed structure the Fairplay fault.

Because there is no known surface expression of the Fairplay fault, its precise location and orientation are uncertain. The fault location shown on the geologic map was selected because it lies west of all known outcrops of the Oligocene rocks in the paleovalley and east of the Minturn outcrops. Cross section B-B', which approximately follows the axis of the paleovalley and is parallel to the dip of rocks in the paleovalley, suggests a minimum down-to-west displacement of 1,500 feet since eruption of the 33.47 ± 0.15 Ma tuff. If the concealed fault is actually located further west, then the post-tuff displacement would be much greater. The Fairplay fault could potentially connect with the Agate Creek fault to the south, described by De Voto (1971); however, the Laramide movement on the Agate Creek fault was down-to-west. If the two faults are connected, then the post-middle Tertiary movement would be opposite that of the Laramide movement.

The west-tilted Oligocene rocks in the paleovalley not only require the existence of a previously unrecognized major post-middle Tertiary fault, but they also require that all east-dipping Paleozoic rocks within the same fault block have been tilted to the west or unfolded since the middle Tertiary. At the end of the Laramide orogeny the Paleozoic rocks would have dipped more steeply eastward than they do today. The 5 to 25^{o} west dips of the Oligocene rocks need to be added to the modern east dips of the Paleozoic rocks to arrive at their configuration at the end of the Laramide.

MINERAL RESOURCES

OIL AND GAS

The South Park basin, particularly the area between Como and Spinney Mountain Reservoir, has been the target of sporadic oil and gas exploration since the early 1930s. Although no significant commercial production has yet been established in the basin, some encouraging shows have been found. The principal potential reservoir rocks in the basin are the Cretaceous Dakota Sandstone, Fox Hills Sandstone, and sandstone members of the Pierre Shale, such as the Apache Creek member (Clement and Dolton, 1970). The Permian Garo Sandstone also is a potential hydrocarbon reservoir. Most of the wells in the South Park basin were dry, but at least two had oil and gas shows. The South Park Oil & Gas Company State #1 well, drilled in 1937 on the Hartsel anticline about six miles southeast of the Fairplay East quadrangle, reportedly produced over 5,000 barrels of oil (Cappa and others, 1999).

In 1978 and 1982 Amoco Production Company drilled two wildcat wells in the northeastern and east-central parts of the Fairplay East quadrangle on the east side of Reinecker Ridge. The target was the Cretaceous Dakota Sandstone. The State AY # 1 well was drilled in 1978 in the SW¼ SW¼ NW¼ of section 10, T. 10 S., R. 76 W. A prominent disturbed area visible on aerial photography flown in 1982 probably is the reclaimed well site. The well was reportedly spudded in Pierre Shale, deviated from the target structure, and was terminated at a depth of 9,010 feet while still in the Pierre Shale (Groth, 1985). The summarized geologic log from IHS Energy PI Dwights PLUS® database shows that the well re-entered the Pierre Shale at a depth of 2,600 feet. On the basis of the publicly available information for the well, our interpretation of geophysical logs run in the well, and the geologic map, we suspect the well was spudded in Pierre Shale and then drilled through one of the faults within the South Park fault system at a relatively shallow depth. The well probably penetrated the South Park Formation in the foot wall of the fault before re-entering the underlying Cretaceous rocks at or several hundred feet above a depth of 2,600 feet. It is uncertain whether the apparently thick Pierre section was a result of drilling through dipping beds or from repetition of Pierre strata due to an unrecognized reverse fault or faults in that interval.

The Reinecker Ridge Gas # 1 well was drilled in 1982 in the NE¼ SW¼ NW¼ of section 34, T. 9 S., R. 76 W. The Amoco geologists interpreted Reinecker Ridge as a large anticlinorial structure in the center of South Park basin (Groth, 1985). Our mapping does not confirm the presence of this large anticlinorial structure. All strata observed on Reinecker Ridge dip to the east, although they are locally cut by faults which caused minor dip changes.

According to the IHS Energy PI Dwights PLUS® database, the Reinecker Ridge well penetrated much of the Cretaceous section, including the Dakota Sandstone, and terminated in the Morrison Formation at a total depth of 7,611 feet. In the geophysical logs for this well, numerous high resistivity units have relatively low gamma response between the bottom of the casing at 759 feet and a depth of 1,750 feet. This interval probably is the South Park Formation. The Pierre Shale underlies the high-resistivity interval and extends from about 1,750 feet to the top of the Niobrara Formation at a depth of 6,028 feet, which indicates the well penetrated 4,278 feet of Pierre Shale. Groth (1985) reported vitrinite reflectance data and suggested that the Reinecker Ridge structure was unlikely to be productive because it formed after oil generation.

In late 1991 and early 1992, Hunt Oil Company drilled the Tarryall Federal 1-17 well in the NE¼ of section 17, T. 10 S., R. 75 W., about four miles east of the Fairplay East quadrangle. This well was spudded close to the surface trace of the Elkhorn thrust fault and was drilled to a total depth of 12,768 feet. Precambrian granite was apparently reached at the bottom of the well. Drill-stem tests (DSTs) were run in the “Hygiene” sandstone of the Pierre Shale between 6,412 feet and 6,547 feet, in the Dakota Sandstone from 10,200 to 10,275 feet, and in the Pierre Shale from 11,140 to 11,164 feet. The tests in the “Hygiene”, a hydrocarbon-producing sandstone member in the Denver basin, and the Pierre Shale yielded gas and gas-cut-mud. The DST in the Dakota was a misrun and yielded no information. No production was established from the well. In 1999, McMurray Oil Company drilled a sidetrack well on this site from a whipstock set at a depth of 10,026 feet. The sidetrack has a total depth of 11,376 feet and also was not successful in establishing production. No DSTs or other tests were reported for the well.

In 1934 the South Park Oil & Gas Company drilled and abandoned the Esche # 1 well in the SE¼ SE¼ NW¼ of section 5, T.9 S., R.76 W. in the Como quadrangle a little over 3 miles north of the Fairplay East quadrangle. The well bottomed in Dakota Sandstone, several shows of oil and gas in Cretaceous rocks were reported, and it flared gas with a four-foot flame (Clement and Dolton, 1970). These shows encouraged the company to continue exploration in the region into the late 1930s.

Two exploratory wells that were drilled in the northwestern part of the Milligan Lakes quadrangle encountered oil and/or gas shows. The Milligan #1 well was drilled to 3,228 feet by South Park Oil & Gas in 1934 in the NE¼ NE¼ SE¼ of section 13, T. 8 S., R. 76 W. In addition to numerous oil shows, light-green oil was recovered from two feet of sandstone at a depth of 2,017 feet (Clement and Dolton, 1970). The Teter #1 well was drilled to 7,475 feet by Tennessee Gas Transmission Company in 1957 in the SW¼ SE¼ NW¼ of section 11, T. 8 S., R. 76 W. Colorado Oil and Gas Conservation Commission records indicate that a gas show was encountered in what was interpreted as the Hygiene Member of the Pierre Shale. The Hygiene Member was later called the Apache Creek member in South Park (Clement and Dole, 1970). A third well in the area, the Shattinger #3, was drilled to a depth of 2,200 feet in the SW¼ NE¼ of section 10, T. 8 S., R. 76 W. by the Geary Oil Company in 1977. The well bottomed in Pierre Shale and was dry.

Hembre and TerBest (1997) stated that “the wide range of good shows from multiple zones” indicates there is petroleum potential in the “eastern South Park sub-basin”, which is the area east of the South Park fault. According to Steyaert and Wandrey (1997), “South Park has reasonable petroleum exploration merit”.

PLACER GOLD

Placer gold was discovered along the South Platte River and other streams in northwestern Park County in the summer of 1859. Quaternary glacial outwash, moraine, and fluvial gravels along the South Platte River near Fairplay and Alma hosted some of the richest placer gold deposits in Colorado and the Rocky Mountain region. Commercial-scale placer mining continued intermittently from the time of discovery until 1952. Some present-day aggregate mining operations along the South Platte River recover gold as a byproduct of gravel production. Small-scale recreational gold panning is still sometimes successful along the South Platte River and other local streams, where outwash gravels and tailings have been reworked by fluvial action and the gold slightly concentrated.

Singewald (1950) reported that between 1859 and 1938, at least $4 million (around 190,000 ounces) of placer gold was produced from Park County. Of that, it is estimated that three-fifths, or 115,000 ounces, came from the South Platte River valley, and most of the rest was from the Tarryall Creek area. Between 1941 and 1952, the South Platte Dredging Company produced about 104,325 ounces (Parker, 1974), most of which came from the Fairplay placers. Production since 1952 has been small, mainly as byproduct from sand and gravel aggregate operations. We estimate that less than 5,000 ounces of placer gold have been produced from the Fairplay-Alma placers between 1952 and 2005. Total placer gold production in the quadrangle probably exceeded 100,000 ounces. At the current price of $540/ounce, this amounts to over $54 million dollars.

The large, intestine-shaped piles of coarse gravel directly southeast of Fairplay and between the Middle Fork of the South Platte River and Highway 9 (fig. 4) are dredge tailings from mining operations on the Fairplay placer, which was one of the main producers of placer gold in the region. The South Platte number 1 dredge (fig. 21) was the largest dredge in Colorado. It was a bucket-line dredge with a maximum processing capacity of 15,000 cubic yards of auriferous gravel per day and could dig to a maximum depth of 96 feet (Parker, 1992). The dredge was built on the South Platte River southeast of Fairplay, began operating in 1941, and eventually produced the majority of the tailings on this placer. Also called the Fairplay dredge, it ceased operations in 1952 and was dismantled in 1980 (Parker, 1992). It was the last large commercial placer gold operation in the state.

Most gold recovered in the Fairplay placer came from the late Pleistocene glacial outwash in unit Qa_2 and Holocene stream alluvium in unit Qa_1, or from underlying buried “clayey gravel” that Parker (1974) believed was Bull Lake outwash (our unit Qa_3). The glacial till in the Fairplay West quadrangle upstream of the main outwash plain in the Fairplay East quadrangle also yielded significant quantities of gold. Most gold was found at the base of the outwash deposits or

Figure 21. Historical photograph of the South Platte number 1 dredge. Image, courtesy Colorado Historical Society (Bob Zellers collection), all rights reserved.

the glacial till, on the bedrock surface beneath the surficial deposits, or along contacts within the sequence of surficial deposits, especially on top of clay layers or clayey gravel beds (Singewald, 1950; Parker, 1974). Some gold is also present in small deposits that largely consist of reworked outwash or moraine. Singewald (1950) believed the unmined, topographically lower and perhaps slightly younger deposits of late Pleistocene alluvial unit two that are across the river from the main tailings piles and which extend south to the confluence of the Middle Fork and Crooked Creek, represent an excellent opportunity for additional prospecting.

The average fineness of placer gold recovered from the Fairplay-Alma region was approximately 800 (Singewald, 1950). The bedrock source for the placer gold is the northeast-trending mineralized belt in the Mosquito Range west and north of Alma.

SAND AND GRAVEL AGGREGATE

Sand and gravel aggregate is the only industrial mineral commodity currently being mined in the Fairplay East quadrangle. The outwash gravels and mine waste along the South Platte River represent a high-quality aggregate resource. The Alpine Rock Company of Breckenridge, Colorado operates the small Fairplay pit in the NE ¼ of section 3, T. 10 S., R. 77 W. in the area of the old placer dredge tailings. Park County operates the small Ansley No. 2 gravel pit in the SW ¼ of section 11, T. 10 S., R. 77 W. Several other active gravel pits are in the Fairplay West quadrangle upstream from the town of Fairplay. Material from some of these pits is also used as riprap and landscaping rock. Some of the active and permitted sand and gravel pits in the Fairplay area produce small quantities of gold as a byproduct of gravel aggregate production (Guilinger and Keller, 2004).

OTHER POTENTIAL INDUSTRIAL MINERAL RESOURCES

The Dakota Sandstone (unit Kd) has been quarried elsewhere in the state for use as dimension stone, silica sand, and crushed-rock aggregate (Schwochow, 1981). Currently, the Dakota Sandstone is being mined primarily for use as riprap at the Table Mountain quarry southwest of Colorado Springs. Clay is mined from the Dakota at places along the eastern base of the Front Range; however, no significant clay zones are known to exist in the Dakota Sandstone in the Fairplay area.

The Pierre Shale (Kp) is a potential source for common clay and lightweight aggregate. Clay from the Pierre Shale is used for manufacturing bricks and tiles, although other formations such as the Laramie and the Dawson are preferred by current manufacturers. Certain horizons in the Pierre Shale are mined and processed for use as lightweight aggregate at a facility near Boulder.

Limestone in the Niobrara Formation (Kn) has been quarried in small quantities in the South Park area for lime (Stark and others, 1949). Limestone beds in the Niobrara are often quite pure, but these beds are seldom greater than one foot in thickness (Stark and others, 1949). The Niobrara is very poorly exposed, and there are no active or abandoned limestone quarries on the Fairplay East quadrangle.

An old timber sled with a large block of granodiorite lies abandoned near the center of the SW ¼ of section 23, T. 10 S., R. 77 W. The rock probably was quarried from the Whitehorn granodiorite near Salida and somehow transported to the Fairplay area. The rock, which is suitable for use as building stone or monuments, was not mined in the quadrangle but likely is of historical interest.

COAL

There are no known coal resources in the Fairplay East quadrangle, and it is unlikely that any undiscovered resources exist. The South Park coal field extends for about 20 miles, from about one mile north of the town of Como south into the Hartsel quadrangle. The only mines with historical production in the South Park coal field are in the Como coal district, where several mines and prospects were active between 1870 and 1905 (Washburne, 1910). The Como coal district lies a short distance north and northeast of the quadrangle (McConnell, 1945; Widmann and others, 2005); however, the Laramie Formation, which hosts the coal beds, does not crop out in the Fairplay East quadrangle.

WATER RESOURCES

The Fairplay East quadrangle is located in the headwaters region of the South Platte River watershed. The Middle Fork of the South Platte River is the largest stream in the quadrangle. This fork of the South Platte originates at the Continental Divide near Hoosier Pass about 14 miles upstream from the quadrangle. The Middle Fork enters the quadrangle near Fairplay, heads southeast until reaching the base of Red Hill, and then turns south, flowing along the west side of

Red Hill until it reaches the water gap cut through Red Hill about a mile south of the quadrangle. The Middle Fork joins the South Fork near Hartsel and forms the South Platte River.

Other perennial streams in the quadrangle include Fourmile, Crooked, and Trout Creeks. Crooked Creek joins the Middle Fork near the center of the quadrangle. Fourmile Creek drains into the South Fork of the South Platte upstream of Hartsel and the confluence of the Middle and South Forks of the South Platte. Trout Creek flows into the Middle Fork above the confluence of the Middle and South Forks. Surface water in the quadrangle historically was used primarily for irrigation, but during the past few decades the adjudicated rights to much of the surface water that flows across the quadrangle have been transferred to the City of Aurora for municipal use.

Real-time flow data is available for perennial streams in and near the Fairplay East quadrangle at http://www.dwr.state.co.us/Hydrology/flow_search.asp. The only readily available annual summaries of stream discharge in and near the quadrangle are found at http://cdss.state.co.us/DNN/Stations/tabid/74/Default.aspx. This database includes flow data from stream gages on the Middle Fork of the South Platte above Fairplay, the Middle Fork near Hartsel and above the confluence with the South Fork, and Fourmile Creek about 3 miles west and upstream of the quadrangle, but only for the short time period from May 1978 through September 1980. During this short time period the mean annual discharge of the Middle Fork of the South Platte above Fairplay was 36,641 acre-feet, whereas the mean annual discharge of the Middle Fork above the confluence with the South Fork was 43,883 acre-feet. The mean annual discharge at the gage on Fourmile Creek was 9,841 acre-feet.

According to water well records held by the Colorado Division of Water Resource, most bedrock formations in the quadrangle are capable of yielding sufficient ground water for domestic purposes. Even the Pierre Shale produces meager amounts of water, although the quality can sometimes be poor. Wells completed in the Dakota Sandstone in Trout Creek valley yield sufficient water to serve the entire needs of the Red Hill Forest Ranch subdivision, but the water contains elevated levels of iron, radon, and radium and must be treated prior to use (Dave Stanford, Aquatest, 2005, personal communication).

Thick deposits of alluvial units one, two, and three also yield adequate ground water for domestic purposes. In the valley of Fourmile Creek the reported depth to water is commonly over 100 feet, which is surprisingly deep considering the creek flows year around.

GEOLOGIC HAZARDS AND GEOTECHNICAL CONSTRAINTS

Geologic hazards and geotechnical constraints in the Fairplay East quadrangle include sediment-laden flooding, debris flows, rockfall, landslides, problematic soils, earthquakes, and perhaps subsidence. Areas underlain by alluvial unit one (Qa1), alluvial units one and two, undivided (Qa), and alluvium and colluvium (unit Qac) are prone to flooding, including sediment-laden flood waters. Debris flows, mudflows, and sheet flooding may affect areas mapped as fan deposits (unit Qf), alluvium and colluvium (unit Qac), and colluvium (unit Qc).

Rockfall hazards exist beneath cliffy outcrops of the Reinecker Ridge Volcanic Member, Dakota Sandstone, and Garo Sandstone on Red Hill and Reinecker Ridge. Although landslides are not abundant in the quadrangle, one large landslide and many smaller ones are present in the quadrangle. They occur in a variety of geologic environments, but they are most common on the east side of Red Hill where east-dipping Cretaceous shales comprise the bedrock and on the west side of Reinecker Ridge in areas underlain by the lower volcaniclastic member and Reinecker

Ridge Volcanic Member. No evidence of historic landslide activity was observed during this study.

Most landslide deposits in the quadrangle probably last moved during the Pleistocene or early Holocene and appear to be stable or quasi-stable under present conditions. Some of the small thin-skinned failures involving residuum and colluvium on steep slopes may have moved during the late Holocene. Natural events such as intense rainfall, rapid snowmelt, ground shaking during earthquakes, and changes in ground-water levels can destabilize slopes and trigger landslides. Human activities, including excavations and earth fills on slopes and changes to the hydrologic environment from irrigation, septic systems, and water impoundments and diversions, also can contribute to slope failure. Future landsliding may not be restricted to areas mapped as landslide deposits (unit Qls); others areas in favorable geologic environments, particularly those where human activities affect slope stability, may also experience slope failures.

Surficial deposits derived from Cretaceous shales rich in smectite clays, especially the Pierre Shale, may have high shrink-swell potential, which can be detrimental to foundations, roads, and other works of humans. Heaving bedrock may also be a problem in areas underlain by beds of steeply dipping Cretaceous shale, as along the east side of Reinecker Ridge. The thin layer of silty clay in the Middle Fork of the South Platte River, which is shown on the geologic map by the wavy pattern superimposed on the color used for unit Qa2, also has high shrink-swell potential (fig. 20). Fine-grained sediments deposited in fan environments and on colluvial slopes may create conditions favorable for hydrocompaction and piping. Such sediments may be found in units Qf, Qc, and Qac. Prior to building foundations in the tuff unit (Tt), the engineering properties of that material should be evaluated.

Fine-grained sediments that are rapidly deposited can be prone to hydrocompaction, which results when deposits with high porosity are wetted. Fan deposits (unit Qf) derived from sedimentary units composed chiefly of siltstone, like the Maroon and Minturn Formations, may be hydrocompactive.

Two topographic depressions of uncertain origin were found in the quadrangle. One depression is in the SE ¼ of section 33, T. 10 S., R. 77 W. It formed in glacial outwash (unit Qa2) that overlies the Minturn Formation on the west side of U.S. Highway 285 near a subdivision. The feature is over 200 feet wide, over 20 feet deep, and is very apparent on aerial photographs (fig. 22) and from U.S. Highway 285. Gullies flow into the depression on its northwest and northeast sides. Shawe and others (1995) concluded the feature resulted from subsidence into a karst void formed in underlying evaporite strata in the Minturn Formation. They reported that surface runoff entering the depression rapidly infiltrated into the materials on the floor of the depression.

A second closed depression is on the northwest side of U.S. Highway 285 about a mile northeast of Fairplay. The depression is about 1,500 feet in length and over 20 feet deep. A lake occupies the floor of the depression. East-dipping mudstones and sandstones and thin limestone beds in the basal part of the Maroon Formation underlie the depression; no evaporitic strata or thick limestone beds are known to exist in the rocks that underlie the depression.

Several closed topographic depressions of uncertain origin exist to the north in the Como quadrangle (Widmann and others, 2005). These depressions formed in Pierre Shale or in surficial deposits that overlie the Pierre. Several closed depressions also were reported to the west in the Fairplay West quadrangle (Widmann and others, 2006). Shawe and others (1995) attributed the depressions in the southern part of that quadrangle to collapse into voids formed in underlying

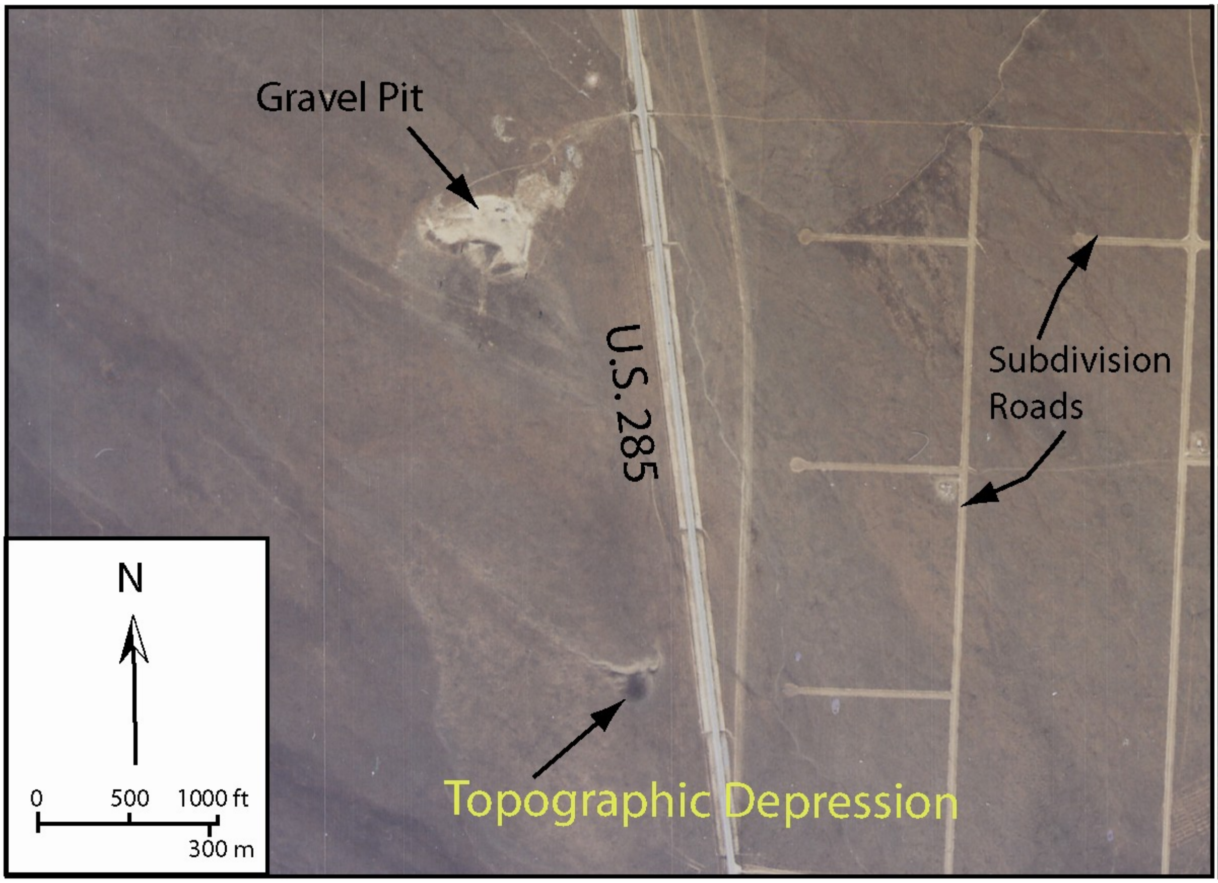

Figure 22. Closed depression on the west side of U.S. Highway 285 near the southwest corner of the quadrangle is very apparent on aerial photographs. (U.S. Bureau of Land Management photograph 11-34-16, project CO-81CC; flown October 6, 1982)

evaporite, but the ones to the north are underlain by clastic sedimentary rocks. This northern group of closed depressions is in outwash near terminal moraines and is suspected to be kettles resultant from the melting of ice blocks. However, if the depressions are a result of subsidence into underground voids, then they pose a threat to structures, roads, and pipelines. Additional investigation of the closed depressions in South Park is needed to determine their origin.

No late Quaternary faults were identified within the quadrangle, but the two topographic benches in eastward-sloping piedmont deposits along the South Park fault in the E ½ of section 33, T. 9 S., R. 76 W. should be further evaluated to determine if they are a result of late Quaternary activity on the fault. The concealed fault on the west side of the Fairplay paleovalley offsets the middle Tertiary tuff and sedimentary rocks an estimated minimum of 1,500 feet. No evidence of fault offset was noted in the Quaternary deposits in the vicinity of the approximately located fault, but the fault should be further evaluated if seismic hazard evaluations of the area are conducted in the future.

Earthquakes due to rupture of nearby faults, like those at Spinney Mountain (Shaffer and Williamson, 1986) or in the upper Arkansas Valley (Ostenaa and others, 1981; Lettis and others, 1996), could cause moderately strong ground motion in the quadrangle. A random or “floating” earthquake along a fault that is deep in the crust and does not rupture the ground surface also could generate moderately strong ground motion. It is our recommendation that structures at least be designed and built to the standards of the current International Building Code or other appropriate building code. Earthquakes can also trigger secondary effects, such as liquefaction, rockfall, and landslides, which potentially can cause great damage.

REFERENCES CITED

Barker, F., and Wyant, D.G., 1976, Geologic map of the Jefferson quadrangle, Park and Summit Counties, Colorado: U.S. Geological Survey Geologic Quadrangle Map GQ-1345, scale 1:24,000.

Beggs, H.G., 1977, Interpretation of seismic reflection data from the central South Park basin, Colorado, *in* Veal, H.K., ed., Exploration frontiers of the central and southern Rockies: Rocky Mountain Association of Geologists Field Conference 1977, p. 67-76.

Bookstrom, A. A., 1989, The Climax-Alma granite batholith of Oligocene age, and the porphyry molybdenum deposits of Climax, Colorado, U.S.A.,: *in* Johnson, A., ed., Richard H. Jahns Memorial Issue: Engineering Geology, v. 27, no. 1-4, p. 534-568.

Bookstrom, A.A., Naeser, C.W., and Shannon, J.R., 1987, Isotopic age determinations, unaltered and hydrothermally altered igneous rocks, north-central Colorado mineral belt: Isochron/West, no. 49, p. 13-19.

Brill, K. G., Jr., 1944, Late Paleozoic stratigraphy, west-central and northwestern Colorado: Geological Society of America Bulletin, v. 55, p. 621-656.

Brill, K.G., Jr., 1952, Stratigraphy in the Permo-Pennsylvanian zeugogeosyncline of Colorado and northern New Mexico: Geological Society of America Bulletin, v. 63, no. 8, p., 809-880.

Brown, G.F., 1940, Late Tertiary sediments in South Park, Colorado: Evanston, Illinois, Northwestern University, M.S. thesis, 43 p.

Bryant, B., Marvin, R.F., Naeser, C.W., and Mehnert, H.H., 1981a, Ages of igneous rocks in the South Park-Breckenridge region, Colorado, and their relation to the tectonic history of the Front Range uplift: U.S. Geological Survey Professional Paper 1199-C, p. 15-26.

Bryant, B., McGrew, L.W., and Wobus, R.A., 1981b, Geologic map of the Denver 1ºx2º quadrangle, north-central Colorado: U.S. Geological Survey Miscellaneous Investigation Series, I-1163, scale 1:250,000.

Burbank, W.S., Lovering, T.S., Goddard, E.N., and Eckel, E.B., compilers, 1935, Geologic map of Colorado: U.S. Geological Survey, scale 1:500,000.

Cappa, J.A., Crane, M.J., Hemborg, H.T., Lehart, T.M., Scarbrough, L.A., and TerBest, H., 1999, Evaluation of mineral and mineral fuel potential of Park County state mineral lands administered by the Colorado State Land Board: Colorado Geological Survey Open-File Report 99-15, CD-ROM.

Chapin, C.E., and Cather, S.M., 1983, Eocene tectonics and sedimentation in the Colorado Plateau-Rocky Mountain area, *in* Lowell, J.D., and Gries, R., eds., Rocky Mountain foreland basins and uplifts: Rocky Mountain Association of Geologists, p. 33-56.

Clement, J.H., and Dolton, G.L., 1970, A chronicle of exploration in South Park basin, Park County, Colorado: The Mountain Geologist, v. 7, no. 3, p. 205-216.

Cruden, D.M., and Varnes, D.J., 1996, Landslide types and processes, *in* Turner, A.K., and Schuster, R.L., eds., Landslides—Investigation and mitigation: National Research Council, Transportation Research Board Special Report 247, p. 36-75.

De Voto, R.H., 1961, Geology of southwestern South Park, Park and Chaffee Counties, Colorado: Golden, Colorado School of Mines, Ph.D. dissertation, T-924, 201 p.

De Voto, R.H., 1964, Stratigraphy and structure of Tertiary rocks in southwestern South Park: The Mountain Geologist, v. 1, no. 3, p. 117-126.

De Voto, R.H., 1965a, Facies relationships between Garo Sandstone and Maroon Formation, South Park, Colorado: American Association of Petroleum Geologists Bulletin, v. 49, no. 4, p. 460-462.

De Voto, R.H., 1965b, Pennsylvanian and Permian stratigraphy of central Colorado: The Mountain Geologist, v. 2, no. 4, p. 209-228.

De Voto, R.H., 1971, Geologic history of South Park and geology of the Antero Reservoir quadrangle, Colorado: Quarterly of the Colorado School of Mines, v. 66, no. 4, 90 p., scale 1:62,500.

De Voto, R.H., 1972, Cenozoic geologic history of South Park: The Mountain Geologist, v. 9, no. 2-3, p. 72-90.

De Voto, R.H., 1980, Pennsylvanian stratigraphy and history of Colorado, *in* Kent, H.C., and Porter, K.W., eds., Colorado geology: Rocky Mountain Association of Geologists, p. 71-101.

De Voto, R.H., 1988, South Park, *in* Sloss, L.L., ed., Sedimentary cover--North American Craton: Geological Society of America, The Geology of North America, DNAG volume D-2, p. 179-182.

Durani, J.A., 1980, Seismic investigation of the tectonic and stratigraphic history of eastern South Park, Park County, Colorado: Golden, Colorado School of Mines, Ph.D. dissertation, T-2346, 138 p.

Emmons, S.F., 1889, Description of the Tenmile district quadrangle: U.S. Geological Survey Geologic Folio 48.

Esser, R.P., 2005, $^{40}Ar/^{39}Ar$ geochronology results from the Culebra Peak and Como quadrangles, Colorado: New Mexico Geochronological Research Laboratory, Internal Report No. NMGRL-IR-493 and 494.

Ettinger, M., 1964, Geology of the Hartsel area, South Park, Colorado: The Mountain Geologist, v. 1, no. 3, p. 127-132.

Fatti, J., 1974, Digital processing of seismic reflection records from South Park Colorado: Golden, Colorado School of Mines, Ph.D. dissertation, T-1653, 159 p.

Folk, R. L., 1980, Petrology of sedimentary rocks: Austin, Texas, Hemphill Publishing Company, 182 p.

Folk, R.L., and Ward, W.C., 1957, Brazos River bar-A study in the significance of grain size parameters: Journal of Sedimentary Petrology, v. 27, p. 3-26.

Fridrich, C.J., Smith, R.P., DeWitt, E., and McKee, E.H., 1991, Structural, eruptive, and intrusive evolution of the Grizzly Peak caldera, Sawatch Range, Colorado: Geological Society of America Bulletin, v. 103, p. 1160–1177.

Gile, L.H., Peterson, F.F., and Grossman, R.B., 1966, Morphological and genetic sequences of carbonate accumulations in desert soils: Soil Science, v. 101, p. 347-360.

Groth, P.K, 1985, Exploration tectonics and virinite reflectance, South Park basin, Colorado [abst.]: American Association of Petroleum Geologists Bulletin, v. 69. no. 5, p. 849.

Guilinger, J.R., and Keller, J.W., 2004, Directory of active and permitted mines in Colorado – 2002: Colorado Geological Survey Information Series 68, CD-ROM.

Guthrie, R.L., and Witty, J.E., 1982, New designations for soil horizons and layers and the new soil survey manual: Soil Science Society of America Journal, v. 46, p. 443-444.

Heckel, P.H., 1986, Sea-level curve for Pennsylvanian eustatic marine transgressive-regressive depositional cycles along Midcontinent outcrop belt, North America: Geology, v. 14, no. 4, p. 330-334.

Hembre, D.R., and TerBest, H., Jr., 1997, Future petroleum potential of Front Range areas, Colorado, *in* Bolyard, D.W., and Sonnenberg, S.A., Geologic history of the Colorado Front Range, 1997 RMS-AAPG field trip #7: Rocky Mountain Association of Geologists, p. 135-144.

Hilgard, E.W., 1892, A report on the relations of soil to climate: U.S. Department of Agriculture, Weather Bureau Bulletin 3, 59 p.

Hungr, O., Evans, S.G., Bovis, M.J., and Hutchinson, J.N., 2001, A review of the classification of landslides of the flow type: Environmental & Engineering Geoscience, v. 7, no. 3, p. 221-238.

Ingram, R.L., 1989, Grain-size scale used by American geologists, *in* Dutro, J.T., Jr., Dietrich, R.V., and Foose, R.M., eds., AGI data sheets for geology in the field, laboratory, and office: Alexandria, Va., American Geological Institute, Data Sheet 29.1.

International Commission on Stratigraphy, 2005, International stratigraphic chart: downloaded January 2006 from the International Commission on Stratigraphy website, www.stratigraphy.org/chus.pdf.

Jackson, J.A., ed., 1997, Glossary of geology, 4th ed.: Alexandria, Va., American Geological Institute, 769 p.

Johnson, J.H., 1935, Stratigraphy of the northeastern and north-central parts of South Park, Colorado: American Association of Petroleum Geologists Bulletin, v. 19, no. 9, p. 1339-1356.

Johnson, J.H., 1937, Tertiary depositions of South Park, Colorado, with a description of Oligocene algal limestones: Boulder, University of Colorado, Ph.D. dissertation, 68 p.

Koschmann, A.H., and Wells, F.G., 1946, Preliminary report of the Kokomo mining district, Colorado: Colorado Scientific Society Proceedings, v. 15, p. 59-70.

Le Bas, M.J., LeMaitre, R.W., Streckeisen, A.I., and Zanettin, B., 1986, A chemical classification of volcanic rocks based upon the total alkali-silica diagram: Journal of Petrology, v. 27, p. 747-750.

Lettis, W., Noller, J., Wong, I., Ake, J., Vetter, U., and LaForge, R., 1996, Draft report, Seismotectonic evaluation; Colorado River storage project-Crystal, Morrow Point, Blue Mesa dams; Smith Fork project-Crawford dam, west-central Colorado: report prepared by William Lettis & Associates, Inc., Woodward-Clyde Federal Services, and Seismotectonics and Geophysical Group of the U.S. Bureau of Reclamation for the U.S. Bureau of Reclamation in Denver, Colorado, 177 p.

Lozano, E., 1965, Geology of the southwestern Garo area, South Park, Park County, Colorado: Golden, Colorado School of Mines, M.S.thesis T-1057, 206 p.

Machette, M.N., 1985, Calcic soils of the southwestern United States, *in* Weide, D.L., ed., Soils and Quaternary geology of the southwestern United States: Geological Society of America Special Paper 203, p. 1-21.

Mallory, W. W., 1972, Pennsylvanian arkose and the Ancestral Rocky Mountains, in Mallory, W. W., ed., Geologic atlas of the Rocky Mountain region: Denver, Rocky Mountain Association of Geologists, p. 131-132.

Martinson, D.G., Pisias, N.G., Hays, J.D., Imbrie, J., Moore, T.C., Jr., and Shackleton, N.J., 1987, Ag dating and the orbital theory of the ice ages; Development of a high-resolution 0 to 300,000-year chronostratigraphy: Quaternary Research, V. 27, P. 1-29.

Maughan, E.K., and Perry, W.J., 1986, Lineaments and their tectonic implications in the Rocky Mountains and adjacent plains region, *in* Peterson, J.A., ed., Paleotectonics and sedimentation in the Rocky Mountain region: American Association of Petroleum Geologists, Memoir 41, p. 41-53.

McConnell, C.M., 1945, Compilation of data, Como coal district, Park County, Colorado: U.S. Geological Survey unpublished report, 4 p.

McDowell, F.W., 1971, K-Ar ages of igneous rocks from western Unites States: Isochron/West, no. 2, p. 1-16.

McIntosh, W.C., and Chapin, C.E., 2004, Geochronology of the central Colorado volcanic field, *in* Cather, S.M., McIntosh, W.C., and Kelley, S.A., eds., Tectonics, geochronology, and volcanism in the southern Rocky Mountains and Rio Grande rift: New Mexico Bureau of Geology and Mineral Resources, Bulletin 160, p. 205-237.

Miller, H.W., 1937, The geology of the Dakota hogback, South Park, Colorado: Evanston, Illinois, Northwestern University, M.S. thesis, 115 p.

Navas, J., 1966, Geology of the Como area, South Park, Park County, Colorado: Golden, Colorado School of Mines, M.S. thesis, 145 p.

Okulitch, A.V., 2002, Geological time chart: Geological Survey of Canada, Open File 3040 (National Earth Science Series, Geological Atlas)-Revision.

Ostenaa, D.A., Losh, S.L., and Nelson, A.R., 1981, Evidence for recurrent late Quaternary faulting, Sawatch fault, upper Arkansas Valley, Colorado, *in* Junge, J.R., ed., Colorado tectonics, seismicity, and earthquake hazards; Proceedings and field trip guide: Colorado Geological Survey Special Publication 19, p. 27-29.

Parker, B.H., Jr., 1961, The geology of the gold placers of Colorado: Golden, Colorado School of Mines, Ph.D. dissertation, 578 p.

Parker, B.H. Jr., 1974, Gold placers of Colorado: Quarterly of the Colorado School of Mines, v. 69, no. 3, 268 p.

Parker, B.H., Jr., 1992, Gold panning and placering in Colorado, how and where: Colorado Geological Survey Information Series 33, 83 p.

Poole, F.G., and Stewart, J.H., 1964, Chinle Formation and Glen Canyon Sandstone in northeastern Utah and northwestern Colorado: U.S. Geological Survey Professional Paper 501-D, p. D30-D39.

Raynolds, R.G., 2003, Laramide synorogenic strata bounding the Front Range, Colorado, *in* Raynolds, R.G., and Flores, R.M., eds, Cenozoic systems of the Rocky Mountains: Society of Economic Paleontologists and Mineralogists, Rocky Mountain section, p. 355-368.

Ross, C.A., 1985, Late Paleozoic depositional sequences are synchronous and worldwide: Geology, v. 13, no. 3, p. 194-197.

Sawatsky, D.L., 1964, Structural geology of southeastern South Park: The Mountain Geologist, v. 1, no. 3, p. 133-139.

Sawatsky, D.L., 1967, Tectonic style along the Elkhorn thrust, eastern South Park and western Front Range, Park County, Colorado: Golden, Colorado School of Mines, Ph.D. dissertation, T-1044, 206 p.

Schenk, C.J., 1989, Sedimentology and stratigraphy of the Eagle Valley Evaporite (Middle Pennsylvanian), Eagle Basin, northwest Colorado: Boulder, University of Colorado, Ph.D. dissertation, 172 p.

Schwochow, S.D., 1981, Inventory of nonmetallic mining and processing operations in Colorado: Colorado Geological Survey Map Series 17, 39 p.

Shaffer, M.E., and Williamson, J.V., 1986, Seismic evaluation of Spinney Mountain dam, *in* Rogers, W.P., and Kirkham, R.M., eds., Contributions to Colorado tectonics and seismicity--A 1986 update: Colorado Geological Survey Special Publication 28, p. 104-121.

Shannon, J.R., 1988, Geology of Mount Aetna cauldron complex, Sawatch Range: Golden, Colorado School of Mines, Ph.D. dissertation, 434 p.

Shawe, D.R., Steven, T.A., Taylor, R.B., and Maxwell, C.H., 1995, Photogeologic map showing distribution of sinkholes south of Fairplay, Park County, Colorado--A possible geologic hazard: U.S. Geological Survey Miscellaneous Field Study Map MF-2295, scale 1:24,000.

Shoffner, D.A., 1974, Geology of Reinecker Ridge – Bald Hill area, South Park, Park County, Colorado: Golden, Colorado School of Mines, Masters thesis, T-1493, 82 p.

Singewald, Q.D., 1942, Stratigraphy, structure, and mineralization in the Beaver-Tarryall area, Park County, Colorado: U.S. Geological Survey Bulletin 928A, 44 p.

Singewald, Q.D., 1950, Gold placers and their geologic environment in northwestern Park County, Colorado: U.S. Geological Survey Bulletin 955-D, 172 p.

Soil Survey Staff, 1975, Soil taxonomy: U.S. Department of Agriculture Handbook 436, 754 p.

Stark, J.T., Johnson, J.H., Behre, C.H., Jr., Powers, W.E., Howland, A.L., Gould, D.B., and others, 1949, Geology and origin of South Park, Colorado: Geological Society of America Memoir 33, 188 p.

Steyaert, D.J., and Wandrey, C., 1997, Petroleum potential of the South Park basin, Park County, Colorado, *in* Bolyard, D.W., and Sonnenberg, S.A., Geologic history of the Colorado Front Range, 1997 RMS-AAPG field trip #7: Rocky: Rocky Mountain Association of Geologists, p. 145-154.

Taranik, J.V., 1974, Stratigraphic and structural evolution of Breckenridge area, central Colorado: Golden, Colorado School of Mines, Ph.D. dissertiation, 222 p.

Tillman, R.W., 1966, Petrology and paleoenvironments of the Robinson Member, Minturn Formation, Eagle Basin Colorado: Boulder, Colorado, University of Colorado, Ph.D. dissertation, 227 p.

Tillman, R W., 1971, Petrology and paleoenvironments, Robinson Member, Minturn Formation (Desmoinesian), Eagle Basin, Colorado: American Association of Petroleum Geologists Bulletin, v. 55, no. 4, p. 593-620.

Topper, R., Spray, K.L., Bellis, W.H., Hamilton, J.L., and Barkmann, P.E., 2003, Ground water atlas of Colorado: Colorado Geological Survey Special Publication 53, 210 p.

Treviño, L., and Keller, G.R., 2004, Structure of the North Park and South Park basins, Colorado – An integrated geophysical study, *in* Karlstrom, K.E., and Keller, G.R., The Rocky Mountain region – An evolving lithosphere – Tectonics, geochemistry, and geophysics: American Geophysical Union Geophysical Monograph Series, v. 154, p. 91-97.

Tweto, O., 1949, Stratigraphy of the Pando area, Eagle County, Colorado: Colorado Scientific Society Proceedings, v. 15, p. 149-235.

Tweto, O., 1974a, Geology of the Mount Lincoln 15-minute quadrangle, Eagle, Lake, Park, and Summit Counties, Colorado: U.S. Geological Survey Miscellaneous Field Studies Map MF-556, scale 1:62,500.

Tweto, O., 1974b, Reconnaissance geologic map of the Fairplay West, Mount Sherman, South Peak, and Jones Hill 7 ½ minute quadrangles, Park, Lake, and Chaffee Counties, Colorado: U.S. Geological Survey Miscellaneous Field Studies Map MF-555, scale 1:62,500.

Tweto, O., 1974c, Geology of the Holy Cross 15-minute quadrangle, Eagle, Lake, Pitkin, and Summit Counties, Colorado: U.S. Geological Survey Miscellaneous Geologic Investigations Map I-830, scale 1:24,000.

Tweto, O., 1979, compiler, Geologic map of Colorado: U.S. Geological Survey, scale 1:500,000.

Tweto, O., and Lovering, T.S., 1977, Geology of the Minturn 15-minute quadrangle, Eagle and Summit Counties, Colorado: U.S. Geological Survey Professional Paper 956, 96 p.

Walker, T.R., 1972, Bioherms in the Minturn Formation (Des Moinesian age), Vail-Minturn area, Eagle County, Colorado: Colo. Sch. Mines Quarterly, v. 67, no. 4, p. 249-278.

Wallace, C.A., Keller, J.W., McCalpin, J.P., Bartos, P.J., Route, E.E., Jones, N.N., Gutierrez, F., Williams, C.L., and Morgan, M.L., 2003, Geologic map of the Breckenridge quadrangle, Summit and Park Counties, Colorado: Colorado Geological Survey Open-File Report 02-7, scale 1:24,000.

Washburne, C.W., 1910, The South Park coal field, Colorado: U.S. Geological Survey Bulletin 381, p. 307-316.

Widmann, B.L., Bartos, P.J., Madole, R.F., Barbá, K.E., and Moll, M.E., 2004a, Geologic map of the Alma quadrangle, Park and Summit Counties, Colorado: Colorado Geological Survey Open-File Report 04-3, scale 1:24,000.

Widmann, B.L., Bartos, P.J., McCalpin, J.P., and Jackson, J., 2004b, Geologic map of the Copper Mountain quadrangle, Summit, Eagle, Lake, and Park Counties, Colorado: Colorado Geological Survey Open-File Report 03-20, scale 1:24,000.

Widmann, B.L., Kirkham, R.M., Houck, K.J., and Lindsay, N.L., 2006, Geologic map of the Fairplay West quadrangle, Park County, Colorado: Colorado Geological Survey Open-File Report 06-xx, scale 1:24,000.

Widmann, B.L., Kirkham, R.M., Keller, J.W., Poppert, J.T., and Price, J.B., 2005, Geologic map of the Como quadrangle, Park County, Colorado: Colorado Geological Survey Open-File Report 05-4, scale 1:24,000.

Widmann, B.L., Morgan, M.L., Bartos, P.J., Shaver, K.C., Gutierrez, F., and Lockman, A., 2002, Geologic map of the Keystone quadrangle, Summit County, Colorado: Colorado Geological Survey Open-File Report 02-03, scale 1:24,000.

Wyant, D.G., and Barker, F., 1976, Geologic map of the Milligan Lakes quadrangle, Park County, Colorado: U.S. Geological Survey Geologic Quadrangle Map GQ-1343, scale 1:24,000.

APPENDIX A. Whole-rock major-element geochemical analyses.

[All analyses were performed by ALS Chemex using the XRF method. Sample descriptions and locations are listed below the table. Sample locations also are shown on the geologic map.

Sample no.	SiO_2	Al_2O_3	Fe_2O_3	CaO	MgO	Na_2O	K_2O	Cr_2O_3	TiO_2	MnO	P_2O_5	SrO	BaO	LOI*	Total
							(in	Weight	%)						
E142	39.25	2.77	0.95	22.41	5.53	0.20	0.65	0.01	0.18	0.03	0.09	0.08	0.06	27.50	99.71
E266	67.39	15.00	1.81	0.95	2.39	2.41	3.99	0.01	0.37	0.06	0.07	0.06	0.18	4.94	99.67
E309P	66.31	14.59	1.90	2.63	1.46	2.05	3.52	0.02	0.28	0.07	0.07	0.05	0.20	6.64	99.79

* LOI = loss on ignition

E142: light-gray silty clay that overlies glacial outwash of unit Qa2; UTM 417565 E, 4333040 N

E266: whole-rock sample of tuff (unit Tt); megascopic xenolithic clasts were excluded from the sample; UTM 415205 E, 4335253 N

E309P: pumice fragment from tuff (unit Tt); UTM 415199 E, 4335298 N

APPENDIX B. $^{40}Ar/^{39}Ar$ step heat analysis of CGS samples.

$^{40}Ar/^{39}Ar$ step heat analysis of CGS Samples

For:
John Keller
Colorado Geological Survey

Prepared by:

Paul Layer & Jeff Drake
Geochronology Laboratory
University of Alaska Fairbanks

May 3, 2006

Summary of the Analysis

For $^{40}Ar/^{39}Ar$ analysis, 6 samples were submitted to the Geochronology laboratory at UAF. One, (FW-161) was rejected due to absence of datable mineral phases. The others were crushed, washed and sieved to either 100 – 250 or 250 – 500 micron size fractions, and hand picked for datable mineral phases (one per sample). The monitor mineral MMhb-1 (Samson and Alexander, 1987) with an age of 513.9 Ma (Lanphere and Dalrymple, 2000) was used to monitor neutron flux (and calculate the irradiation parameter, J). The samples and standards were wrapped in aluminum foil and loaded into aluminum cans of 2.5 cm diameter and 6 cm height. The samples were irradiated in position 5c of the uranium enriched research reactor of McMaster University in Hamilton, Ontario, Canada for 20 megawatt-hours.

Upon their return from the reactor, the samples and monitors were loaded into 2 mm diameter holes in a copper tray that was then loaded in a ultra-high vacuum extraction line. The monitors were fused, and samples heated, using a 6-watt argon-ion laser following the technique described in York et al. (1981), Layer et al. (1987) and Layer (2000). Argon purification was achieved using a liquid nitrogen cold trap and a SAES Zr-Al getter at 400C. The samples were analyzed in a VG-3600 mass spectrometer at the Geophysical Institute, University of Alaska Fairbanks. The argon isotopes measured were corrected for system blank and mass discrimination, as well as calcium, potassium and chlorine interference reactions following procedures outlined in McDougall and Harrision (1999). System blanks generally were $2x10^{-16}$ mol ^{40}Ar and $2x10^{-18}$ mol ^{36}Ar which are 10 to 50 times smaller than fraction volumes. Mass discrimination was monitored by running both calibrated air shots and a zero-age glass sample. These measurements were made on a weekly to monthly basis to check for changes in mass discrimination.

The age, Ca/K and Cl/K spectra plots are on pages 5 – 9 and detailed analyses are given on pages 10 – 13 . A summary of all the $^{40}Ar/^{39}Ar$ results is given in Table 1, with all ages quoted to the +/- 1 sigma level and calculated using the constants of Steiger and Jaeger (1977). The integrated age is the age given by the total gas measured and is equivalent to a potassium-argon (K-Ar) age. The spectrum provides a plateau age if three or more consecutive gas fractions represent at least 50% of the total gas release and are within two standard deviations of each other (Mean Square Weighted Deviation less than ~2.5).

Lanphere, M.A., and Dalrymple, G.B., 2000, First-principles calibration of ^{38}Ar tracers: Implications for the ages of $^{40}Ar/^{39}Ar$ fluence monitors, U.S. Geological Survey Professional Paper 1621, 10 p.

Layer, P.W., 2000, Argon-40/argon-39 age of the El'gygytgyn impact event, Chukotka, Russia, Meteroitics and Planatary Science, v. 35, 591-599.

Layer, P.W., Hall, C.M. & York, D., 1987. The derivation of $^{40}Ar/^{39}Ar$ age spectra of single grains of hornblende and biotite by laser step heating, *Geophys. Res. Lett.,* **14**, 757-760.

McDougall, I. and Harrison, T.M., 1999, Geochronology and Thermochronology by the 40Ar/39Ar method-2nd ed, Oxford University Press, New York, 269pp.

Samson S. D., and Alexander E. C. (1987) Calibration of the interlaboratory 40Ar/39Ar dating standard, MMhb1. Chem. Geol. **66**, 27-34.

Steiger, R.H. and Jaeger, E., 1977, Subcommission on geochronology: Convention on the use of decay constants in geo and cosmochronology, Earth and Planet Science Letters, v. 36, p. 359-362.

York, D., Hall, C.M., Yanase, Y., Hanes, J.A. & Kenyon, W.J., 1981. $^{40}Ar/^{39}Ar$ dating of terrestrial minerals with a continuous laser, *Geophys. Res. Lett.,* **8**, 1136-1138.

Brief discussion of analyses

FW-161: This intermediate intrusive was highly altered. XRD analysis showed that it contained chlorite, not biotite as was hoped. It also contained altered feldspar and quartz. Therefore this sample was rejected for geochronologic analysis.

05-447A: Hornblende from this sample did not appear to be suitable for dating, so biotite was chosen. A single step-heating run shows a well defined plateau with an age of 32.4 ± 0.3 Ma and little or no subsequent argon loss. Based on the quality of the spectrum, we feel that this age reflects cooling of this intrusive rock.

JK083: Biotite was separated from this andesite clast from a Tertiary conglomerate. A single step-heating run shows a well defined plateau with an age of 66.4 ± 0.4 Ma and little or no subsequent argon loss. Based on the quality of the spectrum, we feel that this age reflects cooling of this andesite.

JK099: Biotite was separated from this intermediate intrusive clast from a Tertiary conglomerate. A single step-heating run shows a well defined plateau with an age of 66.6 ± 0.5 Ma, identical in age to JK083, and little or no subsequent argon loss. Based on the quality of the spectrum, we feel that this age reflects cooling of this sample.

JK119: Hornblende was separated from this volcanic rock. The hornblende looked fresh (unaltered) and we were able to extract a pure separate. Two runs of this separate were done. Both show results consistent with each other, and both show a very complex age spectrum. The first ~10% of gas release is characterized by low Ca/K and Cl/K ratios, and based on experience with other samples, probably reflects some sort of biotitic alteration. The spectra from ~20% to 80% of ^{39}Ar release are characterized by relatively constant Ca/K (~8 – 9) and Cl/K (~ 0.1 – 0.15) ratios, but the age spectra show a 'stair-step' down pattern indicative of excess argon. This portion could either represent a 'pure' hornblende phase which has excess argon, or a mixed phase of some biotite and some hornblende). The last part of the release shows slightly higher Ca/K and Cl/K ratios, but a fairly consistent age of about 68.8 ± 0.8 Ma. Although the ages from the two runs do not meet the criteria for plateaus, we feel that this age most accurately reflects the cooling age of this hornblende. Petrographic analysis of this amphibole might provide insights into the state of preservation of this mineral and the reason for the variations in Ca/K and Cl/K during step-heating.

E309P: This rhyolitic or trachytic tuff contained both biotite and large feldspar phenocrysts. Based on discussions with CGS, it was decided to focus on the feldspar, believed to be sanidine, which tends to be a more reliable chronometer in these felsic volcanics. Two runs were done, the first on an aggregate of three grains, and the second on a single large crystal. The most striking result was that this mineral is not sanidine, but rather a different feldspar, presumably plagioclase. Evidence for this is that the total Ca/K ratio is 16 – 17 for each of the runs. I do not know of an instance where sanidine contains so much potassium. Therefore the runs reflect the age of plagioclase for this tuff. Both samples show some evidence of argon loss at low 39Ar release, and a very old age (> 40 Ma) for the high temperature steps, which could be excess argon, which is often seen in plagioclase. The best age for this sample is seen by run 1, where fractions accounting for 40% release have an age of 32.6 ± 0.5 Ma. This is not a plateau age because of insufficient 39Ar release, but is the best age we have for this sample. If desired, biotite could be separated from this sample, however it would take ~ 1 month to analyze.

Table 1 Interpretive Details

Sample	Min.	Integrated Age (Ma)	Plateau Age (Ma)	Plateau Information
05-447A	BI	32.2 ± 0.3	**32.4 ± 0.3**	8 fractions 88% ^{39}Ar released MSWD = 0.2
JK083	BI	65.8 ± 0.4	**66.4 ± 0.4**	10 fractions 96% ^{39}Ar released MSWD = 0.8
JK099	BI	**65.8 ± 0.5**	**66.6 ± 0.5**	9 fractions 89% ^{39}Ar released MSWD = 1.3
JK119	HO#1	74.2 ± 0.6	69.0 ± 1.0*	4 fractions 23% ^{39}Ar released MSWD = 0.8
	HO#2	*71.2 ± 0.5*	68.3 ± 1.4*	7 fractions 32% ^{39}Ar released MSWD = 3.8
		Weighted Average	**68.8 ± 0.8**	
E309P	FS#1	39.2 ± 0.4	32.6 ± 0.5*	8 fractions 40% ^{39}Ar released MSWD = 1.1
	FS#2	35.3 ± 1.4	31.8 ± 3.0*	8 fractions 36% ^{39}Ar released MSWD = 0.3
		Weighted Average	**32.6 ± 0.5**	

Bold: Preferred age for each sample (ages reported at ± 1 sigma)
Plateau: 3+ consecutive fractions, MSWD < ~2.7, more than ~50% 39Ar release.
* Sample does not meet criteria for plateau, sample is weighted mean age of ‘plateau-like’ fractions.

For Weighted mean ages, the error on the age includes the scatter between fractions represented by the higher MSWD values.

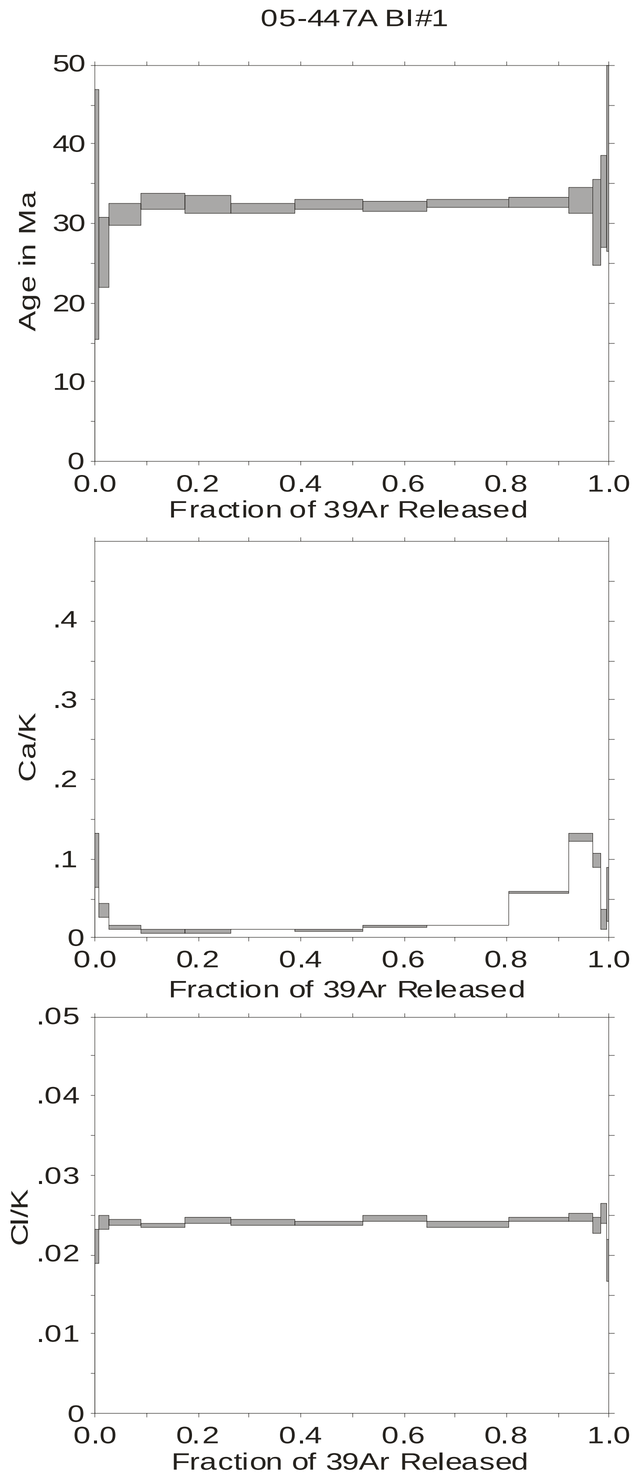
05-447A BI#1
Age in Ma
50
40
30
20
10
0
0.0
0.2
0.4
0.6
0.8
1.0
Fraction of 39Ar Released
Ca/K
.4
.3
.2
.1
0
0.0
0.2
0.4
0.6
0.8
1.0
Fraction of 39Ar Released
Cl/K
.05
.04
.03
.02
.01
0
0.0
0.2
0.4
0.6
0.8
1.0
Fraction of 39Ar Released

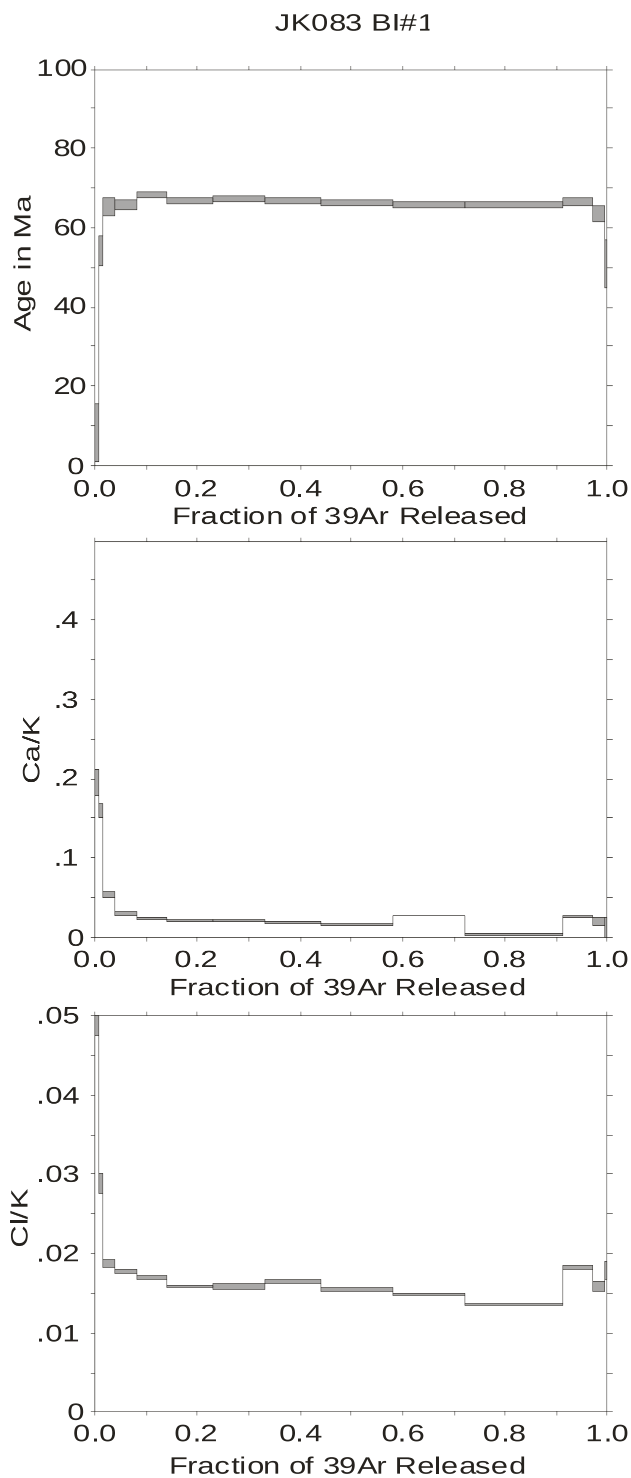
JK083 BI#1
Age in Ma
100
80
60
40
20
0
0.0
0.2
0.4
0.6
0.8
1.0
Fraction of 39Ar Released
Ca/K
.4
.3
.2
.1
0
0.0
0.2
0.4
0.6
0.8
1.0
Fraction of 39Ar Released
Cl/K
.05
.04
.03
.02
.01
0
0.0
0.2
0.4
0.6
0.8
1.0
Fraction of 39Ar Released

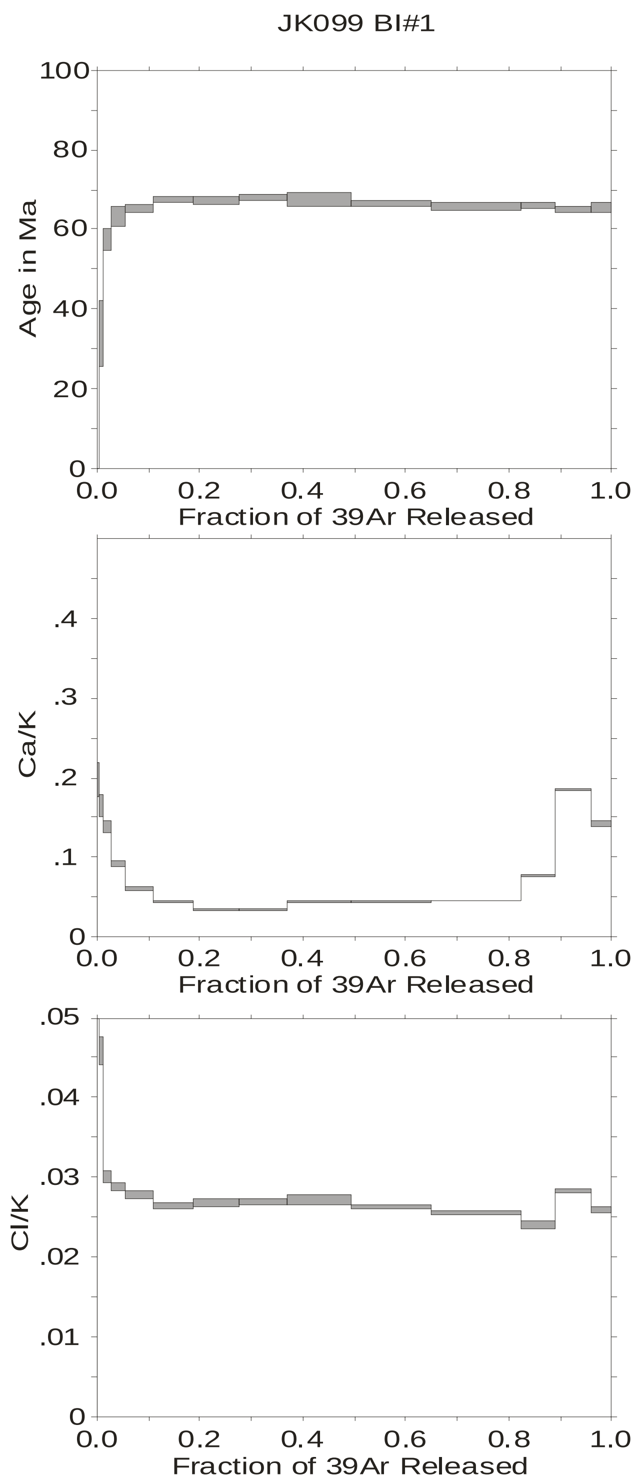
JK099 BI#1
Age in Ma
0
20
40
60
80
100
0.0
0.2
0.4
0.6
0.8
1.0
Fraction of 39Ar Released
Ca/K
0
.1
.2
.3
.4
0.0
0.2
0.4
0.6
0.8
1.0
Fraction of 39Ar Released
Cl/K
0
.01
.02
.03
.04
.05
0.0
0.2
0.4
0.6
0.8
1.0
Fraction of 39Ar Released

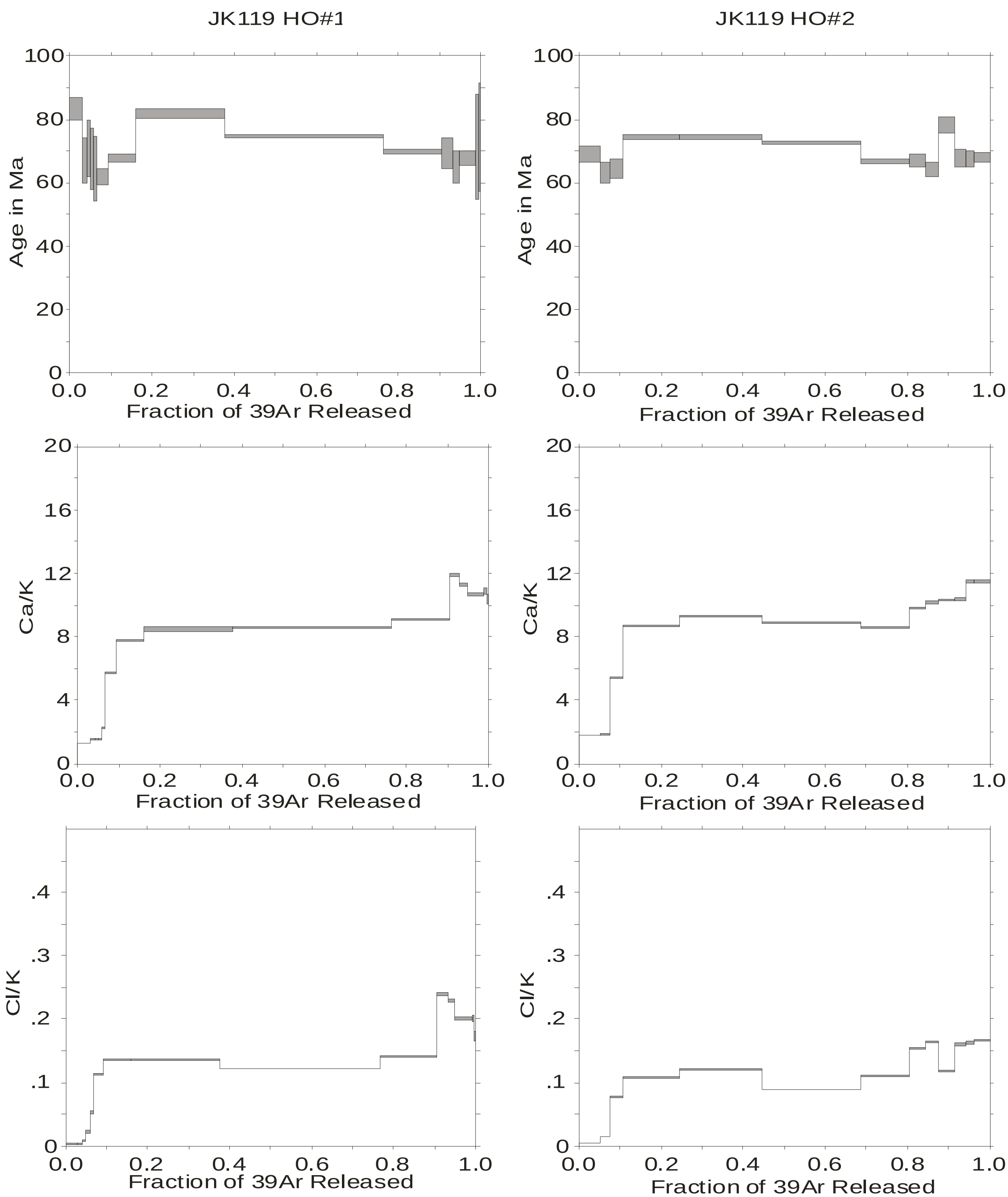
JK119 HO#1
JK119 HO#2
Age in Ma
Ca/K
Cl/K
Fraction of 39Ar Released
100
80
60
40
20
0
16
12
8
4
.4
.3
.2
.1
0.0
0.2
0.4
0.6
0.8
1.0

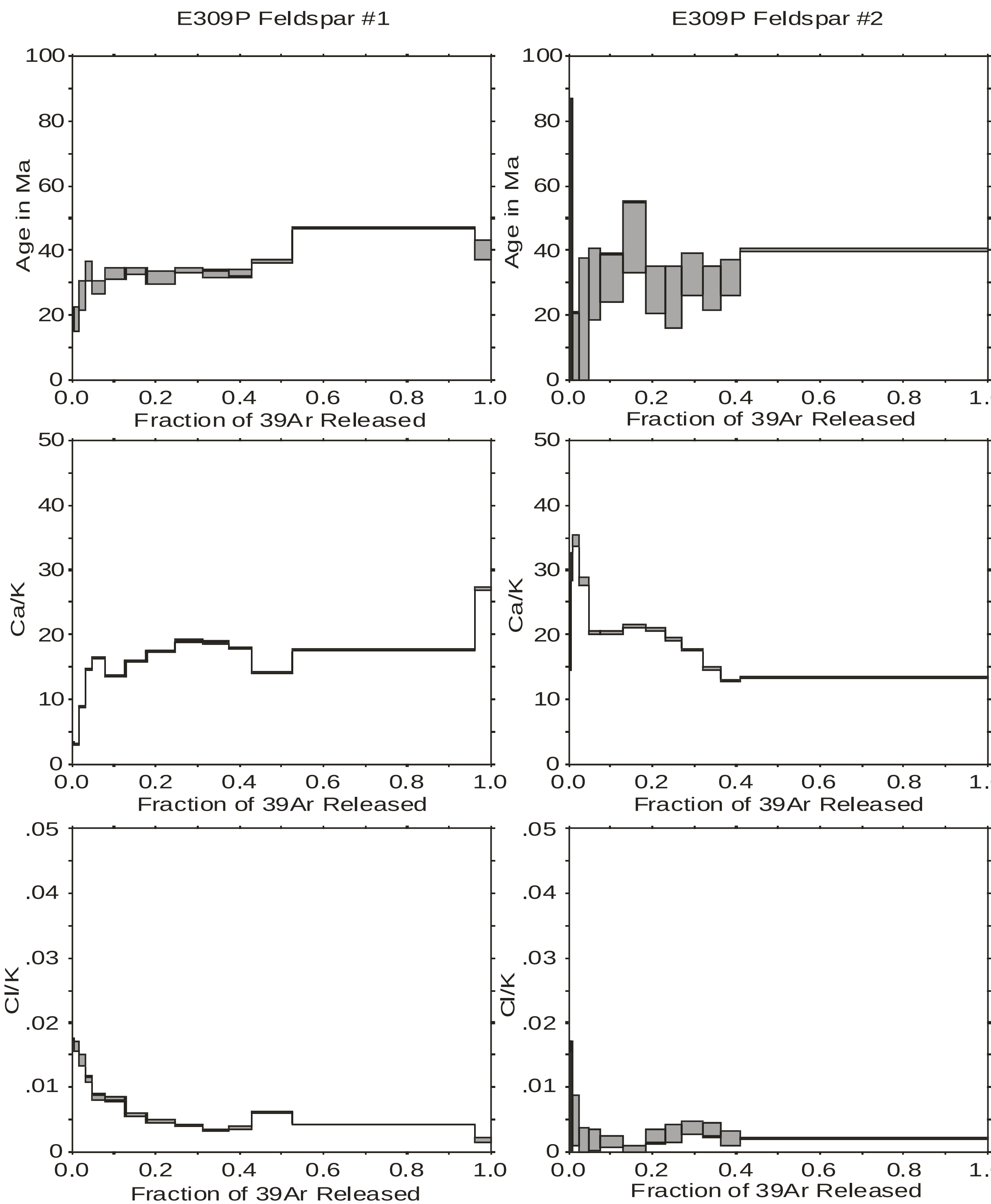
E309P Feldspar #1
E309P Feldspar #2
Age in Ma
Ca/K
Cl/K
Fraction of 39Ar Released
0
20
40
60
80
100
10
30
50
.01
.02
.03
.04
.05
0.0
0.2
0.4
0.6
0.8
1.0

05-447A Bl#1 Weighted average of J from standards = 0.002351 +/- 0.000011

Laser (mW)	Cum. ^{39}Ar	$^{40}Ar/^{39}Ar$ measured	+/-	$^{37}Ar/^{39}Ar$ measured	+/-	$^{36}Ar/^{39}Ar$ measured	+/-	% Atm. ^{40}Ar	Ca/K	+/-	Cl/K	+/-	$^{40}Ar^*/^{39}Ar_K$	+/-	Age (Ma)	+/- (Ma)
300	0.0053	57.297	1.215	0.0539	0.0186	0.1688	0.0131	87.1	0.0989	0.0341	0.02097	0.00217	7.383	3.776	31.0	15.7
500	0.0259	23.404	0.502	0.0193	0.0047	0.0580	0.0034	73.2	0.0354	0.0086	0.02397	0.00086	6.254	1.051	26.3	4.4
700	0.0887	11.298	0.099	0.0076	0.0016	0.0131	0.0011	34.3	0.0139	0.0029	0.02404	0.00046	7.406	0.328	31.1	1.4
900	0.1745	9.473	0.083	0.0052	0.0013	0.0055	0.0008	17.3	0.0096	0.0023	0.02368	0.00035	7.808	0.244	32.8	1.0
1100	0.2621	9.657	0.082	0.0047	0.0011	0.0064	0.0009	19.7	0.0087	0.0020	0.02432	0.00035	7.729	0.286	32.5	1.2
1400	0.3859	9.536	0.107	0.0062	0.0006	0.0065	0.0005	20.1	0.0113	0.0010	0.02407	0.00036	7.601	0.165	32.0	0.7
1700	0.5208	9.057	0.097	0.0059	0.0006	0.0044	0.0004	14.4	0.0108	0.0011	0.02394	0.00032	7.727	0.141	32.5	0.6
2000	0.6446	8.984	0.096	0.0077	0.0009	0.0044	0.0004	14.6	0.0142	0.0016	0.02452	0.00037	7.648	0.146	32.1	0.6
2500	0.8039	8.597	0.079	0.0089	0.0004	0.0028	0.0003	9.7	0.0163	0.0007	0.02389	0.00038	7.739	0.124	32.5	0.5
3000	0.9204	8.543	0.081	0.0320	0.0007	0.0026	0.0005	8.9	0.0586	0.0013	0.02440	0.00029	7.759	0.157	32.6	0.7
3500	0.9687	8.375	0.084	0.0695	0.0027	0.0018	0.0013	6.1	0.1275	0.0049	0.02473	0.00043	7.834	0.400	32.9	1.7
4000	0.9829	8.179	0.088	0.0532	0.0048	0.0034	0.0044	12.3	0.0975	0.0088	0.02369	0.00112	7.145	1.300	30.1	5.4
6000	0.9962	8.326	0.090	0.0131	0.0064	0.0017	0.0047	6.0	0.0240	0.0118	0.02533	0.00126	7.800	1.394	32.8	5.8
9000	1.0000	9.237	0.264	0.0305	0.0187	-0.0063	0.0162	-20.2	0.0560	0.0344	0.01931	0.00254	11.067	4.790	46.3	19.8
Integrated		9.701	0.032	0.0141	0.0003	0.0068	0.0002	20.7	0.0258	0.0006	0.02411	0.00012	7.672	0.075	32.3	0.3

JK083 Bl#1 Weighted average of J from standards = 0.002351 +/- 0.000011

Laser (mW)	Cum. ^{39}Ar	$^{40}Ar/^{39}Ar$ measured	+/-	$^{37}Ar/^{39}Ar$ measured	+/-	$^{36}Ar/^{39}Ar$ measured	+/-	% Atm. ^{40}Ar	Ca/K	+/-	Cl/K	+/-	$^{40}Ar^*/^{39}Ar_K$	+/-	Age (Ma)	+/- (Ma)
300	0.0055	26.661	0.579	0.1061	0.0089	0.0833	0.0059	92.4	0.1946	0.0163	0.04980	0.00229	2.016	1.733	8.5	7.3
500	0.0151	23.823	0.334	0.0872	0.0054	0.0366	0.0030	45.4	0.1599	0.0099	0.02891	0.00124	12.989	0.919	54.3	3.8
700	0.0377	19.986	0.144	0.0294	0.0018	0.0145	0.0017	21.5	0.0540	0.0034	0.01872	0.00056	15.670	0.519	65.3	2.1
900	0.0807	18.033	0.171	0.0164	0.0012	0.0076	0.0008	12.4	0.0301	0.0022	0.01771	0.00028	15.771	0.279	65.7	1.1
1100	0.1408	17.040	0.172	0.0127	0.0008	0.0021	0.0005	3.6	0.0234	0.0014	0.01702	0.00029	16.404	0.220	68.3	0.9
1400	0.2293	16.721	0.142	0.0118	0.0005	0.0024	0.0005	4.2	0.0217	0.0009	0.01592	0.00020	15.999	0.193	66.6	0.8
1700	0.3292	16.414	0.191	0.0115	0.0006	0.0007	0.0004	1.3	0.0210	0.0011	0.01592	0.00034	16.172	0.229	67.3	0.9
2000	0.4391	16.363	0.170	0.0107	0.0006	0.0011	0.0003	1.9	0.0196	0.0011	0.01644	0.00020	16.026	0.189	66.7	0.8
2500	0.5812	16.306	0.113	0.0084	0.0005	0.0012	0.0002	2.1	0.0154	0.0009	0.01546	0.00022	15.931	0.130	66.3	0.5
3000	0.7193	16.124	0.115	0.0152	0.0004	0.0009	0.0003	1.7	0.0278	0.0008	0.01491	0.00019	15.825	0.146	65.9	0.6
3500	0.9140	16.048	0.178	0.0019	0.0004	0.0008	0.0002	1.4	0.0036	0.0008	0.01371	0.00013	15.796	0.192	65.8	0.8
4000	0.9711	16.370	0.152	0.0139	0.0008	0.0011	0.0008	2.0	0.0254	0.0014	0.01818	0.00029	16.008	0.281	66.6	1.2
6000	0.9937	16.204	0.139	0.0112	0.0027	0.0033	0.0016	6.0	0.0206	0.0050	0.01582	0.00062	15.211	0.496	63.4	2.0

9000	1.0000	16.496	0.281	0.0067	0.0064	0.0145	0.0051	26.0	0.0122	0.0117	0.01779	0.00115	12.182	1.512	50.9	6.2
Integrated		16.617	0.054	0.0117	0.0002	0.0027	0.0001	4.7	0.0214	0.0004	0.01600	0.00008	15.806	0.067	65.8	0.4

JK099 Bl#1 Weighted average of J from standards = 0.002351 +/- 0.000011

Laser (mW)	Cum. ^{39}Ar	^{40}Ar/^{39}Ar measured	+/-	^{37}Ar/^{39}Ar measured	+/-	^{36}Ar/^{39}Ar measured	+/-	% Atm. ^{40}Ar	Ca/K	+/-	Cl/K	+/-	^{40}Ar*/^{39}Ar$_K$	+/-	Age (Ma)	+/- (Ma)
300	0.0041	67.436	2.057	0.1083	0.0115	0.2412	0.0121	105.7	0.1987	0.0212	0.06254	0.00351	-3.871	3.192	-16.5	13.7
500	0.0110	28.313	0.436	0.0899	0.0078	0.0686	0.0068	71.6	0.1650	0.0143	0.04592	0.00176	8.034	2.002	33.8	8.3
700	0.0271	20.610	0.240	0.0752	0.0040	0.0231	0.0024	33.1	0.1380	0.0073	0.03003	0.00077	13.769	0.725	57.5	3.0
900	0.0557	18.770	0.184	0.0504	0.0018	0.0121	0.0019	19.1	0.0924	0.0033	0.02884	0.00048	15.166	0.567	63.2	2.3
1100	0.1099	17.774	0.171	0.0328	0.0011	0.0070	0.0006	11.6	0.0602	0.0020	0.02782	0.00052	15.680	0.241	65.3	1.0
1400	0.1876	17.275	0.121	0.0239	0.0010	0.0034	0.0005	5.8	0.0439	0.0019	0.02647	0.00032	16.241	0.191	67.6	0.8
1700	0.2757	17.065	0.244	0.0193	0.0007	0.0029	0.0006	5.0	0.0354	0.0013	0.02684	0.00044	16.182	0.285	67.4	1.2
2000	0.3695	16.983	0.131	0.0191	0.0006	0.0022	0.0005	3.8	0.0351	0.0011	0.02688	0.00031	16.308	0.183	67.9	0.8
2500	0.4941	16.829	0.410	0.0242	0.0007	0.0019	0.0003	3.3	0.0443	0.0013	0.02725	0.00064	16.250	0.411	67.6	1.7
3000	0.6497	16.715	0.130	0.0241	0.0005	0.0025	0.0004	4.4	0.0442	0.0009	0.02619	0.00026	15.958	0.165	66.4	0.7
3500	0.8251	16.496	0.215	0.0249	0.0006	0.0022	0.0004	3.9	0.0457	0.0011	0.02563	0.00023	15.826	0.247	65.9	1.0
4000	0.8887	16.838	0.121	0.0422	0.0011	0.0033	0.0006	5.8	0.0775	0.0021	0.02398	0.00045	15.842	0.220	66.0	0.9
6000	0.9585	16.893	0.115	0.1011	0.0011	0.0043	0.0006	7.4	0.1854	0.0020	0.02829	0.00033	15.611	0.220	65.0	0.9
9000	1.0000	17.133	0.129	0.0779	0.0017	0.0048	0.0009	8.2	0.1429	0.0031	0.02590	0.00045	15.699	0.293	65.4	1.2
Integrated		17.294	0.074	0.0349	0.0003	0.0050	0.0002	8.5	0.0641	0.0005	0.02687	0.00013	15.795	0.088	65.8	0.5

JK119 HO#1 Weighted average of J from standards = 0.002351 +/- 0.000011

Laser (mW)	Cum. ^{39}Ar	^{40}Ar/^{39}Ar measured	+/-	^{37}Ar/^{39}Ar measured	+/-	^{36}Ar/^{39}Ar measured	+/-	% Atm. ^{40}Ar	Ca/K	+/-	Cl/K	+/-	^{40}Ar*/^{39}Ar$_K$	+/-	Age (Ma)	+/- (Ma)
300	0.0282	34.675	0.308	0.6859	0.0077	0.0495	0.0028	42.1	1.2591	0.0141	0.00340	0.00059	20.081	0.862	83.2	3.5
500	0.0405	21.548	0.684	0.8245	0.0315	0.0186	0.0057	25.2	1.5136	0.0579	0.00417	0.00112	16.109	1.765	67.1	7.2
700	0.0501	22.398	0.257	0.8506	0.0224	0.0182	0.0074	23.8	1.5616	0.0412	0.00883	0.00143	17.060	2.202	70.9	9.0
900	0.0585	20.156	0.262	0.8357	0.0207	0.0136	0.0079	19.6	1.5342	0.0380	0.02247	0.00144	16.184	2.353	67.4	9.6
1100	0.0670	18.531	0.287	1.2422	0.0245	0.0106	0.0084	16.5	2.2811	0.0450	0.05247	0.00215	15.470	2.484	64.4	10.2
1400	0.0936	17.476	0.152	3.1232	0.0338	0.0097	0.0020	15.1	5.7424	0.0622	0.11354	0.00182	14.850	0.620	61.9	2.5
1700	0.1590	18.188	0.157	4.2158	0.0363	0.0077	0.0008	10.7	7.7567	0.0670	0.13509	0.00140	16.258	0.286	67.7	1.2
2000	0.3763	21.227	0.393	4.6179	0.0655	0.0063	0.0003	7.1	8.4988	0.1209	0.13534	0.00167	19.748	0.392	81.9	1.6
2500	0.7648	19.107	0.115	4.6434	0.0348	0.0050	0.0002	5.9	8.5458	0.0643	0.12200	0.00078	18.013	0.123	74.8	0.5
3000	0.9058	17.979	0.099	4.9248	0.0317	0.0054	0.0005	6.8	9.0654	0.0585	0.14053	0.00081	16.789	0.172	69.8	0.7
3500	0.9311	17.375	0.125	6.4391	0.0497	0.0042	0.0038	4.4	11.8646	0.0920	0.23923	0.00179	16.655	1.141	69.3	4.7

4000	0.9488	16.765	0.132	6.1129	0.0571	0.0057	0.0042	7.3	11.2612	0.1055	0.22963	0.00219	15.569	1.263	64.8	5.2
5000	0.9899	16.864	0.133	5.7961	0.0436	0.0036	0.0020	3.8	10.6753	0.0806	0.20079	0.00179	16.259	0.595	67.7	2.4
6000	0.9961	15.622	0.256	5.9019	0.0889	-0.0035	0.0137	-9.4	10.8710	0.1643	0.20152	0.00541	17.123	4.086	71.2	16.7
9000	1.0000	14.528	0.441	5.6423	0.1640	-0.0100	0.0141	-23.3	10.3911	0.3031	0.17324	0.00673	17.941	4.199	74.5	17.1
Integrated		19.592	0.098	4.4845	0.0202	0.0071	0.0003	9.0	8.2526	0.0373	0.12963	0.00050	17.852	0.125	74.2	0.6

JK119 HO#2

Weighted average of J from standards = 0.002351 +/- 0.000011

Laser (mW)	Cum. ^{39}Ar	^{40}Ar/^{39}Ar measured	+/-	^{37}Ar/^{39}Ar measured	+/-	^{36}Ar/^{39}Ar measured	+/-	% Atm. ^{40}Ar	Ca/K	+/-	Cl/K	+/-	^{40}Ar*/^{39}Ar$_K$	+/-	Age (Ma)	+/- (Ma)
500	0.0526	32.806	0.277	0.9679	0.0096	0.0551	0.0019	49.4	1.7770	0.0176	0.00467	0.00043	16.590	0.573	69.0	2.3
800	0.0765	20.721	0.156	0.9986	0.0146	0.0191	0.0028	26.9	1.8336	0.0268	0.01471	0.00048	15.136	0.835	63.1	3.4
1100	0.1061	19.163	0.135	2.9693	0.0245	0.0131	0.0025	19.0	5.4588	0.0450	0.07821	0.00105	15.528	0.744	64.7	3.1
1500	0.2427	20.416	0.119	4.7410	0.0281	0.0096	0.0005	12.2	8.7261	0.0520	0.10784	0.00082	17.953	0.174	74.6	0.7
1750	0.4453	19.298	0.116	5.0291	0.0328	0.0061	0.0003	7.3	9.2581	0.0606	0.12005	0.00098	17.915	0.150	74.4	0.6
2000	0.6854	18.677	0.115	4.8515	0.0311	0.0054	0.0004	6.6	8.9300	0.0575	0.08901	0.00068	17.473	0.162	72.6	0.7
2250	0.8048	17.575	0.122	4.6493	0.0365	0.0065	0.0006	9.0	8.5568	0.0674	0.10988	0.00079	16.017	0.199	66.7	0.8
2500	0.8434	18.358	0.116	5.3323	0.0383	0.0092	0.0016	12.6	9.8181	0.0707	0.15444	0.00137	16.081	0.484	66.9	2.0
2750	0.8753	18.692	0.120	5.5272	0.0452	0.0126	0.0020	17.7	10.1782	0.0836	0.16439	0.00152	15.420	0.613	64.2	2.5
3000	0.9170	21.611	0.129	5.6034	0.0393	0.0107	0.0021	12.8	10.3192	0.0726	0.11722	0.00135	18.899	0.640	78.4	2.6
3500	0.9418	18.122	0.140	5.6181	0.0532	0.0077	0.0022	10.3	10.3463	0.0984	0.15981	0.00190	16.288	0.673	67.8	2.8
4000	0.9613	18.124	0.182	6.2247	0.0629	0.0081	0.0021	10.7	11.4679	0.1163	0.16363	0.00223	16.227	0.644	67.5	2.6
9000	1.0000	18.669	0.143	6.2358	0.0582	0.0096	0.0012	12.7	11.4885	0.1077	0.16759	0.00146	16.345	0.381	68.0	1.6
Integrated		19.799	0.046	4.6680	0.0121	0.0103	0.0003	13.6	8.5912	0.0224	0.10619	0.00032	17.137	0.086	71.3	0.5

E309P Feldspar #1

Weighted average of J from standards = 0.002351 +/- 0.000011

Laser (mW)	Cum. ^{39}Ar	^{40}Ar/^{39}Ar measured	+/-	^{37}Ar/^{39}Ar measured	+/-	^{36}Ar/^{39}Ar measured	+/-	% Atm. ^{40}Ar	Ca/K	+/-	Cl/K	+/-	^{40}Ar*/^{39}Ar$_K$	+/-	Age (Ma)	+/- (Ma)
300	0.0009	2249.640	132.591	2.2622	0.1551	7.6765	0.4569	100.8	4.1570	0.2855	0.02727	0.01453	-18.647	25.186	-80.9	111.7
500	0.0044	659.146	11.916	1.9426	0.0446	2.1955	0.0486	98.4	3.5690	0.0820	0.02153	0.00388	10.509	9.594	44.0	39.7
700	0.0177	48.434	0.439	1.6681	0.0226	0.1491	0.0031	90.7	3.0640	0.0416	0.01640	0.00076	4.490	0.897	18.9	3.8
900	0.0306	15.694	0.319	4.8376	0.0913	0.0333	0.0037	60.6	8.9043	0.1686	0.01416	0.00084	6.197	1.110	26.1	4.6
1100	0.0481	10.927	0.092	7.9339	0.0745	0.0119	0.0023	26.8	14.6332	0.1381	0.01124	0.00046	8.015	0.687	33.7	2.9
1400	0.0791	9.042	0.074	8.8710	0.0756	0.0100	0.0016	25.4	16.3716	0.1403	0.00850	0.00042	6.767	0.470	28.5	2.0
1700	0.1270	11.062	0.069	7.3636	0.0486	0.0130	0.0014	29.9	13.5762	0.0901	0.00827	0.00034	7.773	0.426	32.7	1.8
2000	0.1775	8.850	0.045	8.6234	0.0555	0.0051	0.0008	9.8	15.9121	0.1030	0.00574	0.00023	8.000	0.254	33.6	1.1
2500	0.2463	8.722	0.054	9.4648	0.0648	0.0066	0.0015	14.3	17.4743	0.1204	0.00474	0.00020	7.500	0.453	31.5	1.9

3000	0.3130	8.607	0.061	10.3197	0.0770	0.0046	0.0007	6.6	19.0633	0.1433	0.00412	0.00017	8.064	0.211	33.9	0.9
3500	0.3734	8.581	0.061	10.1771	0.0795	0.0053	0.0009	9.4	18.7980	0.1479	0.00343	0.00017	7.802	0.260	32.8	1.1
4000	0.4297	9.164	0.073	9.7260	0.0865	0.0071	0.0008	14.8	17.9595	0.1607	0.00372	0.00019	7.831	0.253	32.9	1.1
5000	0.5265	9.322	0.063	7.7022	0.0609	0.0040	0.0005	6.5	14.2038	0.1129	0.00619	0.00015	8.733	0.148	36.7	0.6
6000	0.9627	12.100	0.076	9.5505	0.0639	0.0055	0.0002	7.5	17.6335	0.1187	0.00424	0.00005	11.235	0.094	47.0	0.4
9000	1.0000	10.015	0.079	14.6590	0.1344	0.0055	0.0024	5.1	27.1564	0.2513	0.00192	0.00040	9.567	0.724	40.1	3.0
Integrated		15.367	0.045	9.2576	0.0304	0.0228	0.0003	39.4	17.0894	0.0565	0.00518	0.00005	9.355	0.084	39.2	0.4

E309P Feldspar #2

Weighted average of J from standards = 0.002351 +/- 0.000011

Laser (mW)	Cum. ^{39}Ar	$^{40}Ar/^{39}Ar$ measured	+/-	$^{37}Ar/^{39}Ar$ measured	+/-	$^{36}Ar/^{39}Ar$ measured	+/-	% Atm. ^{40}Ar	Ca/K	+/-	Cl/K	+/-	$^{40}Ar^*/^{39}Ar_K$	+/-	Age (Ma)	+/- (Ma)
500	0.0009	244.317	156.853	5.5880	3.6307	0.9014	0.7232	108.9	10.2907	6.7105	-0.07370	0.09449	-21.733	129.451	-94.6	578.5
800	0.0036	41.189	5.529	6.9139	0.9339	0.2685	0.1130	191.5	12.7434	1.7292	0.03737	0.02182	-37.830	32.243	-168.0	150.1
1100	0.0094	35.553	2.576	16.4579	1.1862	0.1034	0.0489	82.5	30.5249	2.2238	0.00872	0.00844	6.270	14.459	26.4	60.4
1400	0.0244	13.057	0.342	18.5608	0.4590	0.0534	0.0210	110.5	34.4731	0.8629	0.00486	0.00388	-1.384	6.272	-5.9	26.7
1700	0.0463	8.483	0.190	15.2548	0.3022	0.0182	0.0157	50.0	28.2712	0.5657	0.00157	0.00221	4.268	4.673	18.0	19.6
2000	0.0763	8.163	0.154	10.9748	0.1669	0.0066	0.0089	13.7	20.2821	0.3107	0.00191	0.00166	7.069	2.654	29.7	11.1
2500	0.1295	8.199	0.120	10.9963	0.1578	0.0053	0.0060	9.1	20.3222	0.2938	0.00161	0.00091	7.480	1.788	31.4	7.5
3000	0.1829	8.033	0.091	11.5424	0.1201	-0.0052	0.0089	-30.1	21.3390	0.2238	-0.00035	0.00143	10.493	2.665	44.0	11.0
3500	0.2292	7.968	0.104	11.2771	0.1307	0.0076	0.0059	17.6	20.8450	0.2434	0.00245	0.00107	6.588	1.769	27.7	7.4
4000	0.2709	7.821	0.112	10.4194	0.1275	0.0086	0.0076	22.7	19.2487	0.2371	0.00282	0.00137	6.067	2.269	25.6	9.5
5000	0.3198	9.379	0.099	9.5594	0.0952	0.0079	0.0053	17.4	17.6500	0.1768	0.00375	0.00100	7.776	1.570	32.7	6.5
6000	0.3638	9.187	0.141	7.9999	0.1083	0.0102	0.0055	26.4	14.7555	0.2008	0.00350	0.00110	6.772	1.643	28.5	6.9
7000	0.4092	8.739	0.126	6.9840	0.0960	0.0060	0.0044	14.2	12.8732	0.1778	0.00215	0.00106	7.504	1.312	31.5	5.5
9000	1.0000	10.916	0.090	7.2424	0.0612	0.0064	0.0003	12.3	13.3517	0.1133	0.00207	0.00013	9.596	0.121	40.2	0.5
Integrated		10.422	0.055	8.6380	0.0440	0.0091	0.0011	19.6	15.9393	0.0816	0.00221	0.00021	8.404	0.342	35.3	1.4

APPENDIX C. Supplemental $^{40}Ar/^{39}Ar$ dating of sample E309P by Paul Layer.

E309P

This sample was separated from a rhyolite. The sample contains biotite, quartz and feldspar. Based on morphology, the feldspar was presumed to be sanidine and so it was chosen for analysis. To facilitate handling and analysis, the larger feldspar crystals (~1 mm) were selected. Several of the crystals were clear, while others were cloudy. All appeared to have a sanidine morphology. Sixteen individual mineral grains were step heated and the age spectra analyzed. Most surprising is the Ca/K ratio which averages 14. This is much too high for alkali feldspar, and so most likely the dated phase was a plagioclase feldspar. It should be noted that of the 16 grains dated, none had a Ca/K ratio less than 3, so based on this small sample, and considering that we were trying to select for sanidine, it seems unlikely that there is sanidine in this size fraction of this sample. It is possible that there is sanidine in a smaller size fraction, however we did not select for this, and dated only plagioclase. Most of the dated grains show a stair-step up structure or, at least, a single old fraction. We interpret this old fraction to reflect either inheritance or excess argon. For 15 of the 16 grains there were at least 3 consecutive fractions of consistent age for which we could calculate a mean. The clearer grains tended to have the youngest ages and flattest spectra (e.g. grains 3, 19 and 16). The specimen mean ages are plotted on the probability diagram below. As can be seen, there is a dominant mode at about 33.5 Ma, and two smaller peaks at older ages. We interpret this main mode, consisting of 10 samples, to be the age of eruption of this rhyolite and the older ages (from 5 samples) to reflect inheritance. The weighted average age of the 10 samples forming the mode is 33.47 ± 0.15 Ma.

The samples were dated against standard MMhb-1 with an age of 513.9 Ma (see original report). Standard TCR-2 (Taylor Creek rhyolite sanidine) with an age of 27.87 Ma was also run and the J values are within 0.2%, less than the error on J, so using either standard will give essentially identical results. TCR-2 has a Ca/K ratio of 0.034.

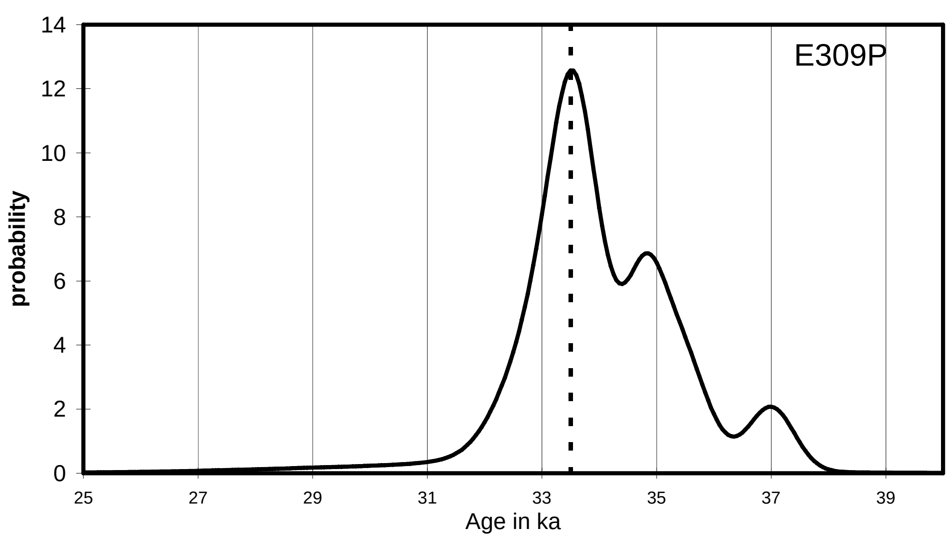

Table 1

Mineral	Integrated Age (Ma)	Plateau or weighted mean Age (Ma)	Plateau details	Ca/K
FS#1	39.2 ± 0.4	32.6 ± 0.5	8 fractions 40% ^{39}Ar released MSWD = 1.1	17
FS#2	35.3 ± 1.4	31.8 ± 3.0	8 fractions 36% ^{39}Ar released MSWD = 0.3	16
FS#3	33.0 ± 1.5	33.5 ± 0.4	6 fractions 95% ^{39}Ar released MSWD = 0.5	24
FS#4	35.9 ± 0.3	33.5 ± 0.4	3 fractions 22% ^{39}Ar released MSWD = 0.8	14
FS#5	43.3 ± 0.4	35.3 ± 0.5*	3 fractions 53% ^{39}Ar released MSWD = 2.8	14
FS#6	41.3 ± 0.3	33.3 ± 0.6	3 fractions 25% ^{39}Ar released MSWD = 0.8	17
FS#7	56.3 ± 0.6	None*	-	17
FS#8	34.5 ± 0.3	34.8 ± 0.3*	5 fractions 89% ^{39}Ar released MSWD = 2.8	6
FS#9	47.2 ± 0.4	33.3 ± 1.1	4 fractions 21% ^{39}Ar released MSWD = 1.6	8
FS#10	33.3 ± 0.3	33.6 ± 0.3	6 fractions 96% ^{39}Ar released MSWD = 0.7	3
FS#11	37.4 ± 0.4	37.0 ± 0.4*	5 fractions 95% ^{39}Ar released MSWD = 0.6	11
FS#12	35.8 ± 0.7	35.4 ± 0.5*	6 fractions 98% ^{39}Ar released MSWD = 6.0	14
FS#13	41.0 ± 0.4	33.6 ± 0.6	3 fractions 35% ^{39}Ar released MSWD = 0.2	18
FS#14	34.6 ± 0.6	34.9 ± 0.6*	6 fractions 99% ^{39}Ar released MSWD = 2.7	12
FS#15	35.6 ± 0.3	33.2 ± 0.4	3 fractions 39% ^{39}Ar released MSWD = 1.1	29
FS#16	33.7 ± 0.5	34.1 ± 0.4	6 fractions 97% ^{39}Ar released MSWD = 1.6	8
Average excluding *		**33.47 ± 0.15**		

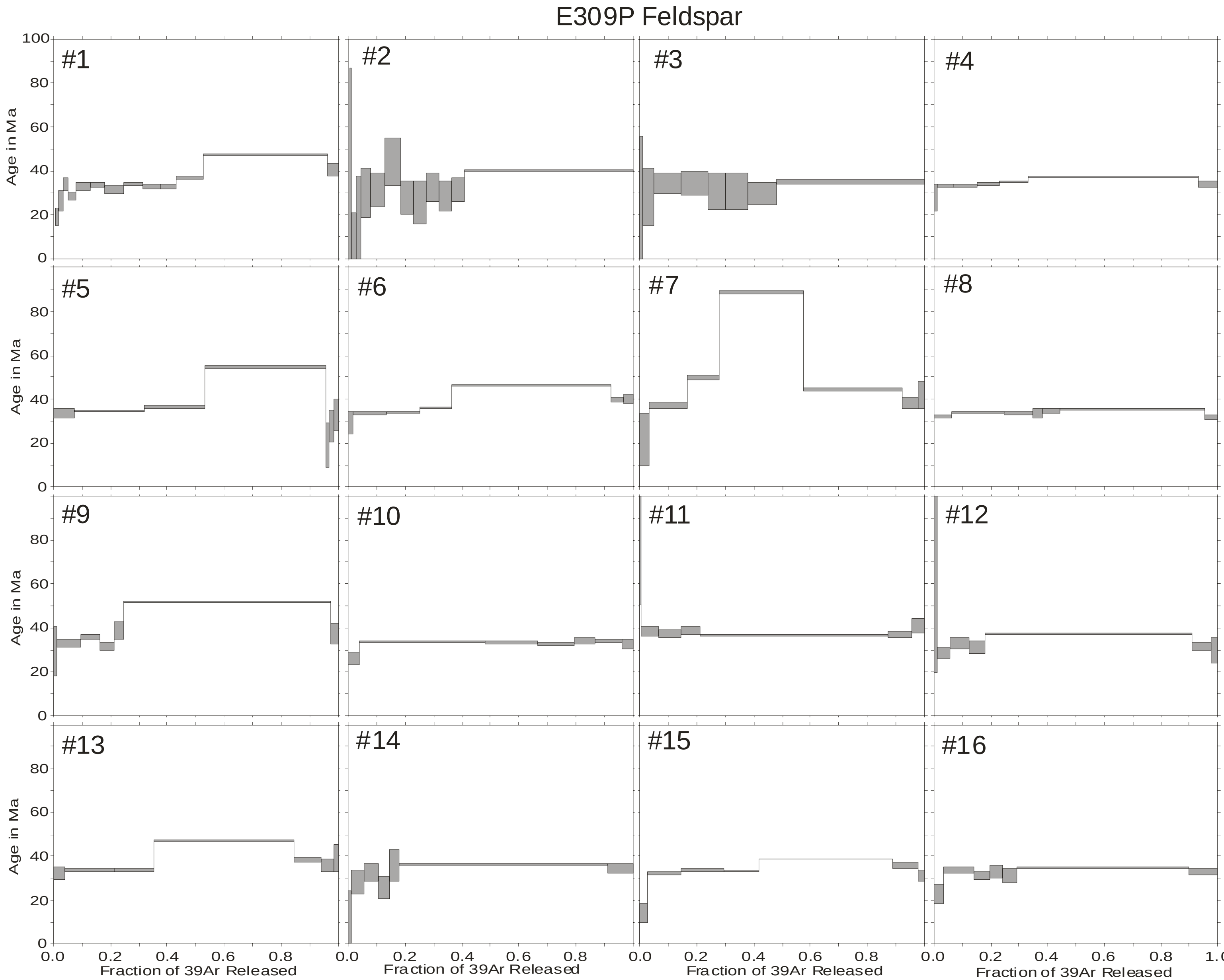
E309P Feldspar
#1
#2
#3
#4
#5
#6
#7
#8
#9
#10
#11
#12
#13
#14
#15
#16
Age in Ma
Fraction of 39Ar Released
0
20
40
60
80
100
0.0
0.2
0.4
0.6
0.8
1.0

E309P Feldspar #1

Weighted average of J from standards = 0.002351 +/- 0.000011

Laser (mW)	Cum. ^{39}Ar	^{40}Ar/^{39}Ar measured	+/-	^{37}Ar/^{39}Ar measured	+/-	^{36}Ar/^{39}Ar measured	+/-	% Atm. ^{40}Ar	Ca/K	+/-	Cl/K	+/-	^{40}Ar*/^{39}Ar$_K$	+/-	Age (Ma)	+/- (Ma)
300	0.0009	2249.64	132.591	2.2622	0.1551	7.6765	0.4569	100.8	4.1570	0.2855	0.02727	0.01453	-18.647	25.186	-80.86	111.70
500	0.0044	659.146	11.916	1.9426	0.0446	2.1955	0.0486	98.4	3.5690	0.0820	0.02153	0.00388	10.509	9.594	44.02	39.70
700	0.0177	48.434	0.439	1.6681	0.0226	0.1491	0.0031	90.7	3.0640	0.0416	0.01640	0.00076	4.490	0.897	18.94	3.76
900	0.0306	15.694	0.319	4.8376	0.0913	0.0333	0.0037	60.6	8.9043	0.1686	0.01416	0.00084	6.197	1.110	26.09	4.64
1100	0.0481	10.927	0.092	7.9339	0.0745	0.0119	0.0023	26.8	14.6332	0.1381	0.01124	0.00046	8.015	0.687	33.67	2.86
1400	0.0791	9.042	0.074	8.8710	0.0756	0.0100	0.0016	25.4	16.3716	0.1403	0.00850	0.00042	6.767	0.470	28.47	1.96
1700	0.1270	11.062	0.069	7.3636	0.0486	0.0130	0.0014	29.9	13.5762	0.0901	0.00827	0.00034	7.773	0.426	32.67	1.77
2000	0.1775	8.850	0.045	8.6234	0.0555	0.0051	0.0008	9.8	15.9121	0.1030	0.00574	0.00023	8.000	0.254	33.61	1.06
2500	0.2463	8.722	0.054	9.4648	0.0648	0.0066	0.0015	14.3	17.4743	0.1204	0.00474	0.00020	7.500	0.453	31.53	1.89
3000	0.3130	8.607	0.061	10.3197	0.0770	0.0046	0.0007	6.6	19.0633	0.1433	0.00412	0.00017	8.064	0.211	33.88	0.88
3500	0.3734	8.581	0.061	10.1771	0.0795	0.0053	0.0009	9.4	18.7980	0.1479	0.00343	0.00017	7.802	0.260	32.78	1.08
4000	0.4297	9.164	0.073	9.7260	0.0865	0.0071	0.0008	14.8	17.9595	0.1607	0.00372	0.00019	7.831	0.253	32.90	1.05
5000	0.5265	9.322	0.063	7.7022	0.0609	0.0040	0.0005	6.5	14.2038	0.1129	0.00619	0.00015	8.733	0.148	36.66	0.62
6000	0.9627	12.100	0.076	9.5505	0.0639	0.0055	0.0002	7.5	17.6335	0.1187	0.00424	0.00005	11.235	0.094	47.02	0.39
9000	1.0000	10.015	0.079	14.6590	0.1344	0.0055	0.0024	5.1	27.1564	0.2513	0.00192	0.00040	9.567	0.724	40.12	3.00
Integrated		15.367	0.045	9.2576	0.0304	0.0228	0.0003	39.4	17.0894	0.0565	0.00518	0.00005	9.355	0.084	39.24	0.39

E309P Feldspar #2

Weighted average of J from standards = 0.002351 +/- 0.000011

Laser (mW)	Cum. ^{39}Ar	^{40}Ar/^{39}Ar measured	+/-	^{37}Ar/^{39}Ar measured	+/-	^{36}Ar/^{39}Ar measured	+/-	% Atm. ^{40}Ar	Ca/K	+/-	Cl/K	+/-	^{40}Ar*/^{39}Ar$_K$	+/-	Age (Ma)	+/- (Ma)
500	0.0009	244.317	156.853	5.5880	3.6307	0.9014	0.7232	108.9	10.2907	6.7105	- 0.07370	0.09449	-21.733	######	-94.60	578.49
800	0.0036	41.189	5.529	6.9139	0.9339	0.2685	0.1130	191.5	12.7434	1.7292	0.03737	0.02182	-37.830	32.243	-168.00	150.07
1100	0.0094	35.553	2.576	16.4579	1.1862	0.1034	0.0489	82.5	30.5249	2.2238	0.00872	0.00844	6.270	14.459	26.39	60.42
1400	0.0244	13.057	0.342	18.5608	0.4590	0.0534	0.0210	110.5	34.4731	0.8629	0.00486	0.00388	-1.384	6.272	-5.88	26.68
1700	0.0463	8.483	0.190	15.2548	0.3022	0.0182	0.0157	50.0	28.2712	0.5657	0.00157	0.00221	4.268	4.673	18.01	19.62
2000	0.0763	8.163	0.154	10.9748	0.1669	0.0066	0.0089	13.7	20.2821	0.3107	0.00191	0.00166	7.069	2.654	29.73	11.07
2500	0.1295	8.199	0.120	10.9963	0.1578	0.0053	0.0060	9.1	20.3222	0.2938	0.00161	0.00091	7.480	1.788	31.44	7.45
3000	0.1829	8.033	0.091	11.5424	0.1201	-0.0052	0.0089	-30.1	21.3390	0.2238	- 0.00035	0.00143	10.493	2.665	43.96	11.03
3500	0.2292	7.968	0.104	11.2771	0.1307	0.0076	0.0059	17.6	20.8450	0.2434	0.00245	0.00107	6.588	1.769	27.72	7.39
4000	0.2709	7.821	0.112	10.4194	0.1275	0.0086	0.0076	22.7	19.2487	0.2371	0.00282	0.00137	6.067	2.269	25.55	9.49

5000	0.3198	9.379	0.099	9.5594	0.0952	0.0079	0.0053	17.4	17.6500	0.1768	0.00375	0.00100	7.776	1.570	32.68	6.54
6000	0.3638	9.187	0.141	7.9999	0.1083	0.0102	0.0055	26.4	14.7555	0.2008	0.00350	0.00110	6.772	1.643	28.49	6.86
7000	0.4092	8.739	0.126	6.9840	0.0960	0.0060	0.0044	14.2	12.8732	0.1778	0.00215	0.00106	7.504	1.312	31.54	5.47
9000	1.0000	10.916	0.090	7.2424	0.0612	0.0064	0.0003	12.3	13.3517	0.1133	0.00207	0.00013	9.596	0.121	40.24	0.50
Integrated		10.422	0.055	8.6380	0.0440	0.0091	0.0011	19.6	15.9393	0.0816	0.00221	0.00021	8.404	0.342	35.29	1.43

E309P Feldspar #3 Weighted average of J from standards = 0.002351 +/- 0.000011

Laser (mW)	Cum. ^{39}Ar	$^{40}Ar/^{39}Ar$ measured	+/-	$^{37}Ar/^{39}Ar$ measured	+/-	$^{36}Ar/^{39}Ar$ measured	+/-	% Atm. ^{40}Ar	Ca/K	+/-	Cl/K	+/-	$^{40}Ar^{*}/^{39}Ar_K$	+/-	Age (Ma)	+/- (Ma)
1000	0.0072	55.679	4.163	2.4403	0.2068	0.1955	0.0528	103.5	4.4848	0.3807	0.01309	0.00960	-1.926	15.040	-8.18	64.07
2000	0.0458	21.718	0.556	8.5339	0.2267	0.0532	0.0104	69.5	15.7460	0.4206	0.01337	0.00269	6.654	3.070	28.00	12.82
3000	0.1450	8.564	0.099	13.3893	0.1522	0.0050	0.0039	5.4	24.7835	0.2842	0.00470	0.00080	8.150	1.176	34.23	4.89
4000	0.2380	8.506	0.086	14.4655	0.1459	0.0049	0.0043	4.2	26.7944	0.2728	0.00106	0.00093	8.198	1.271	34.43	5.29
5000	0.3009	8.487	0.100	14.0316	0.1586	0.0078	0.0066	14.8	25.9834	0.2965	-0.00006	0.00099	7.276	1.964	30.59	8.19
7000	0.3775	8.667	0.095	13.5242	0.1552	0.0083	0.0069	16.6	25.0354	0.2899	0.00025	0.00090	7.265	2.051	30.55	8.55
9000	0.4782	8.761	0.082	12.3886	0.1418	0.0092	0.0039	20.5	22.9162	0.2643	0.00117	0.00081	6.994	1.165	29.42	4.86
9001	1.0000	9.489	0.062	13.1216	0.1471	0.0075	0.0009	13.1	24.2838	0.2747	0.00157	0.00013	8.289	0.260	34.81	1.08
Integrated		9.907	0.041	13.0348	0.0831	0.0104	0.0012	21.1	24.1217	0.1551	0.00213	0.00022	7.858	0.354	33.02	1.48

E309P Feldspar #4 Weighted average of J from standards = 0.002351 +/- 0.000011

Laser (mW)	Cum. ^{39}Ar	$^{40}Ar/^{39}Ar$ measured	+/-	$^{37}Ar/^{39}Ar$ measured	+/-	$^{36}Ar/^{39}Ar$ measured	+/-	% Atm. ^{40}Ar	Ca/K	+/-	Cl/K	+/-	$^{40}Ar^{*}/^{39}Ar_K$	+/-	Age (Ma)	+/- (Ma)
1000	0.0094	74.138	0.565	5.1535	0.0690	0.2299	0.0049	91.2	9.4878	0.1275	0.00838	0.00099	6.572	1.442	27.66	6.02
2000	0.0671	9.520	0.072	8.0661	0.0689	0.0077	0.0005	17.7	14.8782	0.1277	0.00215	0.00012	7.854	0.150	33.00	0.62
3000	0.1550	8.262	0.061	8.0923	0.0630	0.0032	0.0005	4.1	14.9269	0.1168	0.00148	0.00011	7.940	0.172	33.36	0.72
4000	0.2300	8.364	0.060	8.0220	0.0539	0.0030	0.0004	3.4	14.7966	0.0999	0.00196	0.00014	8.093	0.127	34.00	0.53
5000	0.3290	8.786	0.064	6.9878	0.0529	0.0033	0.0003	5.0	12.8802	0.0979	0.00263	0.00013	8.355	0.111	35.09	0.46
7000	0.9293	9.295	0.057	7.3068	0.0456	0.0032	0.0001	4.4	13.4710	0.0844	0.00280	0.00006	8.904	0.064	37.37	0.27
9000	1.0000	8.587	0.057	6.1464	0.0464	0.0034	0.0011	6.5	11.3231	0.0858	0.00146	0.00014	8.037	0.329	33.76	1.37
Integrated		9.655	0.037	7.3396	0.0292	0.0056	0.0001	11.5	13.5319	0.0540	0.00252	0.00004	8.560	0.052	35.94	0.27

E309P Feldspar #5 Weighted average of J from standards = 0.002351 +/- 0.000011

Laser (mW)	Cum. ^{39}Ar	$^{40}Ar/^{39}Ar$ measured	+/-	$^{37}Ar/^{39}Ar$ measured	+/-	$^{36}Ar/^{39}Ar$ measured	+/-	% Atm. ^{40}Ar	Ca/K	+/-	Cl/K	+/-	$^{40}Ar^{*}/^{39}Ar_K$	+/-	Age (Ma)	+/- (Ma)

1000	0.0748	10.716	0.098	8.9585	0.0976	0.0113	0.0016	25.1	16.5341	0.1811	0.00413	0.00021	8.055	0.491	33.84	2.04
2000	0.3204	8.623	0.052	8.0244	0.0553	0.0032	0.0004	4.0	14.8010	0.1026	0.00187	0.00008	8.297	0.123	34.85	0.51
3000	0.5309	9.570	0.058	6.8158	0.0497	0.0048	0.0004	9.4	12.5618	0.0920	0.00318	0.00017	8.681	0.131	36.44	0.54
4000	0.9599	14.051	0.074	7.9375	0.0450	0.0055	0.0003	7.3	14.6398	0.0835	0.00253	0.00006	13.072	0.106	54.60	0.44
5000	0.9708	8.700	0.207	6.6903	0.1259	0.0159	0.0081	48.4	12.3294	0.2330	0.00276	0.00100	4.496	2.392	18.97	10.04
7000	0.9854	8.440	0.124	5.5858	0.0641	0.0077	0.0059	22.0	10.2866	0.1184	0.00093	0.00087	6.587	1.750	27.72	7.31
9000	1.0000	8.232	0.109	5.4084	0.0515	0.0027	0.0059	4.9	9.9587	0.0951	-0.00002	0.00067	7.832	1.759	32.91	7.32
Integrated		11.300	0.036	7.7147	0.0268	0.0053	0.0003	8.8	14.2268	0.0497	0.00257	0.00005	10.335	0.084	43.30	0.40

E309P Feldspar #6

Weighted average of J from standards = 0.002351 +/- 0.000011

Laser (mW)	Cum. ^{39}Ar	$^{40}Ar/^{39}Ar$ measured	+/-	$^{37}Ar/^{39}Ar$ measured	+/-	$^{36}Ar/^{39}Ar$ measured	+/-	% Atm. ^{40}Ar	Ca/K	+/-	Cl/K	+/-	$^{40}Ar^{*}/^{39}Ar_K$	+/-	Age (Ma)	+/- (Ma)
1000	0.0180	35.373	0.566	6.4665	0.0978	0.0977	0.0041	80.3	11.9153	0.1810	0.01078	0.00076	6.982	1.242	29.37	5.18
2000	0.1325	9.196	0.074	10.7933	0.0919	0.0070	0.0005	13.8	19.9443	0.1710	0.00229	0.00014	7.955	0.166	33.42	0.69
3000	0.2521	8.615	0.066	10.7550	0.0935	0.0047	0.0004	6.8	19.8730	0.1740	0.00119	0.00011	8.057	0.124	33.85	0.52
4000	0.3654	8.904	0.058	9.5188	0.0723	0.0036	0.0004	4.0	17.5746	0.1343	0.00161	0.00014	8.575	0.128	36.00	0.53
5000	0.9221	11.628	0.071	8.2815	0.0517	0.0043	0.0001	5.6	15.2778	0.0958	0.00248	0.00005	11.009	0.079	46.09	0.33
7000	0.9674	10.709	0.051	12.5752	0.0691	0.0075	0.0010	12.0	23.2641	0.1289	0.00315	0.00024	9.480	0.309	39.76	1.28
9000	1.0000	10.861	0.070	9.9122	0.0756	0.0069	0.0017	11.9	18.3056	0.1406	0.00142	0.00031	9.601	0.501	40.26	2.08
Integrated		11.039	0.042	9.2215	0.0347	0.0065	0.0002	11.1	17.0225	0.0645	0.00235	0.00004	9.843	0.060	41.26	0.31

E309P Feldspar #7

Weighted average of J from standards = 0.002351 +/- 0.000011

Laser (mW)	Cum. ^{39}Ar	$^{40}Ar/^{39}Ar$ measured	+/-	$^{37}Ar/^{39}Ar$ measured	+/-	$^{36}Ar/^{39}Ar$ measured	+/-	% Atm. ^{40}Ar	Ca/K	+/-	Cl/K	+/-	$^{40}Ar^{*}/^{39}Ar_K$	+/-	Age (Ma)	+/- (Ma)
1000	0.0318	218.075	1.891	10.9370	0.1053	0.7235	0.0103	97.7	20.2118	0.1960	0.00812	0.00083	5.113	2.873	21.55	12.04
2000	0.1679	24.491	0.246	8.9710	0.0649	0.0555	0.0010	64.3	16.5572	0.1205	0.00432	0.00018	8.796	0.348	36.92	1.45
3000	0.2792	12.010	0.093	10.4232	0.0930	0.0030	0.0010	0.8	19.2558	0.1729	0.00262	0.00020	11.971	0.310	50.06	1.28
4000	0.5773	26.274	0.172	9.4733	0.0634	0.0190	0.0006	18.7	17.4901	0.1177	0.00800	0.00016	21.474	0.224	88.84	0.90
5000	0.9200	11.922	0.064	9.4437	0.0579	0.0069	0.0004	11.0	17.4350	0.1076	0.00584	0.00015	10.645	0.129	44.59	0.54
7000	0.9798	9.137	0.064	6.8803	0.0514	0.0018	0.0021	0.3	12.6813	0.0952	0.00580	0.00025	9.126	0.626	38.29	2.60
9000	1.0000	9.070	0.116	6.3671	0.0688	-0.0017	0.0049	-10.8	11.7314	0.1272	0.00292	0.00077	10.060	1.461	42.16	6.05
Integrated		24.253	0.079	9.3296	0.0308	0.0390	0.0004	44.6	17.2232	0.0572	0.00593	0.00008	13.490	0.142	56.32	0.63

E309P Feldspar #8

Weighted average of J from standards = 0.002351 +/- 0.000011

Laser	Cum.	$^{40}Ar/^{39}Ar$	+/-	$^{37}Ar/^{39}Ar$	+/-	$^{36}Ar/^{39}Ar$	+/-	%	Ca/K	+/-	Cl/K	+/-	$^{40}Ar^{*}/^{39}Ar_K$	+/-	Age	+/-

(mW)	^{39}Ar	measured		measured		measured		Atm. ^{40}Ar							(Ma)	(Ma)
1000	0.0636	10.379	0.098	2.6204	0.0268	0.0100	0.0007	26.5	4.8163	0.0494	0.00490	0.00029	7.619	0.219	32.02	0.91
2000	0.2489	8.423	0.061	3.3441	0.0242	0.0020	0.0002	4.0	6.1494	0.0446	0.00087	0.00009	8.073	0.092	33.91	0.38
3000	0.3471	8.500	0.081	3.3686	0.0351	0.0025	0.0006	5.6	6.1946	0.0646	0.00041	0.00022	8.015	0.204	33.67	0.85
4000	0.3817	8.513	0.086	3.3419	0.0360	0.0026	0.0019	6.0	6.1454	0.0663	0.00086	0.00040	7.992	0.570	33.58	2.37
5000	0.4436	8.492	0.088	3.2747	0.0376	0.0016	0.0008	2.6	6.0214	0.0692	0.00075	0.00022	8.261	0.243	34.70	1.01
7000	0.9545	8.612	0.065	3.3410	0.0261	0.0014	0.0001	2.0	6.1437	0.0481	0.00060	0.00006	8.431	0.074	35.40	0.31
9000	1.0000	8.708	0.106	3.4564	0.0442	0.0047	0.0011	13.1	6.3563	0.0815	0.00084	0.00027	7.558	0.335	31.77	1.39
Integrated		8.672	0.038	3.2997	0.0149	0.0024	0.0001	5.3	6.0675	0.0274	0.00093	0.00005	8.207	0.056	34.47	0.28

E309P Feldspar #9

Weighted average of J from standards = 0.002351 +/- 0.000011

Laser (mW)	Cum. ^{39}Ar	$^{40}Ar/^{39}Ar$ measured	+/-	$^{37}Ar/^{39}Ar$ measured	+/-	$^{36}Ar/^{39}Ar$ measured	+/-	% Atm. ^{40}Ar	Ca/K	+/-	Cl/K	+/-	$^{40}Ar^*/^{39}Ar_K$	+/-	Age (Ma)	+/- (Ma)
1000	0.0129	29.548	0.638	2.2825	0.0585	0.0770	0.0091	76.5	4.1944	0.1077	0.00949	0.00214	6.953	2.677	29.25	11.17
2000	0.0925	8.852	0.105	4.3836	0.0601	0.0045	0.0011	11.4	8.0664	0.1109	0.00202	0.00032	7.841	0.350	32.95	1.46
3000	0.1604	8.318	0.091	4.3438	0.0531	0.0004	0.0010	-2.4	7.9929	0.0980	0.00103	0.00033	8.509	0.300	35.73	1.25
4000	0.2099	8.317	0.087	4.2673	0.0440	0.0038	0.0014	9.5	7.8517	0.0812	0.00089	0.00048	7.522	0.428	31.62	1.78
5000	0.2480	8.766	0.095	4.3543	0.0478	-0.0004	0.0030	-5.1	8.0122	0.0882	0.00098	0.00072	9.212	0.906	38.65	3.76
7000	0.9722	13.283	0.073	4.2073	0.0249	0.0039	0.0002	6.2	7.7410	0.0459	0.00130	0.00006	12.463	0.089	52.09	0.36
9000	1.0000	8.940	0.121	4.0018	0.0513	0.0011	0.0039	0.2	7.3619	0.0947	0.00080	0.00090	8.918	1.172	37.42	4.87
Integrated		12.264	0.054	4.2087	0.0193	0.0044	0.0003	8.0	7.7436	0.0355	0.00140	0.00007	11.289	0.095	47.25	0.45

E309P Feldspar #10

Weighted average of J from standards = 0.002351 +/- 0.000011

Laser (mW)	Cum. ^{39}Ar	$^{40}Ar/^{39}Ar$ measured	+/-	$^{37}Ar/^{39}Ar$ measured	+/-	$^{36}Ar/^{39}Ar$ measured	+/-	% Atm. ^{40}Ar	Ca/K	+/-	Cl/K	+/-	$^{40}Ar^*/^{39}Ar_K$	+/-	Age (Ma)	+/- (Ma)
1000	0.0378	14.692	0.293	1.3843	0.0314	0.0291	0.0021	58.0	2.5423	0.0577	0.00496	0.00037	6.163	0.664	25.95	2.78
2000	0.4799	8.266	0.070	1.6936	0.0155	0.0010	0.0001	2.1	3.1109	0.0286	0.00069	0.00003	8.077	0.079	33.93	0.33
3000	0.6644	8.298	0.079	1.6167	0.0183	0.0015	0.0004	4.0	2.9696	0.0337	0.00053	0.00010	7.943	0.129	33.37	0.54
4000	0.7957	8.273	0.099	1.6103	0.0204	0.0020	0.0005	5.8	2.9577	0.0375	0.00059	0.00008	7.776	0.169	32.68	0.70
5000	0.8664	8.292	0.109	1.5863	0.0222	0.0012	0.0010	2.8	2.9136	0.0408	0.00073	0.00025	8.037	0.326	33.77	1.36
7000	0.9626	8.318	0.079	1.6139	0.0186	0.0011	0.0007	2.3	2.9644	0.0342	0.00054	0.00011	8.109	0.230	34.06	0.96
9000	1.0000	8.295	0.107	1.5892	0.0287	0.0023	0.0018	6.9	2.9190	0.0527	0.00150	0.00033	7.701	0.528	32.37	2.20
Integrated		8.523	0.040	1.6376	0.0086	0.0024	0.0002	6.8	3.0080	0.0157	0.00083	0.00004	7.927	0.066	33.30	0.31

E309P Feldspar #11 Weighted average of J from standards = 0.002351 +/- 0.000011

Laser (mW)	Cum. ^{39}Ar	^{40}Ar/^{39}Ar measured	+/-	^{37}Ar/^{39}Ar measured	+/-	^{36}Ar/^{39}Ar measured	+/-	% Atm. ^{40}Ar	Ca/K	+/-	Cl/K	+/-	^{40}Ar*/^{39}Ar$_K$	+/-	Age (Ma)	+/- (Ma)
1000	0.0048	54.036	1.555	4.5011	0.1408	0.1166	0.0270	63.2	8.2831	0.2598	0.01145	0.00266	19.953	7.957	82.69	32.23
2000	0.0658	8.444	0.069	6.3920	0.0617	-0.0007	0.0016	-8.3	11.7775	0.1141	0.00126	0.00037	9.152	0.477	38.40	1.98
3000	0.1462	8.425	0.072	6.0849	0.0526	-0.0003	0.0014	-6.3	11.2093	0.0972	0.00116	0.00043	8.964	0.435	37.62	1.81
4000	0.2127	8.319	0.087	5.7484	0.0662	-0.0016	0.0015	-10.9	10.5872	0.1224	0.00125	0.00023	9.228	0.440	38.72	1.83
5000	0.8728	8.886	0.058	5.9217	0.0393	0.0020	0.0002	1.8	10.9076	0.0727	0.00100	0.00005	8.736	0.081	36.67	0.34
7000	0.9563	8.257	0.054	5.1439	0.0391	-0.0003	0.0012	-5.9	9.4700	0.0723	0.00047	0.00028	8.745	0.373	36.71	1.55
9000	1.0000	8.266	0.086	4.7353	0.0526	-0.0037	0.0025	-17.4	8.7156	0.0972	0.00115	0.00046	9.700	0.761	40.67	3.15
Integrated		8.923	0.040	5.8283	0.0271	0.0015	0.0003	0.2	10.7349	0.0500	0.00106	0.00005	8.909	0.097	37.39	0.44

E309P Feldspar #12 Weighted average of J from standards = 0.002351 +/- 0.000011

Laser (mW)	Cum. ^{39}Ar	^{40}Ar/^{39}Ar measured	+/-	^{37}Ar/^{39}Ar measured	+/-	^{36}Ar/^{39}Ar measured	+/-	% Atm. ^{40}Ar	Ca/K	+/-	Cl/K	+/-	^{40}Ar*/^{39}Ar$_K$	+/-	Age (Ma)	+/- (Ma)
1000	0.0111	1398.813	33.367	8.1112	0.2025	4.6789	0.1158	98.8	14.9620	0.3754	0.02430	0.00358	16.874	12.349	70.17	50.37
2000	0.0587	14.611	0.124	12.0356	0.1282	0.0296	0.0022	53.8	22.2580	0.2390	0.00342	0.00040	6.788	0.645	28.56	2.69
3000	0.1219	8.570	0.072	11.6274	0.1313	0.0056	0.0022	9.3	21.4973	0.2447	0.00177	0.00038	7.808	0.651	32.81	2.71
4000	0.1791	8.970	0.121	10.5227	0.1499	0.0079	0.0022	17.4	19.4409	0.2788	0.00146	0.00034	7.436	0.668	31.26	2.79
5000	0.9065	10.106	0.064	6.9924	0.0456	0.0062	0.0003	13.0	12.8887	0.0845	0.00165	0.00004	8.810	0.096	36.98	0.40
7000	0.9757	9.553	0.067	8.0037	0.0772	0.0089	0.0015	21.2	14.7625	0.1432	0.00120	0.00027	7.549	0.448	31.73	1.87
9000	1.0000	8.388	0.105	5.1313	0.0603	0.0060	0.0047	16.6	9.4468	0.1115	-0.00044	0.00079	6.996	1.407	29.42	5.87
Integrated		25.478	0.120	7.7662	0.0376	0.0594	0.0006	66.7	14.3222	0.0697	0.00190	0.00007	8.530	0.173	35.81	0.74

E309P Feldspar #13 Weighted average of J from standards = 0.002351 +/- 0.000011

Laser (mW)	Cum. ^{39}Ar	^{40}Ar/^{39}Ar measured	+/-	^{37}Ar/^{39}Ar measured	+/-	^{36}Ar/^{39}Ar measured	+/-	% Atm. ^{40}Ar	Ca/K	+/-	Cl/K	+/-	^{40}Ar*/^{39}Ar$_K$	+/-	Age (Ma)	+/- (Ma)
1000	0.0396	16.573	0.314	9.2407	0.1880	0.0325	0.0026	53.9	17.0580	0.3491	0.00614	0.00038	7.680	0.772	32.28	3.22
2000	0.2128	8.532	0.065	10.5098	0.0873	0.0045	0.0005	6.4	19.4168	0.1624	0.00145	0.00011	8.016	0.167	33.68	0.70
3000	0.3538	8.405	0.059	10.3578	0.0843	0.0038	0.0006	4.1	19.1341	0.1568	0.00202	0.00012	8.087	0.189	33.97	0.79
4000	0.8476	11.856	0.079	8.9387	0.0626	0.0043	0.0002	5.1	16.4973	0.1162	0.00361	0.00005	11.284	0.092	47.23	0.38
5000	0.9419	10.082	0.067	9.7799	0.0638	0.0058	0.0009	9.9	18.0598	0.1185	0.00221	0.00015	9.120	0.272	38.27	1.13
7000	0.9832	9.242	0.064	11.4774	0.0991	0.0054	0.0022	7.8	21.2180	0.1845	0.00293	0.00035	8.559	0.649	35.93	2.70
9000	1.0000	10.318	0.155	14.9702	0.2312	0.0074	0.0050	10.3	27.7386	0.4326	0.00483	0.00088	9.316	1.504	39.08	6.24

Integrated		10.679	0.042	9.7090	0.0389	0.0056	0.0002	8.8	17.9280	0.0723	0.00297	0.00005	9.775	0.080	40.98	0.38

E309P Feldspar #14

Weighted average of J from standards = 0.002351 +/- 0.000011

Laser (mW)	Cum. ^{39}Ar	$^{40}Ar/^{39}Ar$ measured	+/-	$^{37}Ar/^{39}Ar$ measured	+/-	$^{36}Ar/^{39}Ar$ measured	+/-	% Atm. ^{40}Ar	Ca/K	+/-	Cl/K	+/-	$^{40}Ar^{*}/^{39}Ar_{K}$	+/-	Age (Ma)	+/- (Ma)
1000	0.0080	43.200	1.765	2.6517	0.1202	0.1481	0.0213	100.9	4.8738	0.2213	0.01115	0.00375	-0.386	6.107	-1.64	25.92
2000	0.0545	8.845	0.640	6.8076	0.0584	0.0090	0.0040	24.4	12.5467	0.1080	0.00276	0.00069	6.695	1.359	28.17	5.67
3000	0.1055	8.354	0.071	7.1855	0.0628	0.0038	0.0033	7.0	13.2464	0.1164	0.00155	0.00068	7.780	0.971	32.69	4.04
4000	0.1445	8.186	0.093	6.9297	0.0714	0.0086	0.0040	24.9	12.7726	0.1321	0.00276	0.00112	6.158	1.180	25.93	4.93
5000	0.1795	8.340	0.128	6.7837	0.1039	0.0008	0.0058	-3.1	12.5024	0.1923	0.00169	0.00093	8.609	1.738	36.14	7.22
7000	0.9111	9.065	0.061	6.5577	0.0478	0.0034	0.0002	5.5	12.0840	0.0884	0.00099	0.00004	8.572	0.090	35.99	0.37
9000	1.0000	8.218	0.071	6.0970	0.0559	0.0017	0.0019	0.7	11.2318	0.1035	0.00114	0.00037	8.169	0.559	34.31	2.33
Integrated		9.155	0.055	6.5518	0.0359	0.0048	0.0005	10.1	12.0731	0.0664	0.00129	0.00009	8.244	0.146	34.62	0.63

E309P Feldspar #15

Weighted average of J from standards = 0.002351 +/- 0.000011

Laser (mW)	Cum. ^{39}Ar	$^{40}Ar/^{39}Ar$ measured	+/-	$^{37}Ar/^{39}Ar$ measured	+/-	$^{36}Ar/^{39}Ar$ measured	+/-	% Atm. ^{40}Ar	Ca/K	+/-	Cl/K	+/-	$^{40}Ar^{*}/^{39}Ar_{K}$	+/-	Age (Ma)	+/- (Ma)
1000	0.0238	23.925	0.411	7.0381	0.1358	0.072	0.004	86.2	12.9733	0.2515	0.01155	0.00068	3.311	1.088	13.99	4.58
2000	0.1435	8.591	0.066	20.6124	0.1800	0.008	0.001	11.2	38.3354	0.3394	0.00323	0.00016	7.710	0.204	32.4	0.85
3000	0.2936	8.726	0.050	18.3050	0.1260	0.007	0.000	8.9	33.9923	0.2369	0.00335	0.00012	8.016	0.111	33.68	0.46
4000	0.4154	8.999	0.055	15.4602	0.1124	0.008	0.000	12.7	28.6557	0.2104	0.00451	0.00012	7.911	0.131	33.24	0.55
5000	0.8910	9.870	0.058	10.8074	0.0694	0.005	0.000	6.8	19.9706	0.1292	0.00301	0.00005	9.239	0.073	38.76	0.3
7000	0.9793	17.632	0.136	24.7013	0.2135	0.037	0.001	51.8	46.0643	0.4046	0.00929	0.00024	8.619	0.362	36.18	1.51
9000	1.0000	11.373	0.122	42.3811	0.4784	0.025	0.002	36.1	79.9698	0.9284	0.01318	0.00087	7.457	0.585	31.35	2.44
Integrated		10.493	0.034	15.4891	0.0521	0.011	0.000	19.8	28.7098	0.0975	0.00424	0.00005	8.478	0.064	35.6	0.31

E309P Feldspar #16

Weighted average of J from standards = 0.002351 +/- 0.000011

Laser (mW)	Cum. ^{39}Ar	$^{40}Ar/^{39}Ar$ measured	+/-	$^{37}Ar/^{39}Ar$ measured	+/-	$^{36}Ar/^{39}Ar$ measured	+/-	% Atm. ^{40}Ar	Ca/K	+/-	Cl/K	+/-	$^{40}Ar^{*}/^{39}Ar_{K}$	+/-	Age (Ma)	+/- (Ma)
1000	0.0356	35.585	0.397	0.7132	0.0154	0.1023	0.0035	84.9	1.3092	0.0282	0.01403	0.00061	5.380	1.027	22.67	4.30
2000	0.1407	8.187	0.069	3.2177	0.0300	0.0016	0.0011	2.7	5.9164	0.0553	0.00608	0.00027	7.958	0.339	33.44	1.41
3000	0.1995	8.246	0.072	4.4382	0.0406	0.0040	0.0015	10.1	8.1671	0.0749	0.00069	0.00044	7.406	0.441	31.13	1.84
4000	0.2433	8.167	0.084	4.3654	0.0436	0.0022	0.0024	3.8	8.0327	0.0804	0.00099	0.00044	7.851	0.722	32.99	3.01
5000	0.2899	8.180	0.090	4.3414	0.0465	0.0035	0.0027	8.6	7.9884	0.0859	0.00039	0.00057	7.473	0.795	31.42	3.31
7000	0.8958	8.762	0.075	4.3954	0.0389	0.0026	0.0002	4.9	8.0881	0.0719	0.00104	0.00006	8.330	0.102	34.98	0.42

9000	1.0000	8.354	0.071	4.1170	0.0371	0.0025	0.0011	5.1	7.5743	0.0685	0.00091	0.00022	7.920	0.335	33.28	1.40
Integrated		9.527	0.051	4.1106	0.0235	0.0061	0.0003	15.7	7.5627	0.0434	0.00197	0.00007	8.028	0.103	33.73	0.45